The Design of Novel Microwave-Heated Reaction Cells for Infrared Spectroscopy

I.P.Silverwood

Ph.D. by Research

University of Edinburgh

2006

Declaration

I hereby declare that I composed this thesis entirely myself and that it describes my own research. The work within has not been submitted for any other degree or professional qualification.

Ian Silverwood
Edinburgh
April 21, 2006

Abstract

Two novel microreactor cells for the investigation of catalysts by *in-situ* infrared spectroscopy under microwave and conventional heating are presented. A transmission infrared microreactor cell is demonstrated which holds a pressed catalyst disc in a controlled atmosphere and allows study of reactions from ambient temperatures to over 473 K. A cell that allows diffuse reflectance spectroscopy under reaction conditions up to 373 K under microwave heating and 423 K under conventional heating is also described. The optical characteristics of these cells are determined by the choice of CaF_2 as the window material, allowing transmission from 77000-1110 cm^{-1}.

An oscillating microwave power heating regime was used to study the oxidation of carbon monoxide in air over the supported platinum catalysts EUROPT-1 and EUROPT-3, and their support oxides in these cells. The reaction was followed by time-resolved infrared spectroscopy and mass spectrometry. Both displayed a number of features that oscillated with the same frequency as the microwave perturbation. Production of CO_2 appeared to vary with temperature in the same manner whether the catalysts were heated conventionally or with microwave radiation.

Although no specific microwave effect for this reaction was observed, accurate thermometry within the cells was limited through the constraints imposed by microwave heating.

Preliminary infrared emission and liquid phase experiments using the transmission cell are also reported.

Acknowledgements

Firstly of course, my grateful thanks to Gordon McDougall, my supervisor and mentor for this project. His guidance was invaluable in determining just what was going on when things seemed to be behaving contrarily just to taunt me. Gavin Whittaker, my second supervisor, taught me everything I know about microwaves and was always willing to indulge my ignorance. Thanks also must go to Ron Brown for assisting in wrangling equipment and many discussions, and Alex Cook who put up with me getting in his way in the lab. Alex was always ready to help with any problem, and also their mellowing in the pub. This work could not have been completed without the skills of David Paden in the mechanical workshop. Thanks for the many hours spent making, modifying and repairing my cells. To those around the who have made my time at KB enjoyable, many thanks; Alex, Trish, Rob, the many people who passed through room 252 and others in the department too numerous to mention. Finally, I would like to thank those who reminded me there was life outside chemistry; Mum and Dad, Tabitha and everyone else who put up with me boring them with my science.

Thanks to you all!

Contents

1 Microwave chemistry **1**

1.1 Introduction 1

1.2 Microwave heating 2

1.3 Materials in the microwave 6

1.4 Microwave transmission 8

1.5 Measuring temperature 9

1.6 Microwave enhanced synthesis 12

2 Microwave catalysis **14**

2.1 Introduction 14

2.2 Proposed mechanisms 17

2.3 Microwave heated catalytic reactions 19

2.4 Aim 22

3 Infrared spectroscopy **23**

3.1 Introduction 23

3.2 Fourier transform spectrometry 24

3.3 Optics 26

3.4 Data manipulation 29

4 Cell Design **33**

4.1 Introduction 33

4.2 Transmission cell construction 33

4.3 DRIFTS cell construction 35

4.4 Using parallel plates . . . 39
4.5 Selection of materials . . . 41
4.6 Maximising energy transfer . . . 41

5 Methods 44
5.1 Infrared spectroscopy . . . 44
5.2 Gas handling and analysis . . . 46
5.3 Microwave source . . . 48
5.4 Catalyst samples . . . 48
5.5 Conventionally heated transmission IR . . . 49
5.6 Microwave heated transmission IR . . . 49
5.7 Conventionally heated emission IR . . . 50
5.8 Microwave heated emission IR . . . 51
5.9 DRIFTS . . . 51

6 Transmission cell experiments 52
6.1 Conventionally heated transmission IR . . . 52
6.2 Microwave heated transmission IR . . . 67
6.3 Conventionally heated emission IR . . . 96
6.4 Microwave heated emission IR . . . 103
6.5 Mass spectrometry . . . 108

7 DRIFTS cell experiments 123
7.1 Conventionally heated DRIFTS . . . 123
7.2 Microwave heated DRIFTS . . . 128

8 Discussion 133
8.1 Temperature . . . 133
8.2 Infared spectroscopy . . . 144
8.3 Mass spectrometry . . . 155
8.4 Assessment of reactions . . . 160
8.5 Evaluation of cell design . . . 162
8.6 Conclusions . . . 163

8.7 Suggested further work 164

Chapter 1

Microwave chemistry

1.1 Introduction

In the Second World War, the magnetron was designed by Randall and Booth and used for RADAR (Radio Detection And Ranging). It was soon recognised that microwaves could heat water in a very effective manner, and microwave-heating appliances became available in the United States from the 1950's. These devices were widespread by the 1980's, and it was around this time that the application of microwave heating upon chemical reactions began to develop [1].

Microwaves are part of the electromagnetic spectrum, with wavelengths of 1 cm to 1 m, corresponding to frequencies of 30 GHz and 300 MHz. As such they have oscillating electrical and magnetic components orthogonal to each other and the direction of propagation. Most of the microwave spectrum is used for telecommunications or RADAR, but a few frequencies are reserved for heating devices, the most common being 2.45 GHz [2]. Microwave heating is due to an electrical field exerting a force on charged particles and dipoles. If the particles can move freely, a current will form. If the charges cannot freely move, they will move until a restoring force of equal magnitude is exerted on them, resulting in a dielectric polarisation. Both mechanisms lead to heating and will be discussed in Sections 1.2.1 and 1.2.2.

The application of microwaves has led to considerable rate enhancements for a number of reactions, and this work aims to develop a method for the investigation of microwave heated reactions using *in-situ* infrared analysis. After an introduction to

the properties of microwave heating and how it applies to the field of heterogeneous catalysis, the manufacture of two microreactor cells which allow microwave heating is described. Their function was confirmed through the use of infrared spectroscopy to follow the heating of carbon monoxide, and the effect of microwave heating on the CO oxidation over supported platinum catalysts is reported. Temperature measurement using thermocouples embedded in the cells and IR emission is then discussed.

1.2 Microwave heating

Although microwaves are best known for their use in the domestic microwave oven, they are used in a wide array of heating applications, from industrial-scale processing [3], through medical use [4], to synthesis in the research laboratory [5]. This is due to various differences in the way a material is heated by microwaves, and the high efficiency that can result from heating only the target rather than maintaining an oven at elevated temperatures.

Temperature is a measure of the average kinetic energy of particles in a system. It is defined thermodynamically as:

$$T = \left(\frac{\delta u}{\delta S}\right)_{v'} \tag{1.1}$$

where u is the energy, S is the entropy and the partial derivative is taken at constant volume. To heat a system, one must increase the average kinetic energy of the components within it. To conserve energy, a system may transfer energy through a change in temperature, or through work, according to the first law of thermodynamics:

$$du = dq - dw \tag{1.2}$$

where q is heat, and w is work. Conventional heating is normally carried out in an oven, which is an inefficient process. The oven walls, and everything contained within the oven is heated along with the sample. The heat slowly penetrates the material through conduction, resulting in a temperature gradient from the outside in. Microwaves cause heating by doing work on the sample and may cause different temperature profiles.

When microwaves penetrate a material it absorbs some of the microwave energy. The energy that is absorbed will vary depending on the properties of both the microwaves and the material itself. Because the microwave is losing energy as it travels through the material, it will at some point have lost all its energy and become extinct. After this point, any heating can not be due to the direct interaction of microwaves with the material, but instead is due to conduction from the regions which have interacted with the microwave radiation. The penetration depth (D_p) is defined as the depth at which the power has fallen to $1/e$ of its incident value, and is dependant on the wavelength and the properties of the material. If a material has a small penetration depth, then all of the power will be lost near the surface of the material, and a similar temperature profile to that of a conventionally heated object will result. If the material has a large penetration depth, heating will occur deeper within the material and can lead to an inverted temperature profile. This phenomenon has been exploited for organic syntheses in solution and is discussed further in Section 1.6. For small samples this means that the radiation may pass through the sample without losing much power and therefore only cause a very slight temperature rise. This can be counteracted by using a reflecting cavity, which allows the radiation to pass through the sample many times to optimise the transfer of energy to the material. Another point to note is that the shape of the sample can affect the power distribution through refraction and diffraction of the microwave radiation. As microwaves are macroscopic, with a wavelength of 12.2 cm at 2.45 GHz, there is also the problem of positioning the sample inside a cavity. As the cavity is usually of similar dimension to the wavelength of the microwaves, standing waves will occur, resulting in an inhomogeneous field. Thus samples at different positions in the cavity will experience different microwave field strengths and will heat at different rates. In domestic microwave ovens, this effect is commonly countered either with a turntable, or a device named a mode-stirrer. A mode stirrer is a rotating metal paddle which reflects the microwaves in different directions. Although these methods produce a more equal exposure to the microwaves over time, they are not ideal for scientific measurements. Instead a tuneable cavity with a single standing wave is normally used, with the sample positioned in the maximum field strength position. This approach does however necessitate the samples to be small

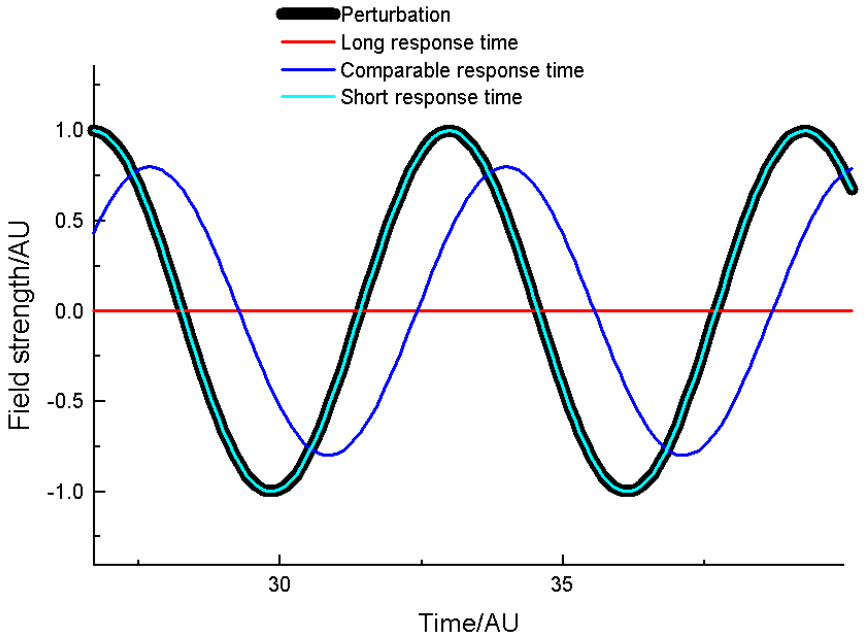

Figure 1.1: Dipole response to microwave radiation

in relation to the wavelength, and creates further difficulties with accurate sample positioning [6].

1.2.1 Dielectric heating

When a dipole is placed in a static electric field, it will align itself with the field to minimise free energy and a finite time, known as the response time, is required for this to occur. If the field is oscillating there are three possibilities. At low frequency the dipole is able to remain aligned with the field as the response time is much smaller than the period of the perturbation. At high frequency the response time is much greater than the period, the dipole is unable to react to the changing field, and remains static. However, at intermediate frequencies where the response time is of the same magnitude as the period of the electric field, the dipole experiences a force that causes a rotation, but the polarisation of the molecules lags behind that of the field. As the dipoles are not in phase with the field, they are not in the lowest energy state, and energy transfer must be occurring. The dipoles are absorbing energy from the electromagnetic field and it is being converted into heat [7]. This is shown in Figure 1.1.

The complex dielectric constant (ε^*) completely describes the dielectric properties of a homogeneous material. It can be expressed as the sum of two parts, the real (ε') and imaginary (ε'') dielectric constants:

$$\varepsilon^* = \varepsilon' + \varepsilon'' \tag{1.3}$$

The real part of the dielectric constant is approximately equal to ε^* at very high or low frequencies and exactly equal in static fields. Where an energy transfer (heating) is occurring ε'' is non-zero. This value is related to the efficiency of conversion between electromagnetic and thermal energy. The loss angle, δ, is also commonly quoted, although usually expressed in the form of its tangent. It is defined thus:

$$\tan\delta = \frac{\varepsilon''}{\varepsilon'} \tag{1.4}$$

The angle δ is the phase difference between the electric field and the polarisation of the material. Magnetic polarisation can also lead to a heating effect in a similar manner, for example in ferrites, although this is much less common [2].

Another form of dielectric heating is seen in materials that are composed of conducting particles suspended in a non-conducting medium. The heating is caused by the accumulation of charge at the interface and is called the Maxwell-Wagner effect [8]. Where a conducting medium is adjacent to a non-conducting medium, the non-conducting medium will oppose polarisation of the conductor. This inhibition results in a heating effect. Although it is possible to create systems that are heated in this way, it is very difficult to model due to the large number of factors involved.

1.2.2 Conduction heating

Another form of heating is cause by the conduction of charged particles such as electrons or ions. Because the time scale of movement for electrons and ions is much shorter than that of microwave radiation, they will couple in phase with the electric field. Conduction heating is the most common mechanism for heating of all solids, and can be sensitive to temperature. Alumina, for example, has a conductivity that rises with temperature, as the number of electrons thermally excited into the conduction band

increases. This can lead to the phenomenon known as thermal runaway. As the temperature rises in the solid, more electrons are excited into the conduction band and more of the microwave energy is absorbed, resulting in a greater heating effect. This positive feedback can lead to a very rapid temperature rise [9].

1.3 Materials in the microwave

1.3.1 Metals

The behaviour of metals in the microwave depends heavily on the geometry of the metal. A bulk metal has many mobile electrons and these can couple with the electric field of the microwave radiation. The coupling is strong, such that the microwaves do not penetrate the metal to any great degree ($D_p \approx 50$ μm). High surface currents are induced in the metal and in a perfect metal, no energy is lost. For a bulk metal, this is an accurate approximation and it can be assumed that all the microwave energy is reflected. This allows construction of waveguides and microwave cavities for the manipulation of microwaves in a controlled manner. These are discussed further in Section 1.4. When the metal is not presented in bulk form, energy may be lost. Sharp corners can result in high electric field stresses which may cause an electrical discharge and damage to the equipment. Other surface defects such as scratches and corrosion can also cause heating. When the metal is present in a form with a very high surface area, such as a powder or foil, these effects dominate and heating can be considerable.

1.3.2 Gases

When in the gas phase, molecules are more rarefied and less likely to interact with each other. In this state, the quantisation of rotational energy levels can be observed. If the molecule contains an electric dipole then it can couple with the electric field of the microwave radiation. Where the frequency of the radiation has the same energy as a rotational transition, a large energy transfer occurs. By measuring the absorbance of a gas over the microwave spectrum a number of well-defined features will be noted. Tunable microwave sources are used in this way for rotational spectroscopy, which can provide information on bond lengths and angles. Rotational spectroscopy is also used

for the identification of molecules in remote planetary and interstellar atmospheres.

Under certain conditions it is also possible for a microwave to induce the gas to form a plasma. In a plasma enough energy has been supplied to the molecules such that they become charged. An approximately equal number of positive and negative species are present such that overall the plasma is charge neutral. Whilst energy is required to sustain a plasma, it can be a relatively stable state when pressure is low. The microwave electric field couples with the valence electrons of the molecules, and causes them to oscillate rapidly in space. These energetic electrons collide with other species, and can cause ionisation of neutral species to create more free electrons. The positively charged species are too massive to attain high velocities. The plasma loses energy to its surroundings through collisions with heavier particles, or through radiative emission, which is often in the visible range. A plasma conducts electricity and can also be caused by high voltage. Lightning, the aurora borealis, stars and neon lighting are all examples of plasmas.

1.3.3 Heterogeneous systems

If defined rigidly, most systems heated with microwaves are heterogeneous. In practical microwave processing air, or another gas is usually present, and food processing and chemical reactions will obviously involve a number of components. Whilst theoretical treatments of multicomponent systems have been used, practical experiments to ascertain whether a differential heating effect is present have not yet been reported. This is partly due to the difficulty of measuring the temperature of mixed components separately, but also that many are prepared to use microwave applicators as a 'black box'. It is possible for many samples to simply take an average of the dielectric properties of the components, and treat it as a homogenous material with a calcuated effective dielectric constant. As mentioned in Section 1.2.1, under certain circumstances interfacial heating may occur, in accordance with the Maxwell-Wagner theory. This has been shown experimentally [8] for copper phthalocyanine inclusions in paraffin wax. However, this study used 3% of the semiconducting copper compound and at higher concentrations the inclusions are unlikely to be completely isolated from each other, causing the effect to break down. Further examples of heterogeneous systems are to be

found in supported metal catalysts, where a large number of small active metal particles are present on a chemically inert support. Theoretical studies have been carried out on this subject, with contradictory results. Perry *et al.* [10] suggest that it is not possible to sustain a temperature gradient between the support and the metal, whereas Thomas [11] claims that it may be possible under ideal circumstances. Thomas also shows that the size of the metal crystallites is important for their heating properties. Clearly, this is an area where further work is needed.

1.4 Microwave transmission

To fully utilise microwaves, it is necessary to control the path of the radiation so that it may be applied wherever it is desired. It is also important to prevent uncontrolled emission of microwaves for safety reasons. Microwaves are generally constrained and transmitted in one of three ways: waveguides, parallel plates and coaxial cable.

Waveguides are hollow metal tubes that are used to provide a path for the conveyance of microwaves. Whilst they can be of any shape, it is common for them to be rectangular and have dimensions that allow standing waves to be formed. This allows very precise positioning of a sample within the microwave field. The microwave cavity can be tuned with a number of plungers which affect the internal waveguide shape to optimise the standing waves.

Parallel plates are simply two conducting plates that are placed parallel to each other. This can be thought of as similar to a rectangular wave guide with the sides removed. Whilst the microwaves can escape if the separation between the plates is large, if they are separated by less than a tenth of the plate's width or length, the loss is negligible.

Coaxial cables consist of a central conducting core, which is surrounded by an insulator and then a external conducting shield. The external cylyindrical conductor is always grounded and the core carries the signal. The main advantage of this system is the flexibility and small volume of the cables. Coaxial cables can therefore be used to transfer microwaves where space is at a premium.

All of these pieces of apparatus are designed to transfer microwaves with minimal

energy dispersion or loss. If microwave heating is desirable however, all of these systems can be used by placing a material with a high dielectric loss in the microwave path. For the coaxial and parallel plate systems this means placing the sample between the two conductors. For a waveguide, the sample must be placed inside the waveguide cavity.

1.5 Measuring temperature

The measurement of temperature under microwave heating is a difficult proposition. As microwaves heat materials differentially depending on their dielectric constant, the introduction of a temperature-measuring device that has a dielectric loss is unsatisfactory. A number of solutions to this problem have been proposed.

1.5.1 Atypical thermometers

A conventional thermometer works through conduction of heat. When a thermometer is brought into contact with a material that is of a different temperature, it will assume the temperature of that material as long as the volume of the material is much greater than that of the thermometer bulb. If the sample is too small, the temperature of the thermometer before it is introduced to the sample to measure can affect the sample's temperature. In other words, a cold thermometer can cool a hot sample, or a warm thermometer can raise the temperature of a cool sample, leading to incorrect temperature readings. The expansive liquid is commonly either mercury or alcohol, both of which couple with microwaves. If these are placed in a sample within a microwave field, they will not only give a measure of the temperature, but also that of the heating effect upon the expansive liquid within the thermometer. It is possible to use a thermometer where the expansive liquid used has a very low dielectric loss tangent such as xylene [2]. Measuring the pressure of a gas in a constant volume has also been demonstrated as a viable method [12]. The necessary volume of sample for these probes prevent them from being used in a small system. Their size will also cause them to demonstrate a time lag in reporting an accurate temperature and will report a temperature average over their contact with the samples, which may prevent identification of localised heating effects. Calibration of atypical thermometers is also

a non-trivial exercise.

1.5.2 Fluoroptic thermometers

All temperature probes rely on a property of a material that varies with temperature. Fluorescent decay has been shown to do this and temperature probes that use this phenomenon are commercially available. A fibre probe is used to illuminate a temperature sensitive phosphor that is attached to the end of the probe. This material fluoresces and the light is transmitted back along the probe to a detector. The time for this to occur is measured and compared with a calibration profile to obtain the temperature [2]. Whilst this method is commonly seen as the 'gold standard' [13] of temperature measurement in a microwave, it is not without drawbacks. The probes are not very durable and have a restricted maximum working temperature. It has also been shown that where an intense illumination source is present, temperature measurements may not be accurate [14].

1.5.3 Infrared emission

A hot body will try to lose energy by emitting radiation. The energy of the radiation that is emitted is a function of the temperature. For a perfect emitter, known as a black body, the relationship is given by the Stefan-Boltzmann law:

$$J^* = \sigma T^4 \tag{1.5}$$

Where J^* is the energy flux density, σ is the Stefan-Boltzmann constant and T is the thermodynamic temperature. For real (non-black-body) emitters, this is only an approximation, but instruments that measure the infrared emission of a sample can give a temperature reading. Optical measurements such as these have the advantage that the instrument does not have to be in contact with the sample. However, as it is only possible to observe radiation from the outside of samples, only the temperature of the surface can be measured. This temperature may not accurately represent the bulk temperature due to surface cooling, or the inverse temperature profile which microwave heating can establish. This method of temperature measurement is also obviously

incompatible with conventional transmission infrared spectroscopy measurements but may possibly be exploited in emission experiments.

1.5.4 Thermocouples

In 1821 the physicist Thomas Seebeck discovered that a potential difference existed between two ends of a metal bar, where a thermal gradient existed in the bar. A thermocouple exploits this effect and consists of two dissimilar metal wires, joined together by welding. A potential difference exists between these two wires which varies with temperature. Because of the thermocouples small size, fast response, flexibility, ruggedness and low cost they are probably the most favoured method of temperature measurement for both conventional and microwave heating. It is not possible to insert wires into a microwave cavity without interference to the microwave field and inducing currents in the wires. A partial solution to the problem is to use a sheathed thermocouple, where the two wires are enclosed within a metal cover. These can be obtained with diameters as small as 0.2 mm. If these are inserted into a cavity whereby the thermocouple is aligned with the direction of microwave travel, the interference will be reduced as the amount of material aligned with the electrical and magnetic field directions is minimised [15]. If a shielded thermocouple is introduced into the cavity in another orientation with the exterior attached to the cavity wall, and therefore grounded, the thermocouple will not be subject to induced currents. However, this will affect the shape of the cavity and and may lead to localised heating, or even arcing. For certain temperature ranges however, thermocouples are the only option.

1.5.5 Not measuring temperature

With the problems described in measuring temperature, and the likelihood of non-equilibrated systems it is worth briefly considering whether or not measuring the absolute temperature will lead to any advancement of theory. Although the activity of reactions is often quoted as a function of temperature, this is usually just an effective shorthand for other properties, such as the energy costs. Furthermore, as temperature can only ever be a bulk property, can it really be applied meaningfully to systems where a temperature differential may be sustained not only through space, but across

components which consist of only a few atoms? As such, although the idea of an absolute temperature for each component may be seductive, it is prudent to view such numbers sceptically. If it is possible to eliminate the measurement of temperature from the meaning of the experiment considered, the interpretation is considerably simplified. Roussy *et al.* have demonstrated this in their work on the isomerisation of C_6 hydrocarbons [16, 17]. By measuring the selectivity as a function of conversion, it is possible to ignore the concept of temperature, but to meaningfully compare the different actions of catalysts under microwave and conventional heating.

1.6 Microwave enhanced synthesis

Microwave heating has been applied to a wide range of reactions with a great degree of success, with the greatest interest in organic syntheses in solution [1, 18]. Due to the nature of microwave heating, in the absence of stirring, superheating of the solvent often occurs. This is a result of the fact that boiling requires nucleation centres for bubble formation. These are generally imperfections at surfaces, such as scratches on the container walls. Microwave dielectric heating allows the core of the solvent to be heated selectively, forming a superheated volume away from nucleation sites. Where the solvent is in contact with surfaces, it is relatively cool. By using readily available containers able to withstand moderate pressures, temperatures of 50-100 K above the standard reflux temperature can be readily achieved [19], although care is needed when handling superheated materials [20]. Whilst in the past arguments have been made for a specific 'microwave effect', this has largely been discounted for liquid-phase reactions as most of the acceleration of reactions can be explained by this superheating effect [21]. It is important to remember that the energy of a microwave photon is far too small to directly break bonds. Whereas ultraviolet light is energetic enough to eject valence electrons from metals, the energy of a microwave photon is approximately 100,000 times smaller. This means that consideration of the methods by which microwave radiation increases reaction rates (if indeed it does) should be restricted to low energy phenomenon.

Reactions involving the heating of solids have also been performed. Microwave

heating was found to be beneficial in the synthesis and processing of ceramics [22]. Solid state reactions have been carried out using microwaves, including the synthesis of metal chalcogenides [23], superconductors [24], sulfides and selenides [25].There has also been some interest in organic reactions on dry media [26]. The precursors are introduced to the support as a concentrated solution before the support is heated using microwaves. The product is then washed off with solvent. This approach significantly decreases the volume of solvents needed and has implications for environmentally friendly synthesis. Finally, there are reports of catalysts being heated using microwaves. These generally show reactions occurring at apparently lower temperature and there are reports of changes in selectivity [15, 27]. Explanations offered for these effects are electrical discharge [28] and uneven heating [29]. Reports have also been published which suggest that catalysts synthesised using microwaves [30, 31] or heated with microwaves [15, 32, 33] have different reactivities when subsequently heated by conventional means.

Chapter 2

Microwave catalysis

2.1 Introduction

Since the earliest days of chemistry, people have striven to achieve chemical transformations to create beneficial products. As the routes have become better characterised, the aims have been to complete the reactions cheaper, faster, with less waste and with a higher purity product. In the practical application of chemistry, catalysis allows these goals to be achieved. It is important to stress that improvements to the efficiency of a catalyst can produce great benefits, and room for improvements is ample. Microwave heating is such an opportunity to improve catalysis. A catalyst is classically defined as a material which changes the rate of a chemical reaction, without being itself consumed.

Catalysis is a purely kinetic phenomenon and cannot alter the equilibrium of a reaction, only the rate at which it is reached. Catalysts work by providing an alternative 'reaction pathway', which allows the reaction to occur *via* an intermediate state of lower energy. Having a lower energy intermediate state means that a greater proportion of the reacting species will have the necessary energy to react. An illustration of how a catalyst works may be seen in Figure 2.1. Using the same type of schematic plot can aid understanding of the more complex catalytic systems that are of interest to study.

For a reaction to occur there is an energy barrier which must first be overcome. This energy is required to bring the reacting molecules into close enough proximity with each other and break the existing chemical bonds. The formation of the new chemical bonds then gives out energy. The action of a catalyst can be visualised if a transitional state is

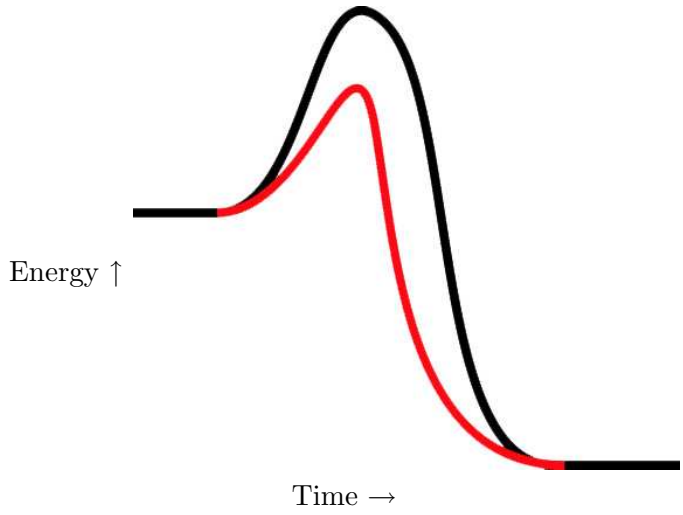

Figure 2.1: Reaction profile for uncatalysed (black) and catalysed (red) reactions

imagined. With an uncatalysed reaction the transition state is formed spontaneously. A catalyst provides an alternative transition state where the activation energy of the reaction is reduced. A simple example of this is the oxidation of hydrogen on platinum. When oxygen and hydrogen adsorb onto the platinum metal surface, they dissociate into their component atoms. The reaction between the adsorbed atoms has a lower activation energy than the free gases and so proceeds faster. The uncatalysed reaction takes the form:

$$2H_2 + O_2 \quad \Rightarrow \quad 2H_2O \tag{2.1}$$

whereas the catalysed reaction can be written:

$$\begin{aligned} H_2 + O_2 + Pt \quad &\rightleftharpoons \quad 2H\text{—}Pt + 2O\text{—}Pt \\ 2H\text{—}Pt + 2O\text{—}Pt \quad &\Rightarrow \quad H_2O + O\text{—}Pt \end{aligned} \tag{2.2}$$

This is represented in the generalised reaction profile shown in Figure 2.2, where ‘a’ is the energy of the adsorbed reactants and ‘b’ is the energy of the adsorbed products. The transition state between these two points (the highest point on the curve) is lower in energy than for the uncatalysed pathway. The figure also shows that the total energy gained from the reaction is identical although the catalytic pathway requires less energy

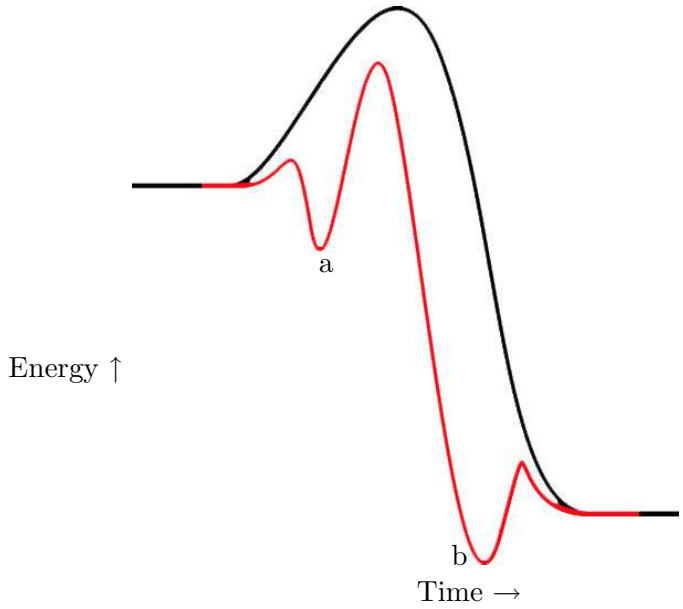

Figure 2.2: Uncatalysed (black) and catalysed (red) reaction profiles for the oxidation of hydrogen

to reach the transition states. The diagram further illustrates that adsorption is an exothermic process with a relatively small activation energy, hence energy is required to desorb the products after the reaction.

The field of catalysis is fundamentally subdivided into two disciplines. Homogeneous catalysis is concerned with catalysts which have the same phase as the reactants. Whilst strictly this involves all phases, by far the greatest area is solution phase chemistry. The catalytic properties of dissolved single metal ions can be manipulated by careful control of the ligands which surround them. This allows for a great range of control over the reactions which occur, but due to the necessity of complex ligands and the difficulty of separating the product from the catalyst, this approach is only feasible for small quantities of high value chemicals. Heterogeneous catalysis focusses on gas or liquid reactions over a solid catalyst. This approach is much more amenable to large scale industrial operations. The catalyst may be held in a bed and the reacting fluid washed through or over it, vastly simplifying the production of a pure product and minimising catalyst losses. Whilst it is not possible to control the reaction as closely as in homogeneous reactions, the financial savings from these catalysts make them the

preferred choice. Heterogeneous catalysts are often metals, either supported on an inert material to maximise the metal surface area, or simply as metal or alloy particles.

2.1.1 The application of microwaves

The phenomenon of microwave heating was first used as a method of heating a reaction in 1986 [1]. The process was rapidly applied to catalysis, and the first report of altered selectivity came in 1989 from Thiebault *et al.* in the transformation of 2-methylpentane [34]. Further reports of different selectivity for the conversion of small organic molecules followed later [15, 32]. Since this time, microwave heating of catalysts has been applied to a number of systems. In the automotive area, microwave heating has been investigated to decrease the cold start problems of three-way catalysts [35], and the catalytic combustion of diesel soot on particulate traps [36]. Synthesis of zeolite catalysts using microwaves has resulted in materials that have different rates and selectivities than those synthesised conventionally [30]. Further studies have been carried out for the oxidative coupling of methane [37, 38, 39], the oxidation of carbon monoxide and hydrocarbons, the reduction of SO_2 and NO_x [40], alkane isomerisation [15, 32] and environmental catalysis [41, 42].

2.2 Proposed mechanisms

There are three main theories that have been proposed for the different activity of catalysts under microwave heating. Firstly there is the idea that the catalyst is modified in some way by the microwave radiation. By a change in the catalyst morphology, a change in the activity or selectivity is easily explained. Studies [15, 32] have shown that catalysts heated under microwaves show a higher activity than those under conventional heating. However, when those catalysts heated under microwaves are subsequently heated conventionally, they retain their enhanced activity. Catalysts produced using microwaves are also reported to show different rates and selectivities [30], with Zhang *et al* recently reporting changes in the catalyst microstructure [33] as a possible cause. However, reports in the literature of the characterisation of catalysts subjected to microwave heating are surprisingly limited.

The second theory is that of an electrical discharge [28, 43]. An electrical discharge is essentially a short-lived plasma. When a high enough potential difference is placed across a gas, it may cause electrical breakdown if the field is high enough to pull electrons out of their orbits. Once enough current has flowed to establish neutral charge, the plasma subsides. Reactions proceeding in a plasma have more energy and are more likely to produce the kinetically favoured product rather than the most thermodynamically stable.

Uneven heating is the third mechanism suggested, and can be divided into two types; selective heating of the metal, and regioselective heating leading to "hot spots". This could lead to different product distributions purely through running the reaction at a higher temperature, but quenching will also become a factor. At a constant high temperature, the thermodynamically favoured products are produced, whereas if the reaction is quenched, the kinetically favoured products will dominate. Where there are reactive regions adjacent to cooler areas, it is conceivable that quenching will occur as the reactants move into a realm of lower temperature. A common method of controlling microwave power is to pulse the source on and off, and it has been suggested that systems using this method will encourage differential heating [44]. This could cause reaction quenching, even if differential heating is not occurring, and thus lead to a different distribution of products. The second mechanism that may lead to quenching has been proposed by Bond *et al.* [29]. They suggest that the microwaves create localised "hot-spots" which are small and mobile, causing characterisation problems. It has been shown that the transition from gamma to alpha alumina has occured in catalysts at measured temperatures 200 K below the literature transition point [45, 46].

It should be pointed out at this stage that all the mechanisms proposed would suggest routes for different activity and selectivity. However, the proposal that the change in morphology causes the enhanced catalytic properties suggests that the measurement of temperature under microwave heating is adequate. As the material shows enhanced activity at reduced temperature whether heated under conventional or microwave regimes, the bulk temperature measured under microwave heating is representative of the entire sample. This is not true of the hot-spot or discharge theories, which rely on the postulation of active sites that are not typical of the bulk and have

a very strong influence on the overall properties of the material.

2.3 Microwave heated catalytic reactions

2.3.1 Alkane isomerisation

The manipulation of hydrocarbons is of great commercial importance for fuels, polymers and as a starting point for production of many industrial chemicals. Should the enhancement of these reactions with microwaves prove possible, vast amounts of energy could be saved. Garin *et al.* [15] have shown a permanent change in the catalytic properties of a platinum/alumina catalyst when heated with microwaves. The isomerisation of 2-methylpentane over their catalyst is markedly more selective when the reaction is heated with microwaves, yet this altered selectivity is retained when the catalyst is subsequently heated conventionally. Roussy *et al.* [32] report a similar effect, with a permanent change in the selectivity for the same reaction over EUROPT-3. However, neither group appears to have characterised the catalysts to any great extent. A wide range of studies involving alkane isomerisation over platinum/alumina catalysts under conventional heating is present in the literature. Of greatest interest in this study is the isomerisation of C_6 hydrocarbons, to allow comparison with the microwave studies. The hydrogenolysis of methylcyclopentane [47, 48, 49] and the isomerisation of 2-methylpentane [48, 50] have both been studied over various Pt/Al_2O_3 catalysts.

2.3.2 Oxidative coupling of methane

The Oxidative Coupling of Methane (OCM) is of great commercial interest as it may provide a route to long chain hydrocarbons from natural gas deposits. As oil reserves dwindle, a source of higher hydrocarbons by this method becomes both more desirable and financially viable. As a result, this is the area of most research in microwave assisted heterogeneous gas phase catalysis. For the reaction to occur, methane is heated with oxygen and a catalyst. The desired reaction is:

$$2CH_4 \Rightarrow C_2H_6 \Rightarrow C_2H_4 \tag{2.3}$$

However, this reaction is problematic, as the products are unstable under conventional reaction conditions and may undergo further oxidation to CO or CO_2. Conventional heating of this reaction typically results in 10–15% methane conversion with 80–85% selectivity for C_2 hydrocarbons [51]. The first report of the application of microwave heating to this reaction was in a review by Bond *et al.* [52] using a sodium aluminate catalyst. Whilst similar selectivities were seen, similar conversions were obtained at observed temperatures that were 400 K lower when under microwave irradiation. This led to the hypothesis that localised 'hot spots' were present. Experiments by Roussy *et al.* [37] found that over a $(SmLiO_2)_{0.8}(CaOMgO)_{0.2}$ catalyst C_2 selectivities of 100% were obtainable under microwave heating. They found that under microwave irradiation the selectivity to C_2 products was 100% at low conversions, but decreased with methane conversion. This was the opposite to what was observed under conventional heating, where selectivity was 0% at low conversion, and increased with greater conversion. Further work by Roussy's group [38] using Li/MgO and $BaBiO_{3-x}$ catalysts showed different results, which are attributed to dissimilar mechanisms. It is claimed that the greater selectivity is due to quenching of the reacting gas, as the microwave system allows more focussed heating of the solid catalyst sample.

2.3.3 Environmental catalysis

Environmental catalysis is an ill-defined term that is generally used to refer to catalysis when applied to reduction or elimination of noxious emissions. This discussion will be restricted to the destruction of unwanted waste gases, such as those formed from combustion or industrial processes. The destruction of volatile and harmful solvents has been demonstrated in a pilot system by the CHA corporation [41]. The output from a fume hood was passed through a mixture of activated carbon and zeolite to absorb airborne pollutants. When the adsorbant mixture is saturated it is heated with microwaves to desorb the volatile solvents, which are then passed through a microwave heated catalytic reactor containing Pd and Pt to form CO_2, H_2O and HCl. The HCl can be removed by a separate system and the CO_2 and H_2O vented to the atmosphere. The decomposition of trichloroethylene over Co/γ-Al_2O_3 and Ni/γ-Al_2O_3 catalysts has also been reported [53].

Automotive three-way catalysis

Whilst the control of solvent vapours is of considerable interest, the pollution caused by the combustion of fossil fuels is of much greater concern. The three way catalyst in vehicle exhaust systems is designed to remove the most harmful components emitted from internal combustion engines and involves the following reactions:

$$\begin{aligned} 2C_xH_y + (2x+y)O_2 &\Rightarrow (2x)CO_2 + y/2\, H_2O \\ 2NO_x + (2x)CO &\Rightarrow N_2 + (2x)CO_2 \\ 2CO + O_2 &\Rightarrow 2CO_2 \end{aligned} \tag{2.4}$$

Automotive catalysts are involved in a complex interplay between these and other reactions under a wide array of conditions and thus contain a veritable cocktail of catalytic metals. A current state of the art catalyst reported by Turner *et al.* [54] contains ten catalytic compounds. Present automotive catalysts are by no means perfect, with their two greatest weaknesses being the cold start problem and their susceptibility to poisoning. Automotive catalysts are not active at ambient temperatures, and only become effective after being heated by the hot exhaust gas from the engine. Microwave heating of the catalyst to reduce emissions immediately after starting the engine has recently been shown to be highly effective, [55] and conversions at abnormally low measured temperatures has been observed [35]. Microwaves have also been reported to reverse the poisoning of the catalyst caused by SO_2 [54].

Reduction of nitrogen oxides

The oxides of nitrogen or NO_x, as they are collectively known, are formed when fuels are burnt and are a sizeable pollution problem. They are also produced naturally from volcanic activity, biological decay and lightning strikes. NO_x contributes to acid rain, smog, eutrophication of water and the formation of toxic compounds in the atmosphere. Reduction of NO_x has been investigated by Wan [40] using copper and nickel catalysts, and Garin *et al.* [56] have worked with a Pt/Al_2O_3 catalyst that showed differences in activity under microwave heating. The direct decomposition has also been carried out over metal-doped zeolites by Zhang [57] and Park [58], both showing novel results.

Reduction of NO with CH_4 under the influence of microwaves has also been studied by Zhang [59]. The reaction occurred at a lower observed temperature over doped zeolite catalysts when heated with microwaves. The control of nitrogen emissions using microwave-generated plasmas in the absence of a catalyst has also been investigated and was the subject of a paper by Wójtowicz *et al.* [60].

Carbon monoxide oxidation

The study of the oxidation of carbon monoxide as a separate oxidation has received little attention, with the work of Perry *et al.* [6, 10, 61] being the sole exception. The research concerns γ-alumina supported Pt and Pd catalysts under conventional and microwave heating. It was concluded that the reaction did not gain any increased activity when under microwave irradiation. A detailed analysis is given of the problems associated with temperature measurement in a microwave field, and it is postulated that any perceived temperature difference between microwave and conventional heating can be assigned to a poor measurement regime. As such they conclude that the metal particles have the same temperature as that of the alumina support. As well as the removal of pollution from vehicle exhausts, the oxidation of CO is important for other applications, such as the purification of gas streams [62] and regeneration of closed-cycle CO_2 lasers [63].

2.4 Aim

The unclear mechanism of catalyst activation under microwave heating is not a subject that has been extensively studied. A great number of the traditional methods for study of these reactions have yet to be applied for the microwave heating regime. Thus the aim of this work was to apply one of the most important investigative tools in the catalytic chemists arsenal to the microwave heating of gas-solid phase catalysis: To develop and test a system that allows interrogation of catalyst samples by infrared spectroscopy under reaction conditions when heated by microwave radiation.

Chapter 3

Infrared spectroscopy

3.1 Introduction

Infra Red (IR) spectroscopy works by measuring the interaction of materials with light of wavelength between about 700 nm and 1 mm (14000-10 cm^{-1}). This is commonly subdivided into three regions; near-, mid- and far-infrared, named for their relation to the visible spectrum. Whilst the boundaries between these regions are not well defined, mid-IR is commonly measured between 4000 and 400 cm^{-1}, with near-IR at higher wavenumber than 4000 cm^{-1}, and far-IR lower than 400 cm^{-1}. The energy of the radiation varies with frequency, thus each region is best suited for the analysis of certain phenomena. The low energy of the far-infrared region is suited to the analysis of the rotational structure of gases, mid-IR is most useful in the study of fundamental molecular vibrations, whilst near-IR can excite vibrational overtones.

Molecular vibrations are quantised and so will absorb or emit energy only in discrete packets. Most of these vibrational transitions have energies which correspond to the energy of light in the mid-infrared region, and so when a sample is illuminated with infrared light, it may excite particular vibrational modes. As the vibrational frequencies of these modes depend on the bonds and atoms involved, it is often possible to relate the absorbed wavelengths with the vibration of a specific bond, and thus molecular form. Similarly, if a substance has an excited vibrational state, decay to a lower energy state will be associated with the emission of radiation. During most forms of infrared spectroscopy, a sample is illuminated with an infrared source which emits

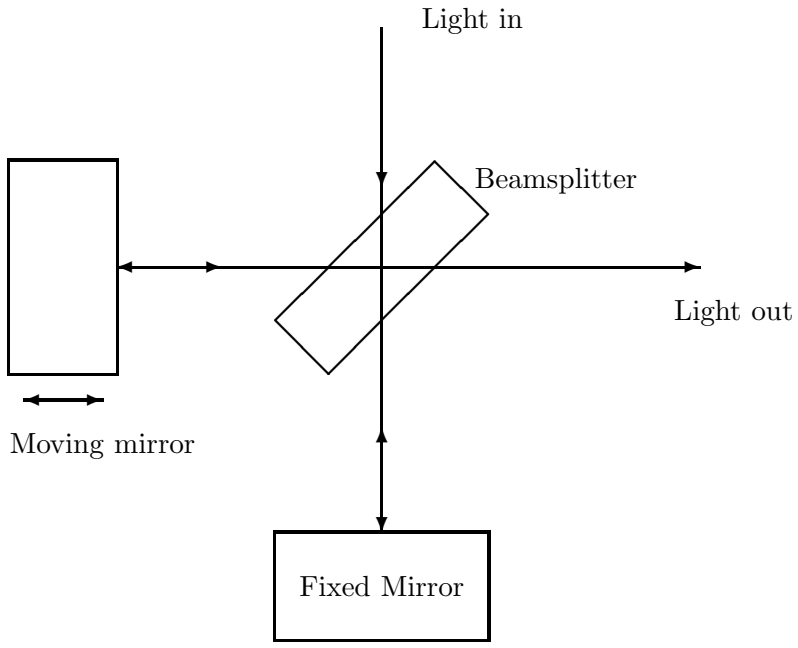

Figure 3.1: The Michelson interferometer

radiation over a wide wavelength range. The light is detected after interaction with the sample, and the wavelengths absorbed can then be related to the molecules present. Emission spectroscopy varies in that the sample is excited by other means such as heat conduction, and the spontaneous emission of infrared light is then detected.

3.2 Fourier transform spectrometry

The central part of a Fourier Transform (FT) spectrometer is an interferometer, which is a piece of apparatus that splits and recombines a beam of radiation to allow analysis of the beam. In a simple form, displayed in Figure 3.1 it consists of a beamsplitter, which transmits and reflects equal portions of the radiation, and two planar mirrors aligned perpendicularly to each other. One mirror is held in a fixed position, whilst the other can be moved to vary the path length the radiation travels. The difference in path length between the two beams is known as the retardation and is equal to double the difference between the distances of the two mirrors from the beamsplitter. When the two mirrors are equidistant from the beamsplitter (zero retardation), the

radiation will take the same amount of time to travel along each path, and will thus be in phase when the two beams are recombined. However, if the moving mirror is displaced by a distance equivalent to a quarter of the wavelength of the incoming radiation (one half-wavelength retardation), the beams will recombine completely antiphase and destructively interfere, resulting in no emitted signal. Retarding the moving mirror by another half wavelength will result in the path difference being one complete wavelength, so that the recombined beams will again be in phase and interfere constructively. If the intensity of the light emitted after the recombination of both beams is plotted against the retardation of the mirror, a plot known as an interferogram is produced. For a monochromatic beam and an ideal interferometer, this is a cosine wave with maxima at each integer wavelength retardation value, and a frequency related to the wavelength of the input radiation and the speed at which the moving mirror is translated. Using this interferogram it is impossible to distinguish the maxima and thus one cannot identify the point at which the two mirrors are equidistant from the beamsplitter.

If the light entering the interferometer is of more than one wavelength, the interferogram will be considerably more complex. At zero retardation, all wavelengths will constructively interfere and the intensity of the light emitted will be high. As the mirror is moved from this point, each separate wavelength will vary cosinusoidally with retardation, but at a different rate. Whilst this can lead to simple repetitive interferograms in cases where only a small number of frequencies are present, if a large number of frequencies are present, the interferogram will have a central intensity maximum at zero retardation. The central burst of intensity will decrease with increasing retardation, as shown by the typical interferogram displayed in Figure 3.2.

Commercially available spectrometers are normally operated in a 'rapid scanning' mode. The moving mirror is translated at constant velocity with its position being monitored by use of a helium-neon laser. The laser is aligned with the IR beam such that it follows a similar path, and encounters the same optics. As it is a monochromatic light source, the interference pattern caused by the laser varies as a cosine function. With the wavelength of the He-Ne laser known, it is possible to follow the displacement of the mirror as constructive interference will occur whenever the retardation is divisible

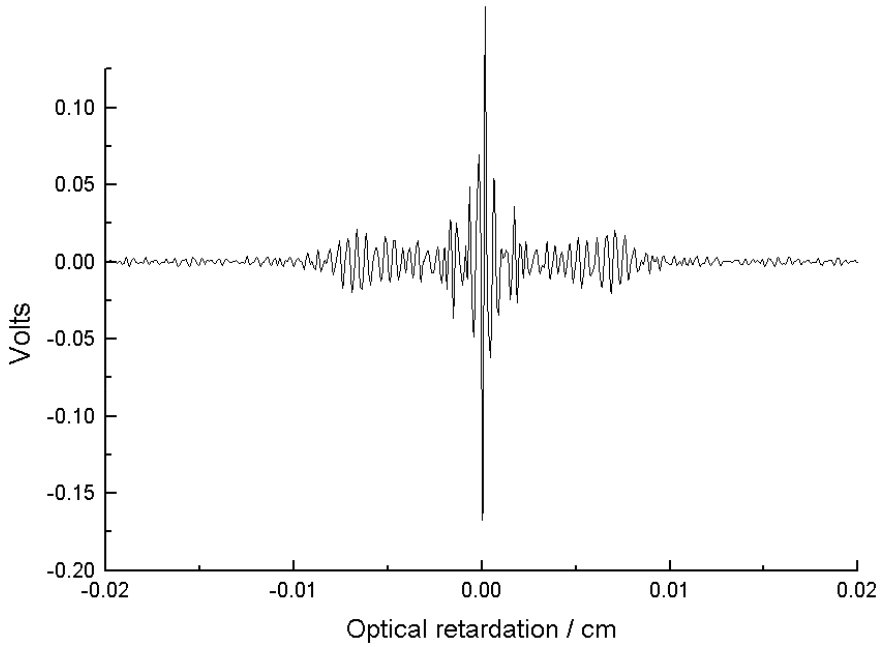

Figure 3.2: A typical interferogram

by one laser wavelength, or 632.8 nm. When a scan begins a trigger initiates counting of the number of maxima in the laser signal to monitor the speed and thus relative position of the mirror. This method of 'fringe counting' allows an accurate measurement of the relative mirror position to be made when collecting the interferogram.

Once the interferogram is collected it is manipulated to give a 'single beam' spectrum by using a Fourier transform. Any waveform can be expressed as the sum of an arbitrary number of sine and cosine waves of different frequencies and magnitudes. The Fourier transform is a mathematical procedure that can resolve, or separate the contribution of these component waves to the interferogram. Thus a spectrum is produced, which is a plot of the intensity of the infrared light detected against frequency.

3.3 Optics

When a light beam encounters a surface, various interactions may occur (Figure 3.3). The beam can be transmitted without attenuation (a), reflected (b), partially transmitted (c) or scattered (d). Whilst all infrared experiments involve a light source, a sample and a detector, a number of techniques exist to deliver and collect the light

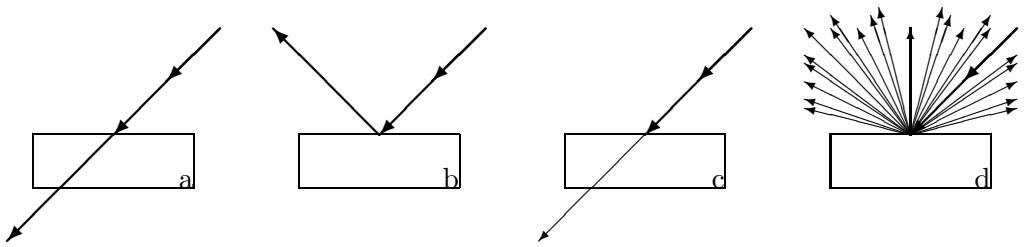

Figure 3.3: Interactions of light with matter

from the sample in a manner suitable to the sample type.

3.3.1 Transmission

The simplest form of IR spectroscopy is transmission. A sample is pressed into a disc and supported in the infrared beam incident on the detector after interaction with the interferometer. The transmitted light detected shows a loss of intensity where vibrating species have absorbed the light. Transmission IR spectroscopy is a technique that has the benefit of simplicity, but is not ideal for the *in-situ* study of the interaction of gases with a solid catalyst. When a catalyst sample is pressed into a disc, this may adversely affect the porosity of the catalyst, depending on the pressing conditions. This restricts the ability of the reacting gases to freely diffuse into the catalyst and access the active metal sites. Another significant problem with transmission studies is the thickness of the adsorbed gas layer. Gas adsorbs on the catalyst surface to the depth of a few molecules, which is many orders of magnitude smaller than the depth of the gas around the sample, and the thickness of the disc itself. As a result, the infrared absorption due to gas phase and bulk catalyst species can be much stronger than those from the species of interest.

3.3.2 Diffuse reflectance

A slightly more complicated method is Diffuse Reflectance Spectroscopy (DRS). The aim of this method is to collect the light that is scattered when interacting with a powdered solid. As the light coming from the sample is distributed across a range of angles, it is also known as diffuse reflectance. The sample is surrounded by elliptical mirrors that are used to illuminate the sample and collect the scattered radiation. Most

of the light beam is reflected so the angle between the reflected beam and the sample is equal to the angle between the incident beam and the sample. Light which is reflected in this manner, as would happen with a mirror, is known as specular reflection and is likely to have interacted little with the sample. The light which is diffusely reflected will exit in every direction and will have transfered energy to the sample. The key to DRS is to maximise the non-specular signal with respect to the specular and thus select the light which has strongly interacted with the sample being studied. The drawback to this technique is that the the ratio of the non-specular reflection to the incident beam is very low, and so a highly sensitive spectrometer must be used. A Fourier Transform (FT) spectrometer is ideal for this and when such a spectrometer is used, the technique may be known as Diffuse Reflectance Infrared Fourier Transform Spectroscopy or DRIFTS. Although the collection of DRIFTS spectra requires careful alignment of mirrors and a highly sensitive spectrometer, it does have one significant advantage. The sample does not need to support itself, so the use of powders is possible. Using a powder sample allows gas to freely diffuse around the material and provides a greater surface area for interaction with gases. Using a sample with as little processing as possible not only decreases the likelihood of the introduction of artefacts due to that processing, but can also save considerable amounts of time.

3.3.3 Emission

As the optics of a spectrometer are designed to efficiently transmit infrared radiation from the source to the detector, it is obvious that to measure the emission from a hot source, one simply needs to replace the source with the sample. However, as the geometry and size of the sample is rarely conducive to this, it is possible to disable the source, and use an alternative beam path. External optics are usually used to collect the radiation from a heated sample, which is then fed to the interferometer in lieu of the radiation from the usual source. The resulting interferogram is then Fourier transformed to give the emission spectrum of the sample.

3.4 Data manipulation

The single beam sprectum obtained from the Fourier transform of the interferogram shows a characteristic shape which depends on the character of the infrared source and detector used in the experiment. For the transmission and DRIFTS experiments, there would ideally be a constant intensity across the entire spectral range being studied. For emission spectroscopy, where the sample acts as the source of radiation detected, it would be best if the sample only emitted through the decay of the vibrations and rotations being studied. In both cases, this is far from what actually occurs and the intensity of emission from the source varies with wavelength in a similar manner to a black body. A black body is a theoretical object that absorbs all the radiation that falls on it, with no energy transmitted or reflected. A black body will also emit radiation dependent on its temperature according to Planck's law:

$$I(\nu) = \frac{2h\nu^3}{c^2} \frac{1}{e^{h\nu/kT} - 1} \tag{3.1}$$

Where I is energy, ν is frequency, h is Planck's constant, c is the speed of light, k is Boltzmann's constant and T is temperature. Figure 3.4 shows simulated black body spectra for 308, 600, 800 and 1500 K which demonstrate a shift in frequency for the emission maximum and an overall intensity increase at higher temperature. A typical infrared spectrometer source is an approximate black body maintained at a temperature between about 1200 and 1700 K that will therefore provide illumination across a broad range of the IR spectrum. The choice of detector may sacrifice the range across which it works in favour of enhanced sensitivity over a specific region of interest. Figure 3.5 shows a number of spectra including simulated black bodies at 308 and 1500 K, with an emission spectrum recorded at 308 K and transmission and DRIFTS spectra at similar temperatures. The spectra are independently scaled for clarity. It can be seen that the interplay of the source and detector produce spectra which display a response that is not consistant across the spectral range. It is therefore greatly beneficial if the spectrometer may negate these effects to give a uniform response and provide spectra that do not depend on the properties of the instrument. Traditional dispersive instruments commonly analyse the difference between two beams collected

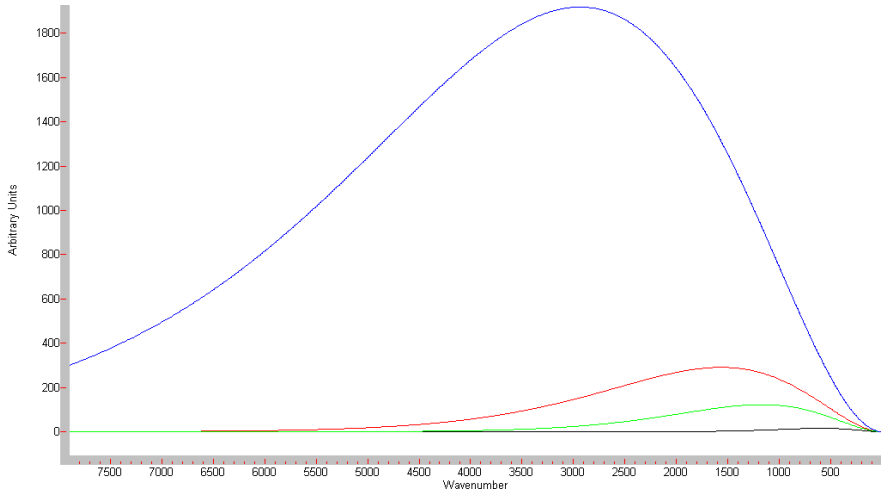

Figure 3.4: Simulated black body spectra at 308, (black) 600, (green) 800 (red) and 1500 K (blue)

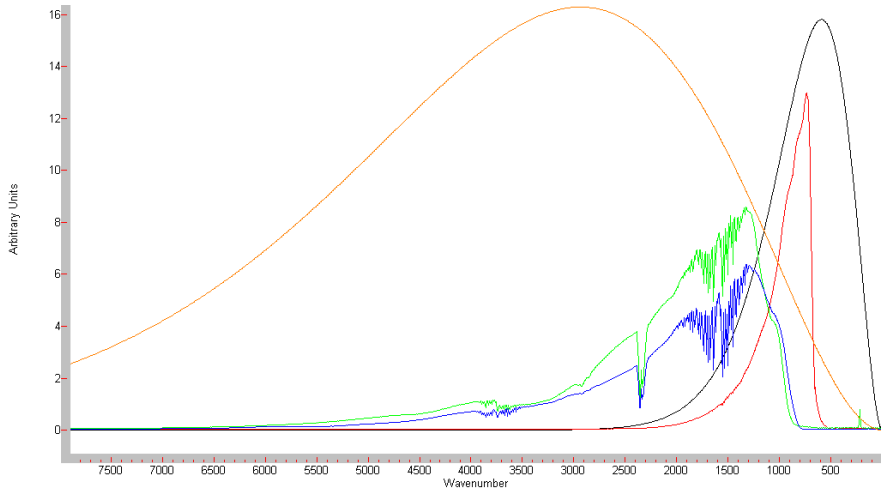

Figure 3.5: Simulated black body spectra at 308 (black) and 1500 K (orange) with emission, (red) transmission (blue) and DRIFTS (green) spectra

simultaneously, one interacting with the sample, and one used as a reference, to give a plot of % transmittance. This method produces a spectrum which shows only the features of the sample as the idiosyncracies shown by the source and detector are common to both beams and hence cancel upon ratioing them together. Also, as the two beams are collected at the same time under virtually identical conditions, temporal fluctuations in the environment within the spectrometer are largely eliminated.

Using a second beam with a different path as an internal reference is an uncommon approach with an FTIR instrument, due to the increased complxity that would be required of the optics. Instead, a single beam spectrum is initially obtained as a background and sample spectra are subsequently acquired and manipulated post collection. Transmission spectra obtained in this way are conventionally plotted as absorbance, which shows positive peaks where a vibration becomes excited by absorbing the light. The absorbance is calculated using:

$$A = -\log_{10}\left(\frac{I}{I_0}\right) \tag{3.2}$$

Where A is absorbance, I_0 is the intensity recorded for the background, and I is the intensity in the sample scan. Whilst this method of subsequent scans is vulnerable to temporal changes after collection of the background spectrum, maintenance of a stable purge atmosphere within a closed spectrometer system can minimise this. Advantages of this technique are greater flexibility in signal processing after collection and a greater ease in obtaining a suitable background. In systems which involve minor spectral changes it is necessary to have a good quality background spectrum to prevent artefacts from background miscancellation obscuring the species of interest. To observe differences in the adsorbed gases on supported metal catalysts under reaction conditions, minimising the signal from gas phase species and the support is of paramount importance. Preparation of two identical catalyst samples and maintenance of identical conditions to ensure a stable baseline before the initiation of an experiment would be necessary in an instrument using two beams. Collection of both spectra using an identical beam path through the same physical sample eliminates this problem.

The DRIFTS and emission techniques described above both suffer from additional

problems when trying to obtain a reasonable background spectrum in systems like heterogeneous gas phase catalysis which require extreme finesse to observe such dimunitive contrasts. The usual interpretation of DRIFTS results involves the use of the Kubelka-Munk theory, which allows quantification of the relationship between the IR absorption and the species absorbing. This involves the measurement of a non-absorbing powder reference material such as KBr and has been shown not to be effective for compounds with an absorbing matrix, such as silica or alumina, present [64]. Introduction of any non-essential variance between the measurement of the background and sample spectra may cause spurious features to obscure the legitimate results. The spectra obtained through DRIFTS were therefore treated in the same manner as those recorded in the transmission paradigm to maximise the visibility of minor changes, whilst maintaining as similar a background as possible.

The quantification of emission spectra conventionally involves the use of an approximate black body for the background [65]. This results in features that are not of interest appearing in the results, due to deviations in the apparatus and sample from the black-body model. In this work therefore, the data was manipulated as for the other samples on an absorbance scale. Although this choice prevents proper quantification of the results, it greatly improves the sensitivity of the spectrum to the desired response and allows a qualitative interpretation that might not otherwise have been possible.

Chapter 4

Cell Design

4.1 Introduction

Infrared spectroscopy is a powerful tool for following the course of a reaction. In many cases it has been possible to devise reaction cells which allow investigation of the reacting species *in-situ* [66, 67, 68]. As the study of microwave enhanced chemistry is a relatively young field, there are no previous reports of microwave-heated reaction cells which allow infrared spectroscopy.

4.2 Transmission cell construction

The basic design of the transmission cell is of a ceramic sample holder between brass parallel plates. An exploded view of the working transmission cell is shown in Figure 4.1 with letters denoting parts. Each applicator plate (a,b) is constructed from two pieces of brass. These are held together by countersunk screws and surround a 13 mm diameter CaF_2 window of 2 mm thickness. The window has a gas tight seal which is a circular gasket of rectangular cross-section, cut from a 0.75 mm thick sheet of Kalrez® compound 4079. The window is covered by a nickel mesh (40 × 40 mesh, 0.13 mm wire diameter), obtained from Strem, that attenuates the infrared signal by about 40%. This is held in place by a brass washer that is wedged into the plate. The thicker half of each applicator plate has a hole drilled to accept a 1/8 inch cartridge heater (c) for conventional heating. The grounded applicator plate (a) has a 1 mm diameter shielded

a: Ground applicator plate
b: Live applicator plate
c: Cartridge heater
d: Thermocouple
e: Sample holder
f: Mounting bracket
g: Clamping plate
h: Clamping plate
i: O-rings
j: Coaxial cable

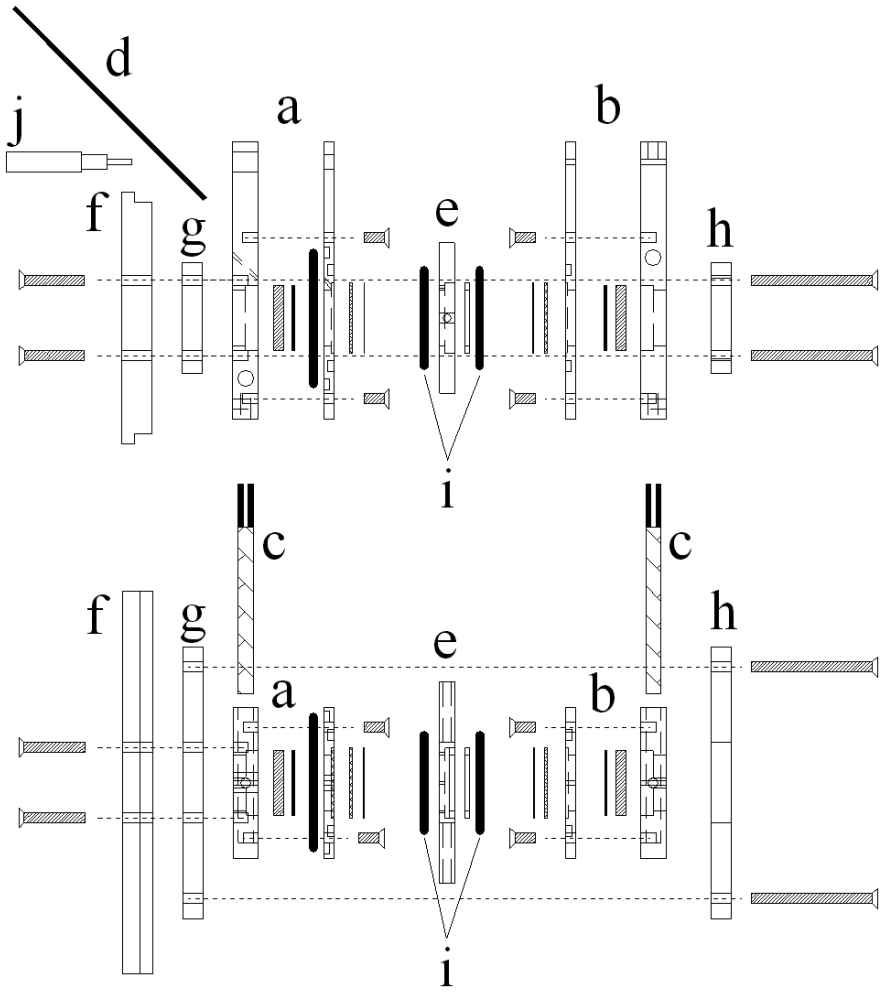

Figure 4.1: Exploded view of transmission cell

k-type thermocouple (d) from Thermocoax running through the plate at angle of 45 degrees. This protrudes from the inner face by about 1.5 mm and is silver-soldered onto the outer face. An extra o-ring between the two pieces of the applicator plate is used to ensure the cell is gas-tight. The central sample holder (e) is manufactured from a 3 mm thick Macor® plate with a central hole for the passage of the infrared beam. A step supports the catalyst disc, with a notch cut out to accept the thermocouple. 1/16 inch holes were drilled from the edges to the center cavity to act as gas guides. Stainless steel pipes of 1/16 inch external diameter were inserted into these and secured using high temperature silicone sealant. A brass mounting bracket (f) designed for a conventional infrared cell mount is attached to the ground plate, as is a stainless steel plate with threaded holes (g) to allow a clamping plate (h) to compress the assembly. The ceramic sample holder seals against the metal applicator plates through Kalrez® (compound 6221) o-rings (i) held in grooves in the applicator plates. The clamping plate is insulated from the signal applicator by a mica sheet. Power is supplied to the cell by a coaxial cable (j) which is soldered to the ground plate, with the central pin fixed in the other plate through a grub screw. The excess energy is dumped to a resistor bank which is connected to the applicator plates by grub screws. A photograph of the assembled cell can be seen in Figure 4.2.

4.2.1 Modification for liquid experiments

The transmission cell was adapted to allow experiments in the liquid phase to be carried out as a proof of concept. A ceramic sample holder had a solvent reservoir attached to its upper gas-guide connection, and a filling tube to the lower connection. This is shown in Figure 4.3 and allowed filling of the sample cavity with a liquid to be investigated. To prevent excessive IR absorption by the solvents used, a CaF_2 window was also placed in the sample cavity to lower the path length of the solvent.

4.3 DRIFTS cell construction

The construction of the diffuse reflectance cell followed a similar pattern to the transmission cell, although various improvements suggested through use of the transmission

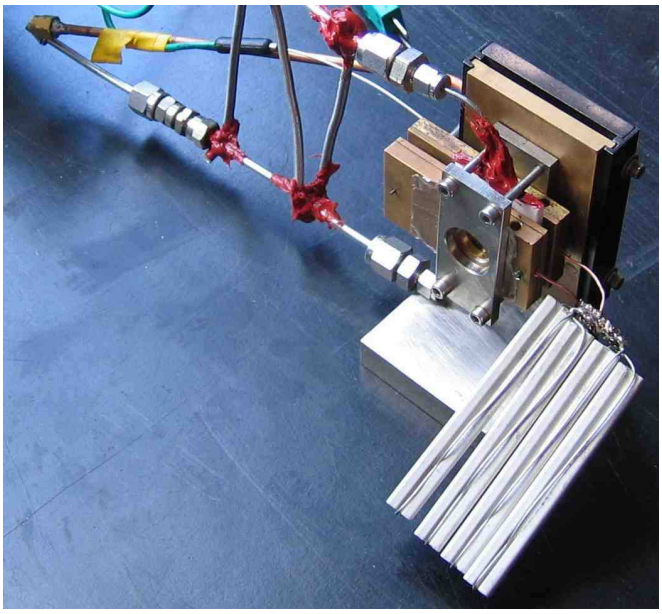

Figure 4.2: Photograph of assembled transmission cell

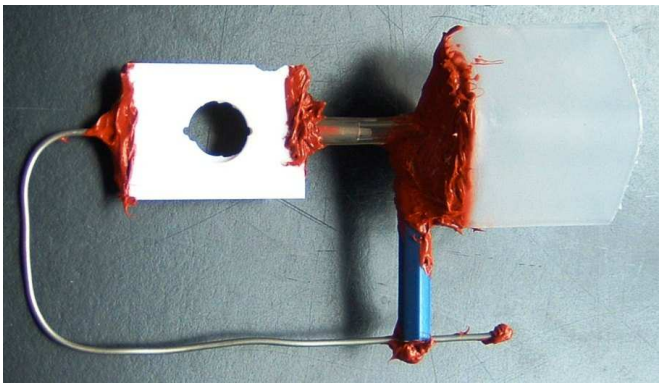

Figure 4.3: Modified sample holder for liquid experiments

Figure 4.4: Catalyst disc showing uneven discolouration

cell were incorporated:

- Screw heads on inner plate face removed
- O-ring grooves on inner plate face removed
- Gauze spot-welded into position
- Fragile joints between sample holder and gas connections eliminated
- Constructed of stainless steel for greater mechanical strength

The first three improvements dealt with deviations from flatness in the parallel plate applicators. While it is not believed that these small deviations from a perfectly flat plate caused a significantly inhomogeneous field, it was considered better to avoid this. The penetratation of the thermocouple into the field distorts the field more significantly and evidence for this was observed in some of the catalyst discs removed after reaction, which discoloured around the thermocouple. An example is shown in Figure 4.4. For this reason, a thermocouple positioned between the parallel plates was omitted from the DRIFTS cell. Instead, the cartridge heater used for conventional heating was chosen to have an internal thermocouple.

a: Inner live applicator
b: CaF_2 window
c: Ni gauze
d: Coaxial cable
e: Outer live applicator
f: O-ring
g: Sample holder
h: Gas supplies
i: Ground applicator
j: Nylon M4 screws
k: Cartridge heater

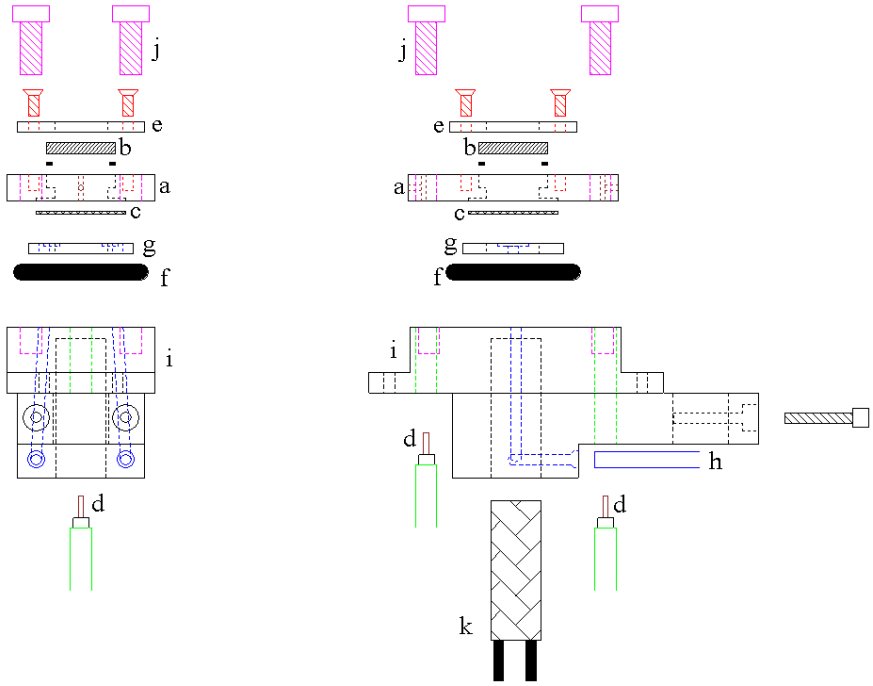

Figure 4.5: Exploded view of DRIFTS cell

The construction of the DRIFTS cell is detailed in Figure 4.5. For clarity some parts with related function are similarly coloured. The main body of the top applicator (a) houses a window (b) covered by a nickel gauze screen (c) that was spot-welded into a recess. This assembly is connected to the inner coaxial conductors (d) *via* grub screws when the cell is assembled. The direction of the screws holding the outer part of the applicator (e) to the inner was reversed, resulting in a flatter surface being presented to the sample. In order to remove the o-ring grooves from the applicator plates, a single o-ring (f) was used to seal between the two applicator plates, completely surrounding the sample holder. Using a larger diameter o-ring also allowed the gauze to be spot-welded to the applicator plate, and thus provide a flatter finish. To allow sealing with a single o-ring, the sample holder (g) was reshaped and the gas supplies (h) enter the cell

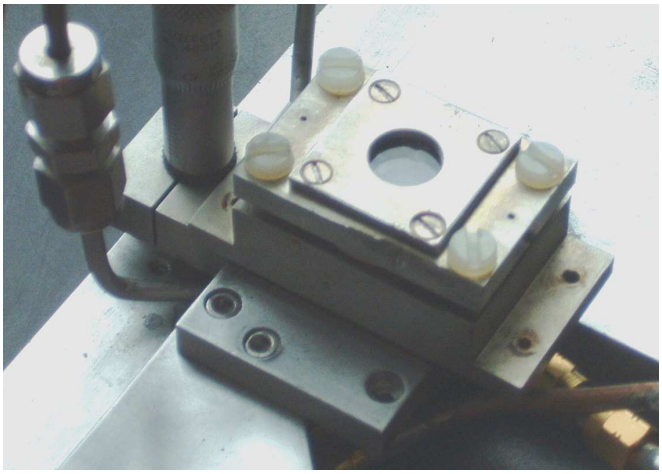

Figure 4.6: Photograph of assembled DRIFTS cell

through the grounded applicator (i). This sealing method differs from that used in the transmission cell, where the applicators seal against the ceramic of the sample holder. Making the seal in this manner increased the dead volume of the cell by a very small amount, but the increased simplicity made the seal more reliable. This also removed the fragile joint between the stainless steel gas supply tubing and the ceramic sample holder. The microwave applicators were clamped together using M4 nylon screws (j), which limited the cell temperature to 423 K under conventional heating and 373 K with microwave irradiation. Excess microwave energy from the cell is first directed along a length of coaxial cable away from the cell before being dumped to a resistor bank. This was necessary to conform to the geometrical constraints of the DRS optics. The increased size of the bottom applicator plate allowed the use of a significantly larger cartridge heater (k), and a heater with an internal thermocouple was selected, which provides a less accurate measurement of temperature, but provides the benefit that it does not disrupt the microwave field. A photograph of the assembled cell is shown in Figure 4.6.

4.4 Using parallel plates

The use of parallel plates to apply the microwave field to the samples was a decision that was made for a number of reasons. The large physical size of waveguides nec-

essary for the transmission of microwaves would prevent any cell from fitting inside the spectrometer sample compartment, requiring complex optics to be manufactured. Furthermore, a waveguide is essentially a closed metal box and although it is possible to cut holes in the waveguide for the IR windows or delivery of gas to the cell, this requires an orthogonal metal tube to act as a 'choke' to prevent leakage. This would futher add to the size of such a cell and introduce a level of complexity in the design and manufacture that was undesirable. To heat a sample in a coaxial waveguide would necessitate positioning of the sample between the inner and outer conductors. Due to the circular shape of this transmission line, design and fabrication of a reliable coaxial cell would also have presented a number of challenges, and it is unlikely that any benefits would have been gained from using such an applicator. Traditional infrared cells often hold the sample between two clamped plates, which is thus easily adapted to the use of parallel plates for microwave heating.

Mounting the pressed disc sample parallel to the applicator plates in the transmission cell allowed minimisation of the plate separation. This allowed small applicators to be used to produce a high microwave field density. The DRIFTS cell has the sample supported as a horizontal disc to interface with the available optics.

Windows in the applicators were chosen to admit the infrared as the alternatives would cause manufacturing difficulties. If the light was transmitted parallel to the plates, the sample holder would need to transmit the radiation. This would require either an IR and microwave transparent material that could be machined, or a much more complicated component containing windows. Using this geometry would also cause the applicator plate separation in the transmission cell to be determined by the diameter of the pressed catalyst discs. This would have increased the size of the cell with all the disadvantages this would have caused. The windows were covered on the inner face of the applicators with a fine wire mesh to create an approximately flat conducting surface to the sample. This method attenuated the infrared beam, but was necessary to ensure homogeneity of the microwave field between the plates.

4.5 Selection of materials

In selecting a high temperature gas tight seal that may be re-used, o-rings manufactured from temperature resistant perfluoroelastomers are often used. DuPont manufacture a range of these under the Kalrez® brand. The usual selection would be Kalrez® compound 4079 or similar, but this contains a powdered carbon black filler material which heats in the microwave. Preliminary experiments showed that Kalrez® compound 6221, a high purity variant developed for food and pharmaceutical use and devoid of this filler, did not heat in a microwave field. As a result this material was used for all seals within the microwave field, whilst any seals needed outside the microwave, such as the seals for the windows in the applicators, were made with the more usual Kalrez® compound 4079.

The material chosen for manufacture of the sample holder was initially Shapal-m®, an aluminium nitride ceramic made by Tokuyama soda, due to its very low interaction with the microwave field. However this proved too fragile and costly for routine use, so all experiments reported in this work were made using sample holders manufactured from Macor®, a ceramic manufactured by Corning incorporated, consisting of approximately 55% fluorophlogopite mica and 45% borosilicate glass. Macor has a slightly higher dielectric loss, although this should be negligible under the conditions used.

The Ni gauze used for covering the windows of the cell was supplied by STREM and was selected as being the most open weave easily available to minimise infrared attenuation. Brass was used for the transmission cell body due to its excellent electrical conductivity and for ease of manufacture. The DRIFTS cell used stainless steel to ensure chemical inertness.

4.6 Maximising energy transfer

In a DC electrical circuit power is lost in different components according to their resistance, taking the form $P = I^2R$. Thus the greater the resistance, the greater the power loss at that point. In an AC system, a similar situation prevails, although this is complicated by the frequency of the signal, and the possibility of a phase lag. For AC systems, there is effectively both a real and imaginary part to the resistance of an

electrical component, with the imaginary part known as the reactance. The sum of these is the impedance and can be stated:

$$Z = R + jX \tag{4.1}$$

Where Z is impedance, j (used to avoid confusion with current) is $\sqrt{-1}$, and X is reactance. The magnitude of Z can be obtained as:

$$|Z| = \sqrt{R^2 + X^2} \tag{4.2}$$

and is equal to the ratio of RMS voltage and current:

$$|Z| = \frac{V_{(RMS)}}{I_{(RMS)}} \tag{4.3}$$

Therefore the power loss in a given component in an oscillating system is given by:

$$P_{(RMS)} = I^2_{(RMS)}|Z| \tag{4.4}$$

To ensure the greatest possible power is dropped across the desired load it is necessary to select the correct impedance and this can be manipulated using a stub tuner. A single T-piece is inserted into the co-axial cable at a specific position, with the side branch of the T holding an adjustable short between the inner and outer conductors of the cable which can be moved to vary the length of the conductor up to $\lambda/2$. This is schematically shown in Figure 4.7. The T must be positioned an odd number of quarter wavelengths ($1/4\lambda$, $3/4\lambda$, $5/4\lambda$ ...) from the position at which the inner co-axial conductor is equidistant from the two applicator plates. Moving the position of the short varies the impedance of the system and consequently the heating of the sample.

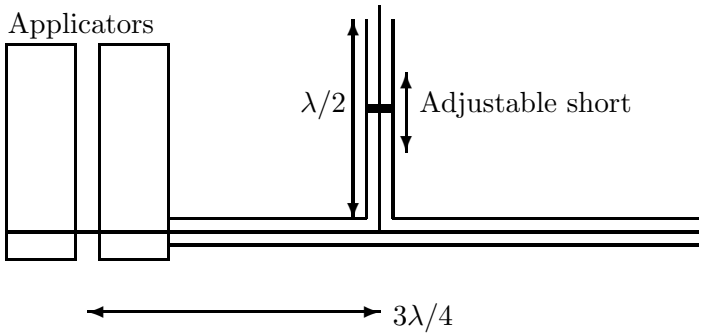

Figure 4.7: Stub tuner used to maximise heating of cell contents

Chapter 5

Methods

5.1 Infrared spectroscopy

The infrared spectrometer used for all data collection was a Bio-Rad FTS-6000 research grade spectrometer equipped with a DC-coupled mercury-cadmium-telluride (MCT) detector. Figure 5.1 shows a picture of the spectrometers optical bench, with the normal IR beam path overlaid in red. The source (a) is mounted in the top right corner, with the laser (b) used for accurately determining the position of the mirror in the top left of the picture. The moving mirror (c) is hidden in the large black casting which dominates the bottom of the picture and houses the air bearing that it moves upon. The KBr beamsplitter (d) is also mounted upon this casting towards the right. The 'fixed' mirror of the interferometer (e) is mounted on piezo-electric transducers and partially hidden under the electrical connections to them in the bottom right of the picture. The transducers can be used to move the mirror a limited distance and alter the angle of reflection. This feature is used in the rapid scan mode to counteract any minor discrepancies in the path of the moving mirror and is commonly known as 'dynamic alignment'. Feedback for optimisation of the signal is provided by a detector array (f) to the right of the mirror adjacent to the beamsplitter housing. The spectrometer case is continuously purged with dry air and has a number of ports which may be opened to allow redirection of the IR beam outside the spectrometer to be used by various instrument accessories. The transmitted beam (g) exits the compartment for the main bench at the bottom right of the picture, where a mirror can be rotated to deflect it

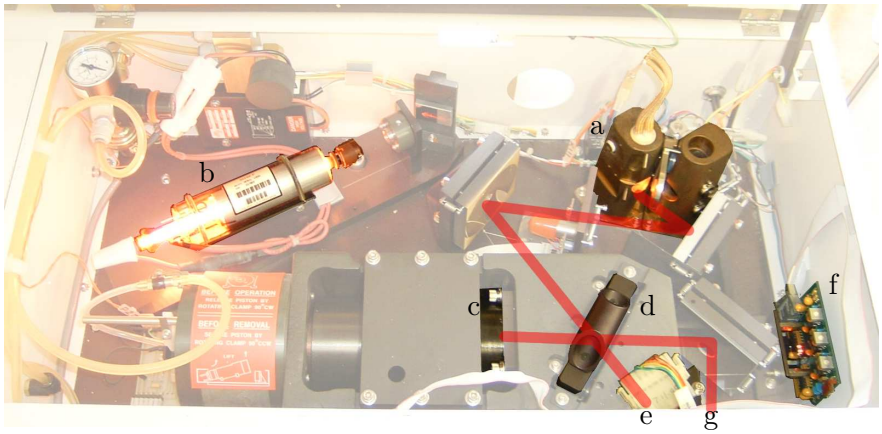

Figure 5.1: The optical bench of the FTS-6000

to external optics, or through the sample compartment.

The infrared experiments used a common gas handling system attached to the different reaction cells, which were placed to be optically accessible by the FTIR spectrometer. Transmission experiments were easily accommodated in the sample compartment of the spectrometer, although the door was replaced with a custom made frame which supported metal plates and plastic sheeting to allow dry air purging. The DRIFTS cell was placed in a 'Praying Mantis'™ DRS accessory from Harrick scientific, a picture of which is shown in Figure 5.2 with the beam path overlaid in red. The elliptical mirrors which supply the beam and focus the collected radiation are offset behind the sample, so that the specular reflectance collected is reduced. This arrangement also leads to more room being available around the sample cup than with other DRIFTS accessories for supplying the necessary services to the controlled atmosphere cell.

For the FTS-6000 a replacement aperture wheel assembly is commercially available which allows use of the emission port situated in the rear of the spectrometer housing. It has previously been reported that basic emission optics are relatively simple to produce oneself [69], and it was in this spirit that the emission optics were prepared in-house.

A table was constructed to attach to mounting holes on the rear of the instrument, such that the table surface was at the same height as the optical bench within the spectrometer. Experimentation with available optics led to the use of a rudimentary

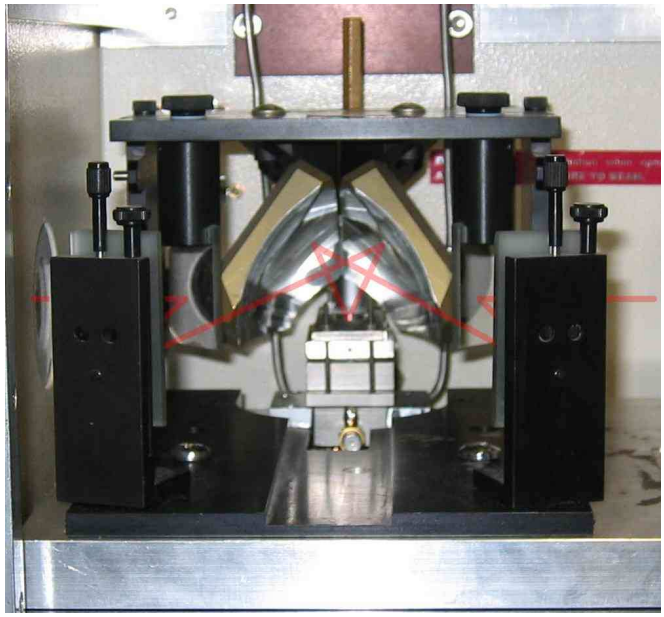

Figure 5.2: Diffuse reflectance infrared accessory

system which is now described and is shown in Figure 5.3. A planar mirror was placed in a similar position to that of the removed aperture to direct the external beam entering through the rear port onto the same path as the conventional source. External to the spectrometer was a periscopic assembly which consisted of a planar and parabolic mirror and the sample was positioned on a movable holder that could be adjusted to obtain the greatest signal strength. The parts of the apparatus external to the spectrometer were covered with plastic sheeting supported by cardboard and secured to the table and spectrometer with adhesive tape. This allowed limited purging of the system with dry air, but was by no means gas-tight.

5.2 Gas handling and analysis

The gases used in the experiments were controlled using a flow system that is shown in Figure 5.4. Gas flow was controlled using four MKS Mass Flow Controllers (model numbers 1159, 1259 and two model 1179), attached to a 247-C four channel readout. Flow rates are adjustable from 0–100 sccm of He for models 1159 and 1259 and 0–20 sccm for the 1179. This system allows complete control of the atmosphere surrounding

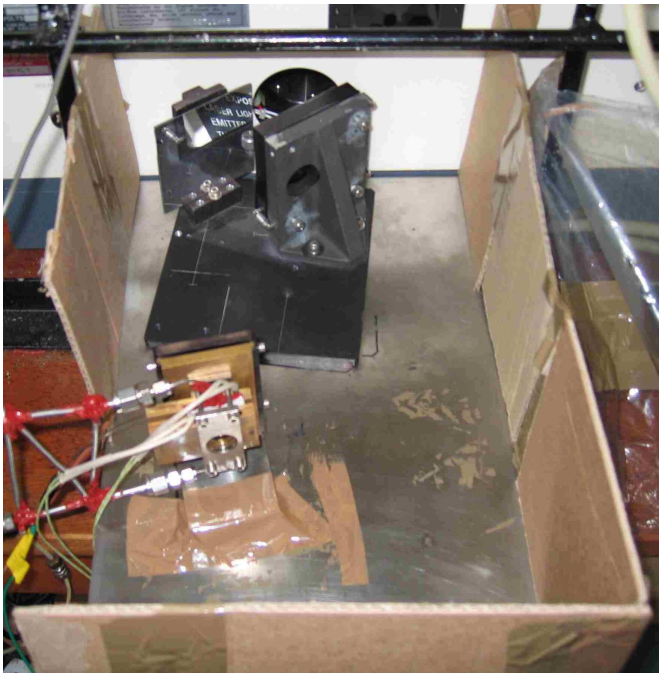

Figure 5.3: Arrangement of optics for collection of emission IR spectra

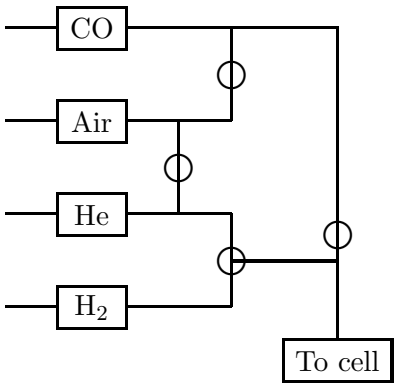

Figure 5.4: Gas handling apparatus

the catalyst for *in-situ* pre-treatment and analysis. Carbon monoxide was supplied by Argo, all other gases were supplied by BOC.

Mass spectrometric analysis of the exhaust gases was conducted with a mobile mass spectrometer, model MMS-070 from Spectra. This system is based around a Microvision Plus quadrupole analyser, with associated vacuum and sample admission systems mounted on a trolley. The gas inlet was *via* a fused silica capillary inserted through an 1/8 inch Swagelok T-piece into the outlet gas connection so that the sampling point was within 8 cm of the catalyst bed. The instrument allows recording of analogue signals through an expansion port, and the data from the thermocouples in the cells were recorded using this method. Masses 18, 28, 32 and 44 were monitored.

5.3 Microwave source

For the microwave experiments an ASTeX AX-2100 microwave generator was used. This is a variable power 2.45 GHz source which allows remote control and can generate up to 1 kW. The source was connected to a Thurlby Thandar TG215 function generator for power control and the power was varied sinusoidally between 0 and 200 W with 0.1 Hz frequency. Microwave heating can lead to a much more rapid and holistic heating effect than that caused by the conduction of heat in the conventional manner. Oscillating the power of the microwave energy applied in this manner allows an insight into the speed of heating and may yield information about the kinetic processes involved in the system.

5.4 Catalyst samples

The suppliers of all the catalysts used in this project are described in Table 5.1. All catalysts were ground to a fine powder in an agate pestle and mortar before use.

For all experiments carried out in the transmission cell *circa* 30 mg of a finely ground catalyst sample was pressed under 10 tonnes for 10 s in a 13 mm die with a hydraulic press. This was carefully transferred to the ceramic disc holder and the reaction cell was assembled. The sample was then pretreated by oxidation in 15 sccm air above 423 K for an hour, followed by reduction under 15 sccm hydrogen at the same

Table 5.1: Summary of catalyst properties

Platinum % by mass	Support	Manufacturer	Designation
0	SiO_2	Crosfield Chemicals	Sorbasil
0	Al_2O_3	ICI	JRS std Alumina
6.3	SiO_2	Johnson Matthey	EUROPT-1
0.3	Al_2O_3	Akzo	EUROPT-3

temperature. The catalyst was allowed to cool under hydrogen, then purged under 20 sccm He for 5 minutes before the reaction mixture of 5 sccm CO and 15 sccm air was passed over the catalyst disc. This was left to equilibrate for at least twenty minutes before the first spectrum was collected.

5.5 Conventionally heated transmission IR

For each experiment a background file was taken at room temperature and then a time-resolved kinetics spectrum (30 s resolution, 120 minutes length) was initiated and the cell heated. Recording of mass spectra was also started at the same time. The voltage to the resistive heaters was increased over a period of 75 minutes, held for 30 and decreased after 105. Infrared data are plotted as a surface with wavenumber along the horizontal and time on the vertical. The surface is coloured according to the infrared absorption value with red being high value, through yellow, green and turquoise, to low values which are displayed as blue.

5.6 Microwave heated transmission IR

5.6.1 Gas/Solid samples without impedance adjustment

Time resolved spectra were also acquired for microwave heated samples, but over a shorter period. Data collection by the infrared and mass spectrometers was initiated and after a short period of *circa* 10–20 s, the varying microwave power was enabled. The collection of data in this manner allows the stability of the system to be confirmed. The time resolution of the infrared spectrum was 1 s, with runs lasting 120 s. The sample temperature was then raised by *circa* 20 K using conventional heating, and

allowed to fully equilibrate. Another background was then taken, and the experiment repeated.

5.6.2 Gas/Solid samples with impedance adjustment

Some experiments in the transmission cell utilised the stub tuner for impedance matching. The cell was assembled and the reacting gas flow was admitted to the cell. Time resolved kinetics data was obtained with the short in many positions and the data compared to find the greatest oscillation in the recorded data. The short was then fixed at the position which gave the greatest oscillation in the infrared data, and the same pre-treatment and experimental regime was then followed as for the other microwave heated transmission experiments.

5.6.3 Liquid samples

The transmission cell was assembled with a CaF_2 window in the cavity of the ceramic sample holder to lower the path length of the infrared beam through the solvent. The solvent was injected through the filling tube of the cell using a syringe. A quantity of the solvent was needed to fill the reservoir above the cell before the syringe was repeatedly injected and withdrawn to eliminate air bubbles in the system. The cell was then placed in the spectrometer and after *circa* 5 minutes a kinetics background was obtained. Time resolved kinetics spectra were then collected at room temperature using the microwave regime previously described.

5.7 Conventionally heated emission IR

During the reduction phase of the pre-treatment, the position of the cell was adjusted to obtain the greatest signal to the infrared spectrometer before sealing the accessory as well as possible with plastic sheet for purging of the optical path with dry air. After cooling and under the reaction mixture single beam spectra were obtained at 5 K intervals, between 323 and 423 K as the sample was heated. Once this temperature was reached, the sample was placed under 20 sccm He flow and cooled. Single beam spectra were again obtained at 5 K intervals, and acted as the corresponding background to

the spectra obtained under heating. This data processing is similar to the transmission experiments, leading to signal intensity being incorrectly reported as absorbance.

5.8 Microwave heated emission IR

The IR signal was again optimised during pretreatment, followed by enclosing the cell in plastic sheet. The heating regime was the same as that for the microwave transmission experiments, with a background taken at a thermal equilibrium, before data collection for two minutes under microwave radiation. The voltage to the resistive heaters was then increased, and the cell allowed to reach equilibrium before another background, and corresponding time-resolved spectrum obtained.

5.9 DRIFTS

All of the DRIFTS experiments utilised the stub tuner for impedance matching, with it positioned 152 mm ($5/4\lambda$) from the center of the gap between applicator plates. Enough powdered sample to fill the sample cup was placed in the DRIFTS cell and the reacting gas flow admitted to the cell. Time resolved kinetics data were collected and the short adjusted to give the greatest variance in signal under oscillating microwave power. The catalyst was then pre-treated under air and hydrogen for an hour each, with gas flow rates the same as for the other experiments. Although the thermocouple was not in direct contact with the sample it was assumed that the temperature difference after a reasonable equilibration time would be negligible. The sample was heated in air, and held for an hour above 423 K, followed by an hour under hydrogen. The sample was then cooled before the reaction mixture was admitted. Due to the temperature limitations of the nylon screws used, microwave heating was restricted to below 373 K.

Chapter 6

Transmission cell experiments

6.1 Conventionally heated transmission IR

6.1.1 CO

In the investigation of the catalytic oxidation of CO, it is beneficial to understand the processes which occur when no catalyst is present. As with any complex system, it is best to begin with a limited number of components and fully comprehend their behaviour before introducing additional factors. Studying the heating of the cell containing only CO therefore not only gives a solid foundation from which to build, but also allows assessment of the suitability of the cell for the investigation of gas phase reactions under conventional and microwave heating.

To obtain a CO absorbance spectrum, a spectrum was collected under He flow and used as a background against which a sample spectrum under CO flow was ratioed. The spectrum thus obtained is presented in Figure 6.1 and shows the strong doublet of the rotational envelope of CO centered around 2143 cm^{-1}. Other features that are present are due to miscancellation caused by variation in the dry air purge supplied to the spectrometer. These features are indicative of CO_2, which displays a doublet centred around 2348 cm^{-1}, and water vapour. The presence of water results in a number of peaks below 1900 cm^{-1} and centred at 1595 cm^{-1} which are due to the resolution of individual rotational transitions. These peaks are minimised through the use of a purge through the instrument, but their total elimination is difficult unless the

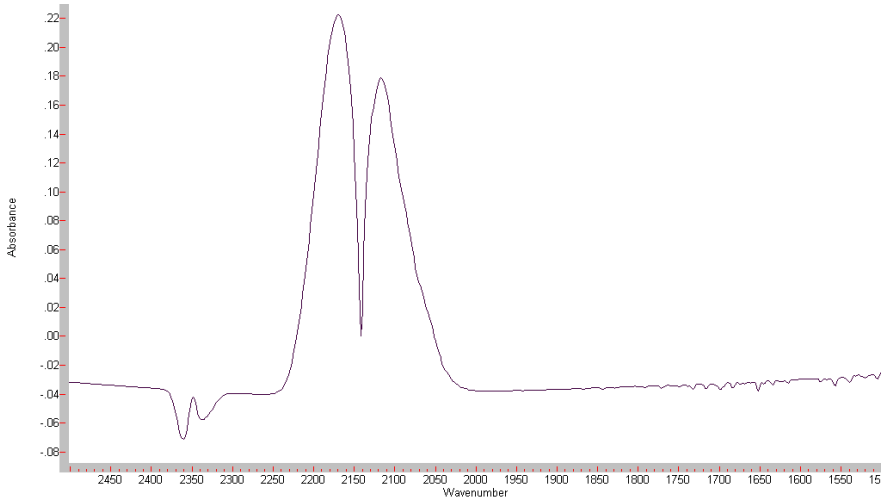

Figure 6.1: IR absorbance spectrum for CO

apparatus is evacuated.

A time resolved kinetics absorbance spectrum was obtained to elucidate the effect of increasing temperature on the CO. The data recorded when the cell was heated containing only CO is shown in Figure 6.2, with red denoting a maximum in absorbance, and blue the minimum. The results show the background of the spectrum increasing throughout the heated portion of the experiment. There are two possible explanations for this effect; increased emission from the body of the cell, and increased absorbance. Whilst these two effects appear contradictory at first glance, their interplay may cause an unexpected change in the spectrum. Increased infrared emission from the heated cell will cause a D.C. bias at the detector in the spectrometer. This results in an increase in the 'effective bath temperature' of the photoconductive detector, thus reducing sensitivity and apparently increasing absorbance across the entire spectral range. As a sample heats, it emits a greater amount of infrared energy. Kirchoff's law of thermal radiation states that at thermal equilibrium, emissivity equals absorptivity, hence the absorbance of a material will be also increase upon heating. This is not the dominant effect for the pure CO sample, as absorbance increases would only be observed at the CO peak position of the spectrum. It can therefore be concluded that the increase in background must be due to the D.C. bias caused by emission from the cell, as it is wavelength independent.

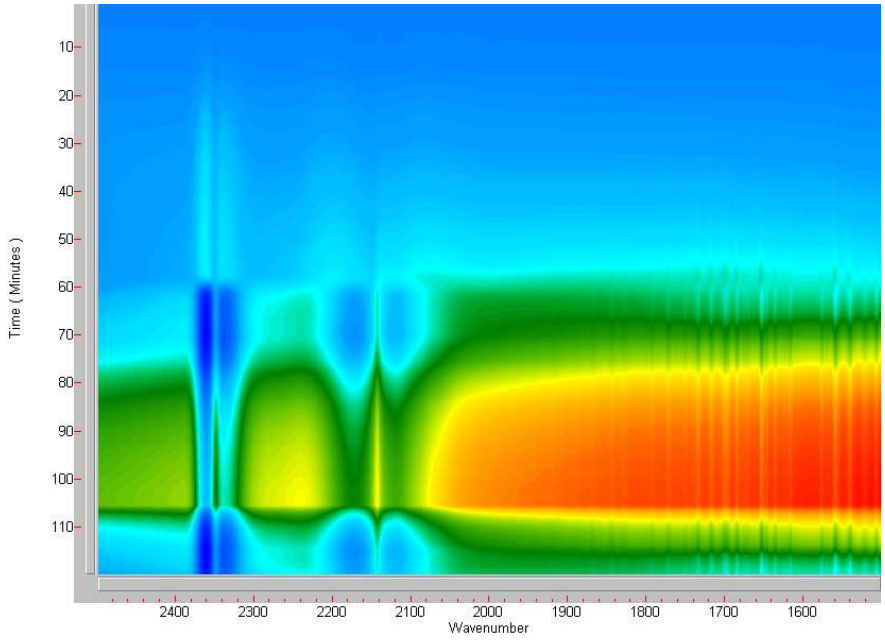

Figure 6.2: Time resolved kinetics IR absorbance spectrum for CO

A strong discontinuity is visible in the spectrum at 60 minutes, which corresponds to approximately 373 K, in both the CO (2143 cm^{-1}) and CO_2 (2348 cm^{-1}) bands, dividing the spectra into two domains. Characteristic spectra from each region are displayed in Figure 6.3 and correspond to the spectra obtained after ten and ninety minutes of heating, at 308 and 426 K respectively. The CO peaks in the low temperature portion of the spectrum show a decrease in intensity at their center, with associated increases occuring to the sides of the main peaks. The shape of a peak in the infrared spectrum is governed by the population of rotational states of the functional group, which are excited as the temperature is raised. Qualitatively therefore, higher temperatures will result in broader peaks, and a more rigorous treatment of this thermal broadening is presented in Section 8.2.2. At lower wavenumber to the main CO feature, a peak is apparent at 2042 cm^{-1}. This peak can be assigned to the interaction of the CO with the nickel gauze covering the windows of the cell, either through production of $Ni(CO)_4$ [70], or simple adsorption of CO on Ni [71]. Water and CO_2 miscancellation are also evident, with positive peaks. In the high temperature domain the H_2O and CO_2 features have both become more negative than the base-

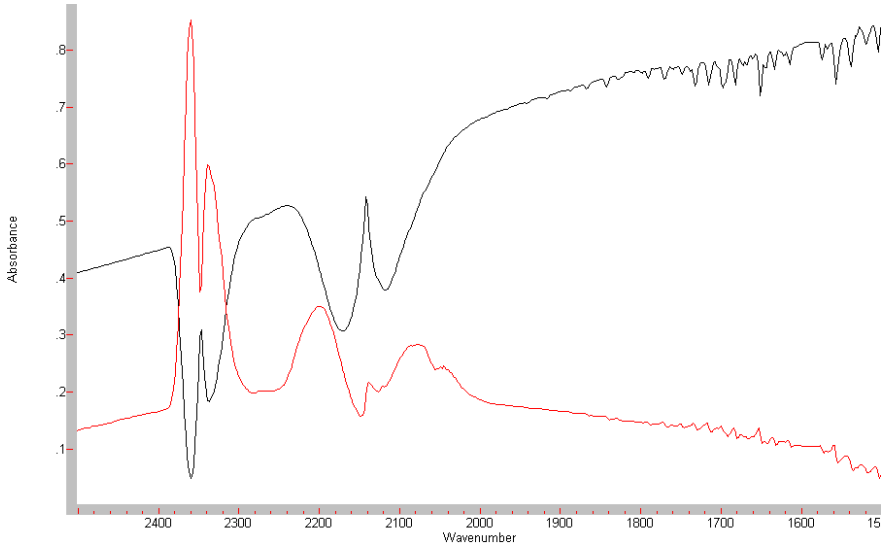

Figure 6.3: Transmission IR spectrum for CO at 10 min/308 K (red) and 90 min/426 K (black)

line. This suggests not that these peaks have strongly varied, but that the increasing baseline artefact has surpassed these features strength. The positive CO side-peaks and the peak at 2042 cm^{-1} have also become overwhelmed by this feature and only negative peaks in the CO region can be seen. The sudden discontinuity in the results is observed as the point at which the shifting baseline surpasses the real peaks, and acts as a warning against using inappropriate background spectra, such as those collected at a significantly lower temperature to the sample spectrum.

6.1.2 CO and Air

The addition of air to the CO gas flow through the cell increases the complexity of the system under study as it increases the number of reactions possible. A typical absorbance spectrum obtained is shown in Figure 6.4, and was generated by the ratio of single beam spectra obtained after the admission of CO and air into the reaction cell at 303 K against the cell filled with He. The P and R branches of the CO stretch are again obvious, as well as features from CO_2 and water vapour. These peaks are no longer purely due to the miscancellation from the purge, as there is a significant contribution due to the CO_2 in the added air flow. As no chemical traps are used on

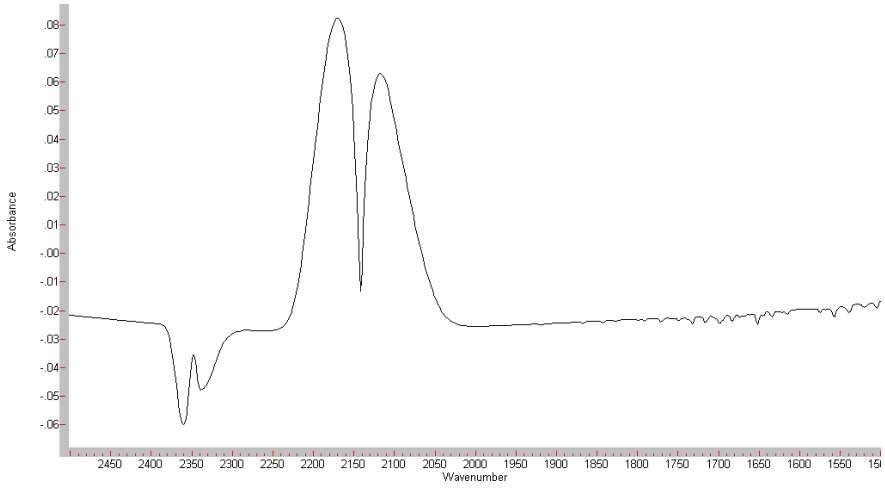

Figure 6.4: Transmission IR spectrum for CO and air at 303 K

the air line, the presence of water is also likely. However, the pathlength through the cell is small when compared to the purge atmosphere and the absorbance spectrum shows negative peaks for both features, demonstrating the strong dependance of the recorded spectra on the natural variance in the purge.

The addition of air to the gas flow in the empty cell has little effect on the time resolved infrared results obtained under conventional heating, as can be seen in Figure 6.5. The discontinuity between the two regions occurs slightly later than for the pure CO, at 65 minutes and 385 K, although the absolute position of this feature is unlikely to have any physical relevance. Representative high and low region spectra are shown in Figure 6.6.

The increase in the spectral baseline is again observed as the temperature increases, and the discontinuities in the CO, CO_2 and H_2O at 60 minutes are also apparent. The broadening of the CO_2 peaks is visible in the low temperature region, and the positive side peaks are lost after the 60 minute period. A major difference in the CO region of the spectrum is the absence of the peak showing the interaction of CO with the Ni window gauze at 2042 cm^{-1}. The loss of this peak suggests that the presence of air either prevents the adsorption of CO onto the Ni, or inhibits the formation of $Ni(CO)_4$. The CO_2 and H_2O that is inevitably admitted to the reaction cell in the sample gas flow has no visible effect on the recorded absorbance spectra as the background spectra

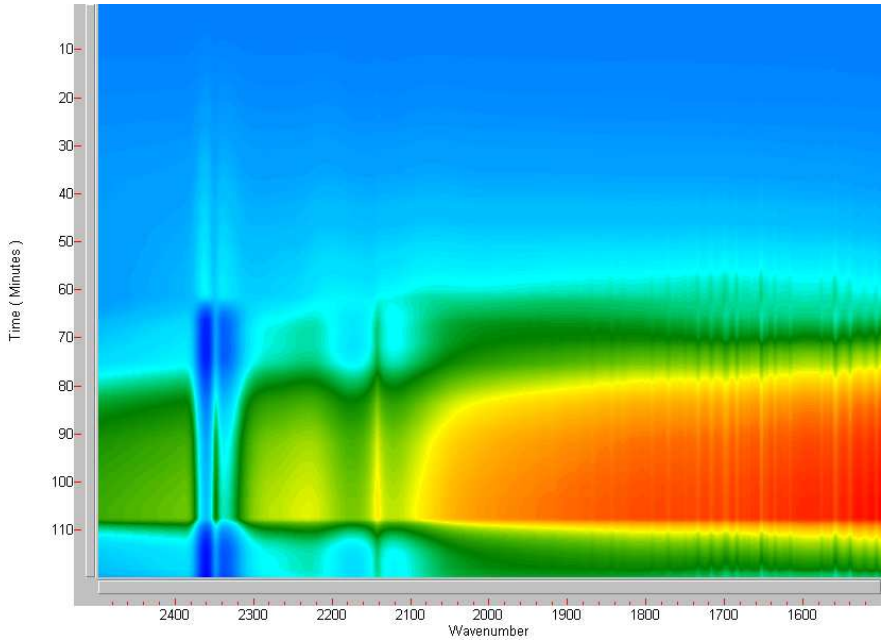

Figure 6.5: Time resolved kinetics IR absorbance spectrum for CO and air

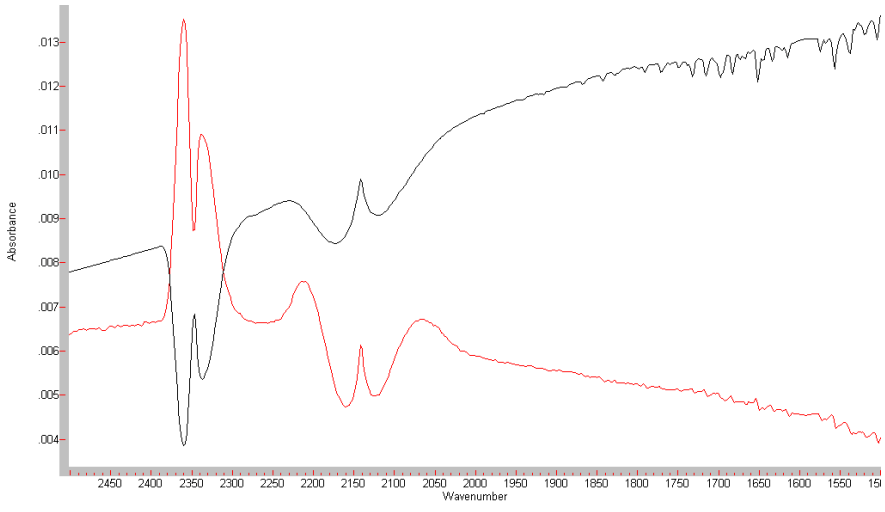

Figure 6.6: IR absorbance spectrum for CO and air at 10 min/309 K (red) and 90 min/428 K (black)

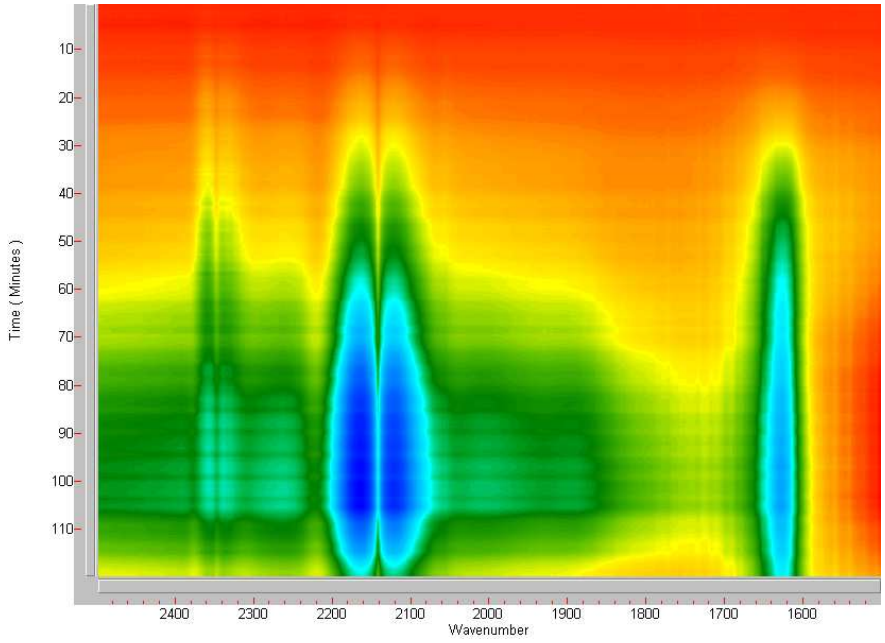

Figure 6.7: Time resolved kinetics IR absorbance spectrum for CO and air over SiO_2

were also recorded under these conditions.

6.1.3 Silica

The addition of a relatively inert catalyst support material to the reacting gas mixture will allow study of any effects caused by the catalyst materials which occur on the support, rather than the catalytic metal. EUROPT-1 is a silica supported Pt catalyst, thus the study of the silica, which is the same as that used in the production of the catalyst, should be enlightening for reactions over EUROPT-1. The time resolved kinetics transmission IR spectrum for a pressed silica disc with CO and air under heating is shown in Figure 6.7. The change with temperature recorded in the baseline of the spectra with silica present is the opposite to that seen for the purely gaseous samples. A decrease in absorption is observed, instead of the increase seen for the gaseous samples. The two mechanisms previously discussed in Section 6.1.1 which can cause changes in the recorded baseline will also be operating for this sample, but with different intensities. The presence of a solid disc in the beam path means that both the emission and absorption of infrared are greatly increased compared with a purely

gaseous sample and lead to an opposite shift being seen in the baseline of the spectrum. The increased temperature will result in a higher D.C. voltage caused by the emission from the cell and sample, whilst the enhanced absorbance, due to the presence of the solid catalyst in the beam, will lead to a decreased A.C. signal at the detector. The complex interplay this causes results in the baseline decrease, although fortunately it does not obscure the development of features due to the reacting species.

Horizontal lines with a four minute period are also present in the kinetics spectrum, appearing after the cessation of heating at 75 min. The magnitude of this effect is relatively feeble compared to the other features, and cannot be attributed to thermal change of the sample. The broad spectral range suggest possible instability in the instrument's performance, possibly either fluctuations in the source or detector, although the diminutive and isolated character of this variation allows this to be ignored. The behaviour of the much larger peaks in the spectrum due to gas phase CO and CO_2 is similar to that seen when no solid is present. Both show a decrease in absorbance at the peak centre with the appearance of positive side bands as heating occurs. Although no gas phase water is seen, a negative peak corresponding to the O-H bending of adsorbed water [72] develops at 1627 cm^{-1}, due to its desorption from the silica. Individual spectra collected at 10 and 90 minutes (309 and 424 K) are shown in Figure 6.8 to demonstrate these features.

6.1.4 Alumina

Whilst EUROPT-1 is a silica supported platinum catalyst, EUROPT-3 has Pt supported on alumina. The study of alumina will therefore give an analogous insight into the mechanism of the reactions (if any) which occur on the support for the EUROPT-3 catalyst.

The time resolved kinetics data for alumina is shown in Figure 6.9 and displays broad similarities with the silica experiment. The desorption of water is the strongest feature seen, with the negative O-H bend peak at 1635 cm^{-1} [73]. However, the peak also shows a weak shoulder at 1578 cm^{-1} which is due to another species entirely. The adsorption of CO onto alumina supported catalysts results in the presence of a broad peak around this point due to the formation of carbonate and carboxylate species [74].

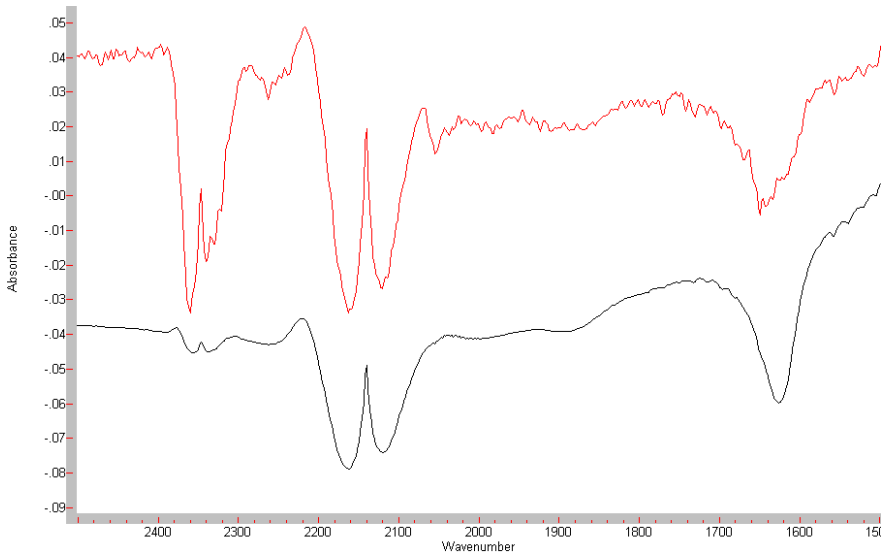

Figure 6.8: IR absorbance spectra for CO and air over SiO_2 at 10 min/309 K (red) and 90 min/424 K (black)

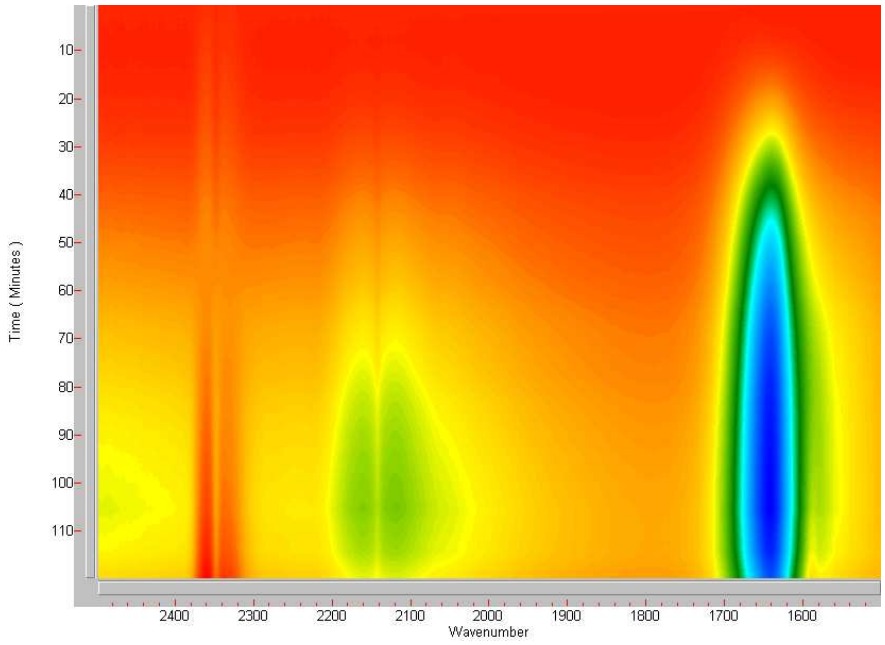

Figure 6.9: Time resolved kinetics IR absorbance spectrum for CO and air over Al_2O_3

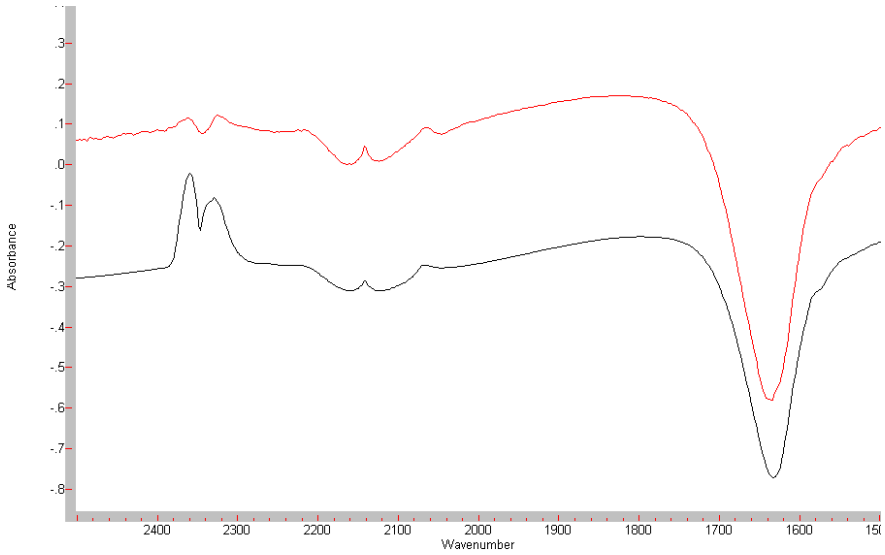

Figure 6.10: IR absorbance spectrum for CO and air over Al_2O_3 at 10 min/309 K and 90 min/429 K

Resolution of the individual species responsible for this peak is not usually possible [75], and a detailed interpretation of this region is therefore difficult. As the O-H bending peak is such a prominent feature compared with that of the carbonate/carboxylate species, evaluation of these compounds is not undertaken.

The background again shows a decrease in absorption as temperature increases, with an increase occuring upon cooling at 105 minutes. The CO peaks show a loss in central intensity possibly due to the thermal peak broadening described above, although the side bands are not as prominent, as can be seen in the spectra shown in Figure 6.10 recorded at 10 and 90 minutes. The CO_2 peaks initially decrease, but cease after 68 minutes, and begin to increase at 84 minutes, probably due to variation in the spectrometer purge.

6.1.5 EUROPT-1

Introducing platinum to the system under study, as EUROPT-1, brings an additional level of complexity and gives a number of extra peaks in the infrared spectrum. A typical absorbance spectrum obtained from the ratio of the spectra of the catalyst under the reacting gases against a background under helium is given in Figure 6.11

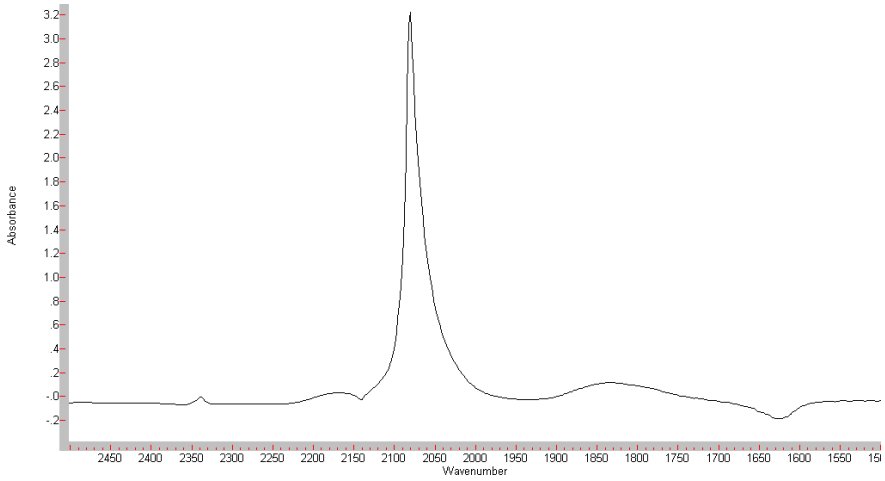

Figure 6.11: IR absorbance spectrum for CO and air over EUROPT-1

and displays one very prominent peak. The peak at 2081 cm^{-1} is due to CO adsorbed on Pt in a linear configuration [71]. The CO is bound to a single metal atom through the carbon, which weakens the intramolecular CO bond and causes a shift in the IR peak from the gas phase value of 2143 cm^{-1}. To display the other spectral features in more detail, an expanded plot is shown in Figure 6.12. The R-branch of the gas phase CO can be seen to the left of this feature, but the P-branch is largely masked by the adsorbed species. The weaker broad peak at 1854 cm^{-1} is due to the bridged CO species where the gas is bound to two metal atoms [71]. Miscancellation of the CO_2 leads to a negative feature, although the addition of the air to the cell would be expected to lead to positive peaks. A loss of water from the support is also visible at 1624 cm^{-1}.

The time resolved spectrum obtained for the heating of EUROPT-1 under the reacting gases is shown in Figure 6.13. The dominant linear adsorbed CO peak is such an efficient chromophore that virtually all the incident infrared light of this wavelength is absorbed by this species, which leads to a noisy signal at this point in the spectrum. Figure 6.14 shows a single absorbance spectrum recorded at 90 minutes and 430 K displaying a strong positive absorbance below 2070 cm^{-1} and a negative feature above 2080 cm^{-1}, either side of the absorbance saturation. This behaviour suggests a shift in the peak to lower wavenumber under heating, which is echoed by the bridged CO

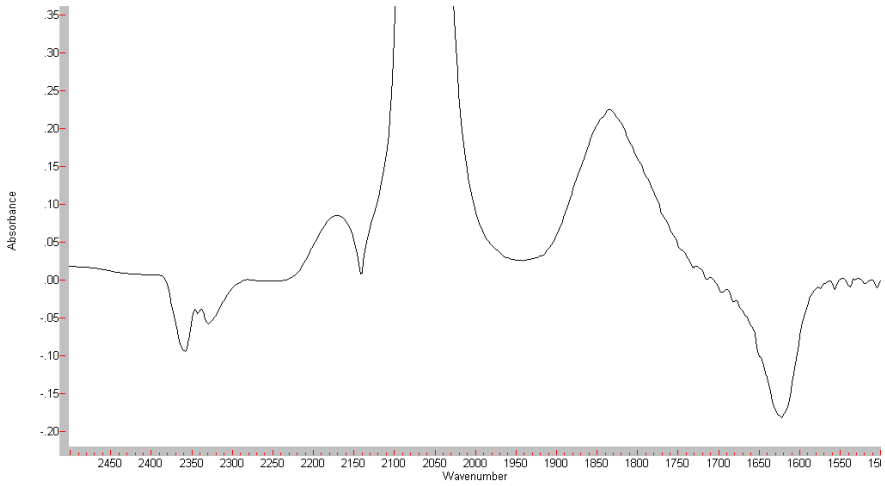

Figure 6.12: IR absorbance spectrum for CO and air over EUROPT-1 (detail)

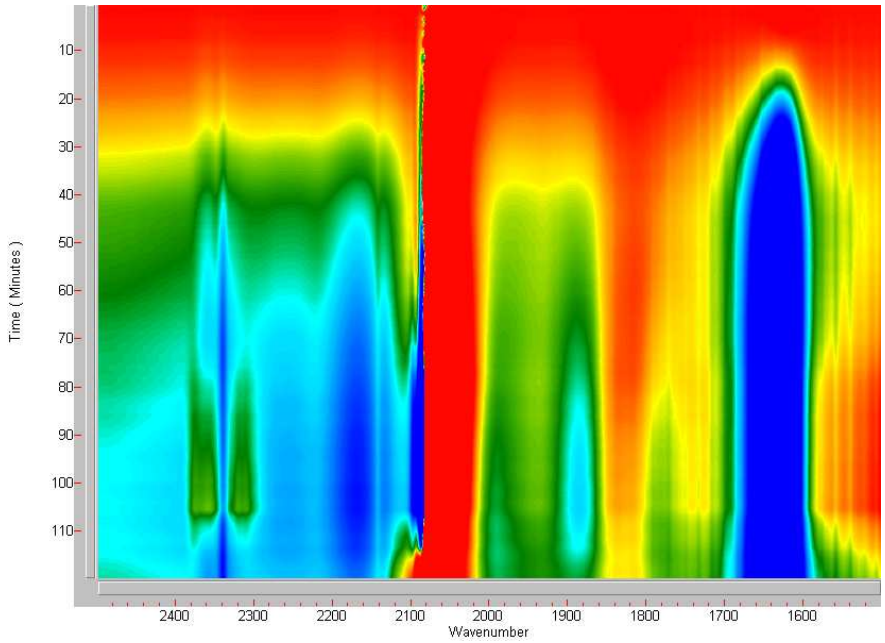

Figure 6.13: Time resolved kinetics IR absorbance spectrum for CO and air over EUROPT-1

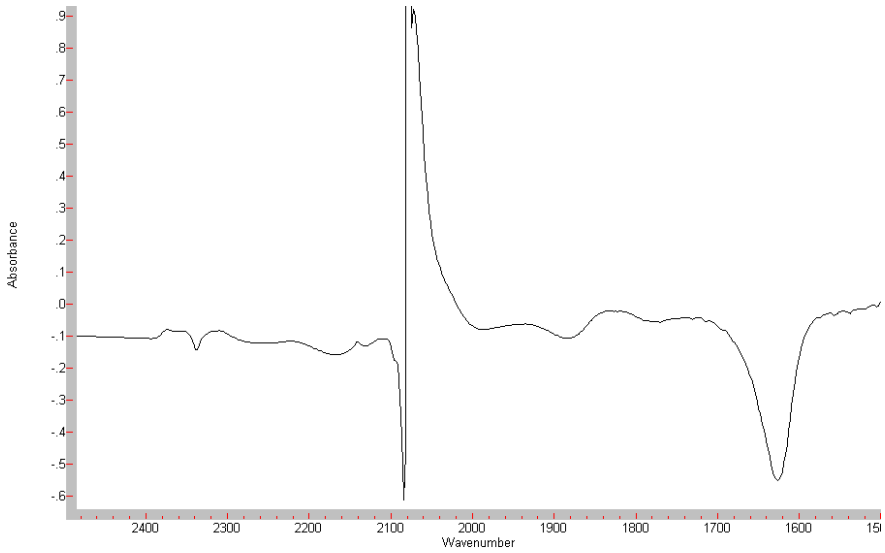

Figure 6.14: IR absorbance spectrum for CO and air over EUROPT-1 at 90 min/430 K

band. There is a loss in intensity at 1885 cm^{-1} and an increase at 1830 cm^{-1}. It is well known that the peak due to the linearly adsorbed CO species on polycrystalline Pt is coverage dependent, shifting to higher wavenumber as coverage increases [71]. The reaction conditions as well as the peak position, suggest that the platinum surface is saturated before the heating is applied, thus the shift to lower wavenumber under heating indicates a lowering of the CO coverage due to its desorption, or conversion to CO_2. The spectral features due to CO_2 are positive which provides further evidence for this, and the oxidation of CO to CO_2 is therefore clearly observable in the IR.

The gas phase CO R-branch shows a negative feature at 2169 cm^{-1}, which could be assigned to the loss of CO through oxidation, or the thermal broadening caused through the elevated temperature. There is a positive feature at 2224 cm^{-1}, which suggests that at least some of the loss of intensity at the CO band center is due to thermal broadening, although this is proportionally much smaller than what has been seen in the previous experiments, and it is therefore likely that both effects are contributing to this peak shape.

The CO_2 peak shows an unusual shape, with the peaks appearing to split into doublets, resulting in four maxima around 2348 cm^{-1}. There are a number of competing effects which may influence the spectrum at this position, such as the baseline change

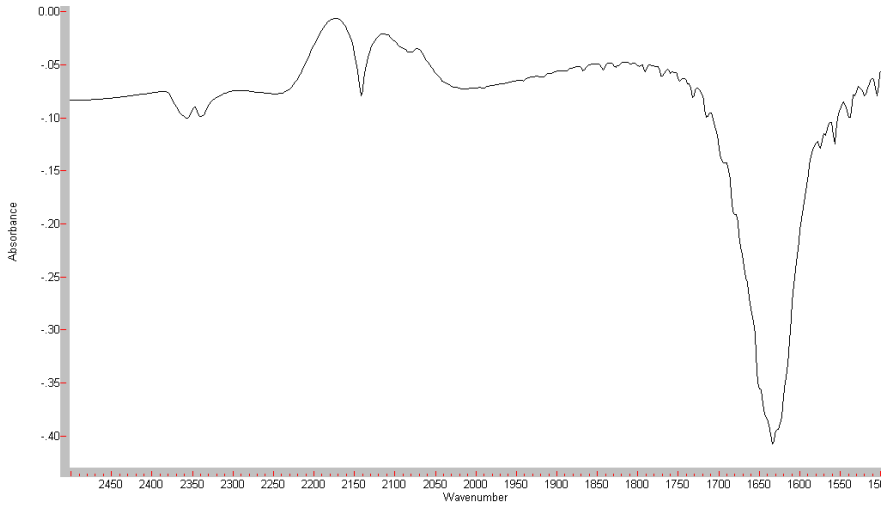

Figure 6.15: IR absorbance spectrum for CO and air over EUROPT-3

brought about by increasing emission, thermal broadening of the peak, observation of the physisorbed species, production of CO_2 from the reaction, and variation in the purge gas. The interplay between these factors is too complex to interpret and results in the presentation of this unusual peak form.

The other major feature in the spectrum is the desorption of water observed at 1628 cm^{-1}. This shows a decrease that continues throughout the course of the experiment. Gas phase water can also be observed in this region of the spectrum, alhough whether this is due to desorption of water within the cell, reaction of hydrogen adsorbed on the catalyst from the pretreatment step, or miscancellation from variations in the instrumental purge, is impossible to say.

6.1.6 EUROPT-3

EUROPT-3 has a significantly lower Pt loading than EUROPT-1 (0.3% compared with 6.3%), resulting in decreased detection of adsorbed species. This can be seen in Figure 6.15, which shows a typical absorption spectra for CO and air over EUROPT-3. The spectrum shows a much weaker linearly adsorbed CO peak than for EUROPT-1, but still positioned at 2080 cm^{-1}. This appears as a shoulder on the gas phase CO envelope, and no peak corresponding to the bridged species is apparent. Minor miscancellation due to gas phase CO_2 and water can be seen, although the greatest

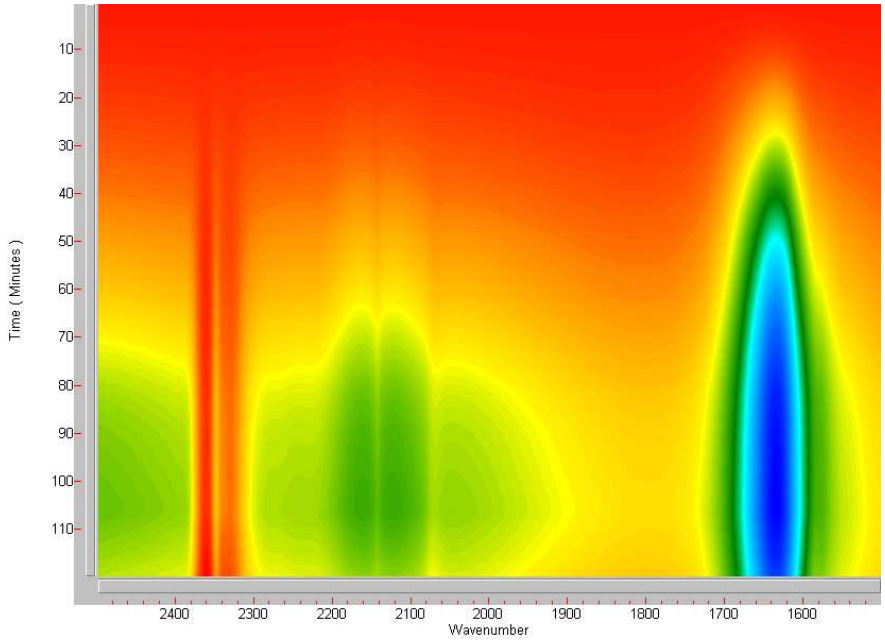

Figure 6.16: Time resolved kinetics IR absorbance spectrum for CO and air over EUROPT-3

feature at 1635 cm^{-1} is due to the O-H bending vibration of adsorbed water. The peak representing carbonate type species seen in the alumina sample is again present as a shoulder at 1578 cm^{-1} on the larger water peak.

The time resolved kinetics spectrum for the heating of EUROPT-3 is shown in Figure 6.16. The most obvious feature is again the desorption of water from the solid catalyst at 1634 cm^{-1}. The baseline of the spectrum once again decreases with rising temperature, and varying features due to CO and CO_2 are obvious. The CO_2 peak decreases for 36 minutes, then increases till 56 minutes, before decreasing again until becoming constant at 80 minutes. Once cooling starts, the signal increases. These seemingly random and relatively minor changes suggests that miscancellation due to purge variations dominates the spectrum at this point. The CO peak structure is dominated by the gas phase, although a single absorbance spectrum collected at 90 minutes and 428 K aids further interpretation of this region and is shown in Figure 6.17. There is little evidence of thermal peak broadening apparent for these results, as although there is a significant decrease in the central band intensity, there is only one feature that could possibly be construed as a side peak. This positive feature appears at 2067

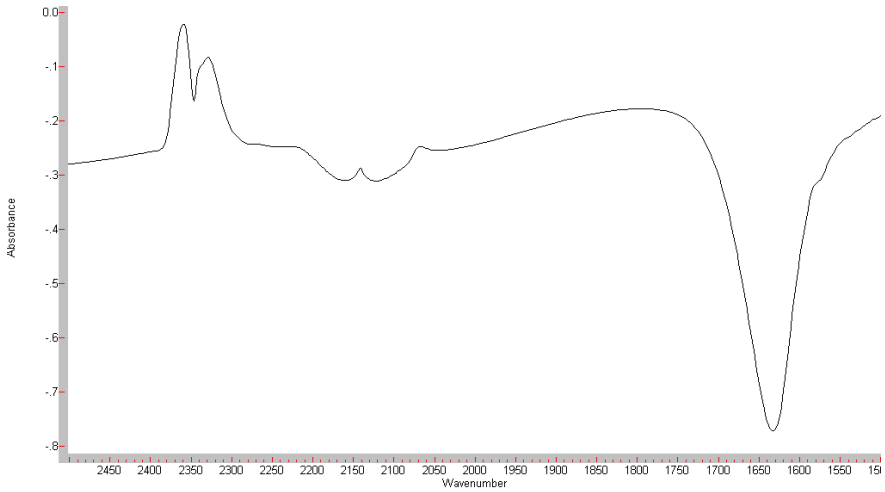

Figure 6.17: IR absorbance spectrum for CO and air over EUROPT-3 at 90 min/428 K

cm^{-1} and because it is convoluted with the decrease, is not easily identifiable. It is most likely that this peak is due to CO adsorbed on the Pt of the catalyst, with the relatively low wavenumber for this feature caused by its convolution with the gas phase peak. Another possibility is that this is a side peak, and the other increases at the edge of the gas phase bands are being obfuscated by the artefact that is the thermally induced movement of the baseline. The total lack of the side peak at higher wavenumber however, suggests that this is less likely.

6.2 Microwave heated transmission IR

6.2.1 Gas/Solid samples without stub tuner

Carbon monoxide

The time resolved transmission infrared data for the heating of pure CO using oscillating microwave power is detailed in Figure 6.18. The spectrum is initially reasonably flat and uniform, with no features observable. At 20 s, the microwave power was enabled and a prominent negative doublet of peaks due to CO appear centred around 2142 cm^{-1}. These clearly oscillate with a frequency of 0.1 Hz, which is the same as that of the microwave power. An increase in absorbance intensity outside these negative bands at 2235 and 2033 cm^{-1}, suggests a thermal widening of the peak structure

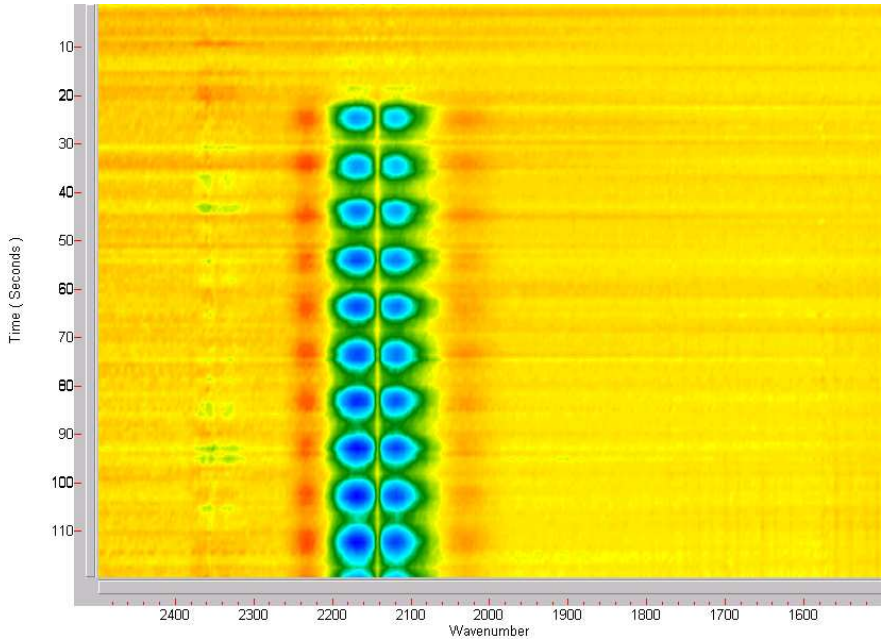

Figure 6.18: Oscillating microwave power infrared absorbance spectrum for CO with no catalyst

as seen in the conventionally heated spectra. The oscillations do not vary around a fixed position, instead they follow a trend in the direction they first appear. This can be seen in Figure 6.19, which shows the intensity changes at 2118 and 2033 cm^{-1} as time progresses. The 2118 cm^{-1} peak corresponds to the minimum feature in the CO P-branch and shows an overall decrease allied to an oscillation. Similarly the maximum of the CO side band at 2033 cm^{-1} shows an overall increase, although this is much reduced in intensity and opposite in direction. Thus both positive and negative peaks develop in average strength as time progresses. The oscillations also appear slightly damped, becoming weaker as time progresses. A typical spectrum extracted from the time resolved kinetics results to show the positions of the developing peaks is presented in Figure 6.20. In addition to the CO peak broadening a small amount of random variation can be seen in the CO_2 and water peaks due to miscancellation of the background, although these are very minor features that appear unaffected by the application of the microwave radiation.

The temperature data recorded from the thermocouple in the cell shows a regular oscillation of the same frequency as the microwave power, accompanied by an upward

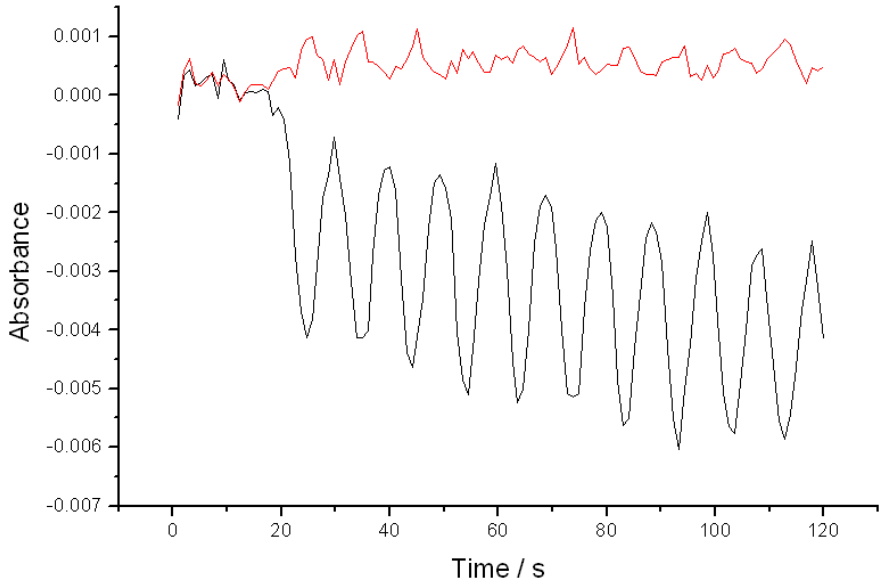

Figure 6.19: Absorbance changes at 2118 cm^{-1} (black) and 2033 cm^{-1} (red) for CO under oscillating microwave power

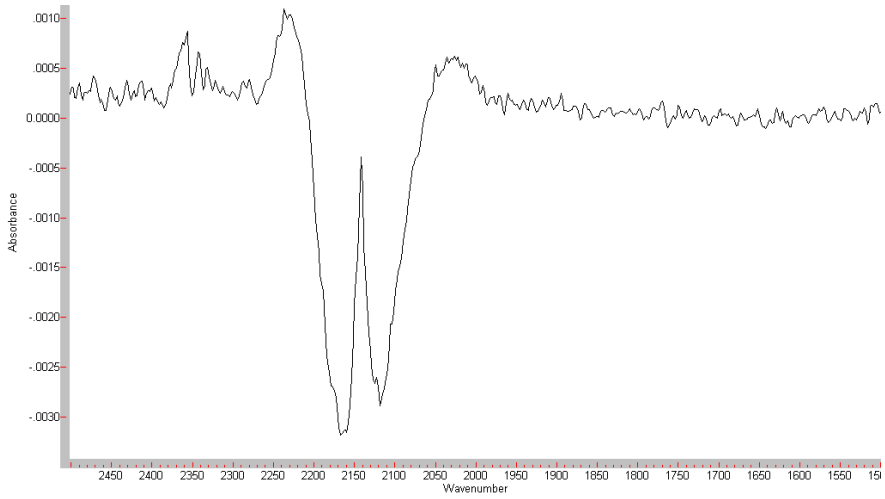

Figure 6.20: Infrared absorbance spectrum for CO with no catalyst

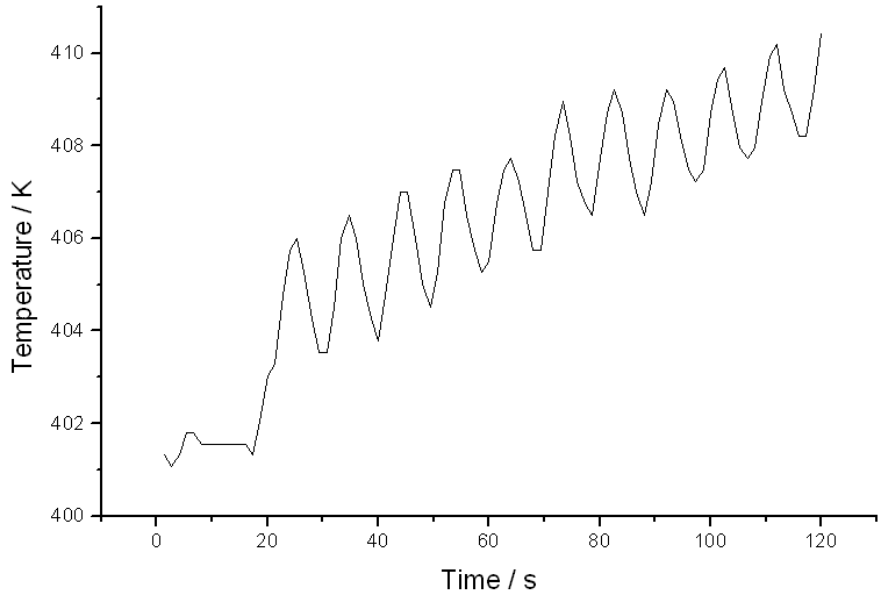

Figure 6.21: Temperature plot for CO with no catalyst

trend through the experiment. This is shown in Figure 6.21, and is typical of the results obtained for all experiments. An initial jump in temperature of *circa* 4 K occurs when the microwave power is enabled. There then follows a series of oscillations at 0.1 Hz of around 2–3 K magnitude. A number of explanations are possible for this behaviour, although a definitive cause can not be determined. An induced current in the thermocouple wires might cause such a rapid initial response, although it would be expected to see an associated linear drop when the microwave was turned off, which is not seen. A very rapid heating may have actually occurred in the first few seconds after the irradiation was begun, but the subsequent rising edges would be expected to show the same magnitude, were this the case. Perhaps the most reasonable explanation is that the profile of power delivered by the microwave generator requires time to settle. If this causes a higher microwave power to be initially applied, the associated temperature rise is likely to follow the observed result. The rising trend of the oscillations indicates that the sample is able to dissipate some, but not all of the heat it obtains under microwave power heating. The oscillating increase in temperature clearly explains the behaviour seen for the CO peaks, as the thermal broadening is very similar to what is seen for the classically heated experiments.

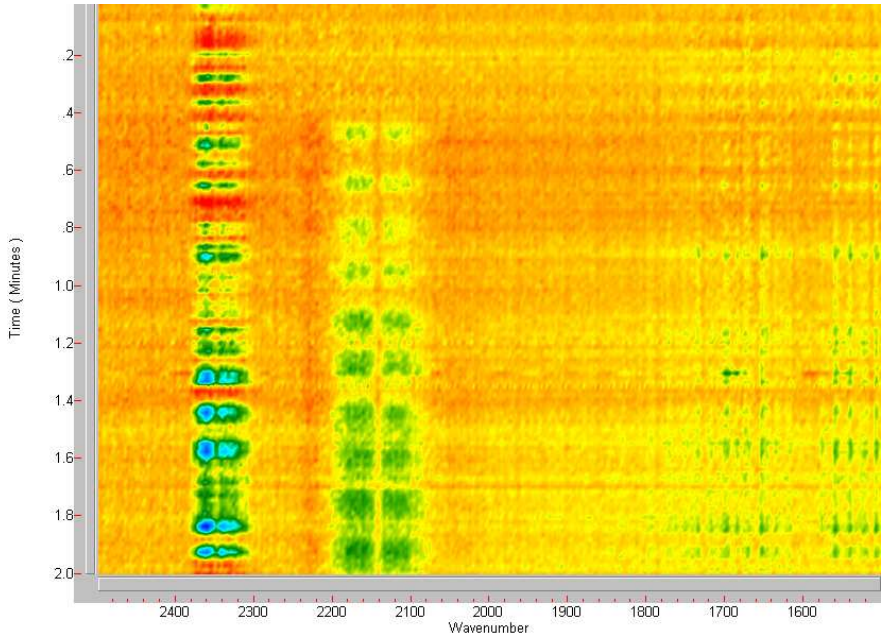

Figure 6.22: Oscillating microwave power infrared absorbance spectrum for CO and air with no catalyst

Carbon monoxide and air

The addition of air to the CO flow through the cell affects the time resolved kinetics data obtained by reducing the quality of the spectra, as can be seen in Figure 6.22. The stability of the system is again demonstrated by the relative lack of features before the application of microwave power. The CO_2 and H_2O features observed in this time region are random, caused by the variation of the purge atmosphere. The CO doublet is centred around 2142 cm^{-1}, and displays oscillations with the same frequency as the microwave power. The magnitude of these is significantly decreased compared with the pure CO experiment, giving a less defined result upon plotting, as can be seen from Figure 6.23 which shows a typical single absorbance spectrum extracted from the time resolved kinetics data. Hints of an intensity increase towards the extremities of the CO bands corresponding to thermal broadening can be seen in the time resolved plot, and the corresponding features in the individual spectrum are noisy at best.

Figure 6.23: Infrared absorbance spectrum for CO and air with no catalyst

Silica

The addition of a solid sample to the cell leads to a significantly different time resolved kinetics spectrum, as can be seen in Figure 6.24. The spectrum is featureless and stable before the initiation of the microwave heating at 0.4 min. After this point, the development of negative CO peaks become visible, although these peaks are relatively weak and do not show any periodic features corresponding to the oscillating microwave power. Even weaker are the changes in absorbance in the CO_2 region of the spectra, which are barely visible and have once again most likely arisen from miscancellation in the background. The feebleness of the infrared absorption changes over the course of the experiment can be assessed against the noise level in Figure 6.25, which shows the spectrum obtained at 1.4 minutes.

A slight banding may also be seen across the entire spectrum, although it appears much stronger at lower wavenumber. This is posited to consist of two components, the first of which is an artefact caused by interference of the microwaves with the spectrometer electronics. This electrical interference is likely to be of constant strength across the entire spectral range, and could possibly be eliminated or attenuated by improving electromagnetic shielding between the cell and the spectrometer. The second component is an increase in thermal infrared emission from the sample which may cause an increased DC bias at the detector. This effect is stronger at lower wavenumber and

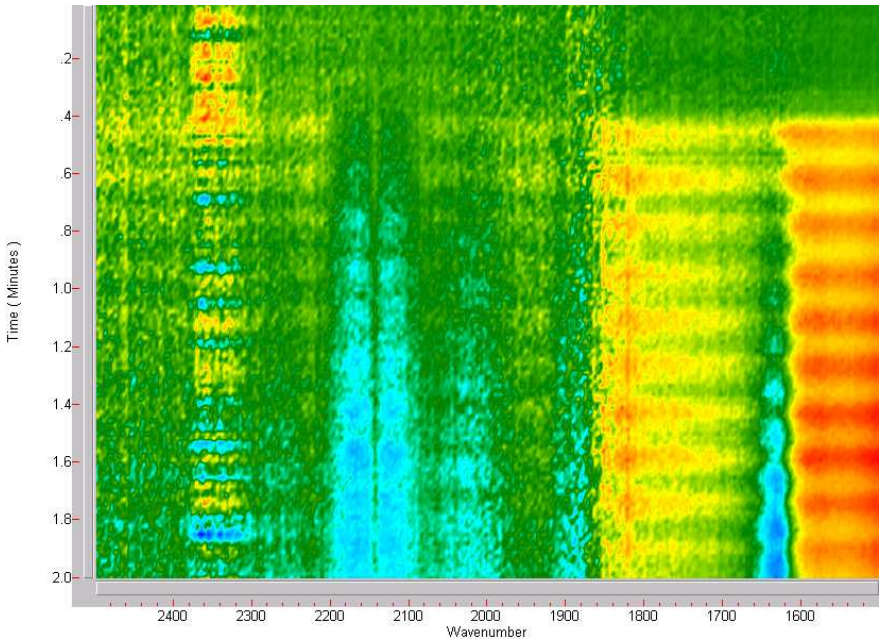

Figure 6.24: Oscillating microwave power infrared absorbance spectrum for CO and air over SiO_2 sample

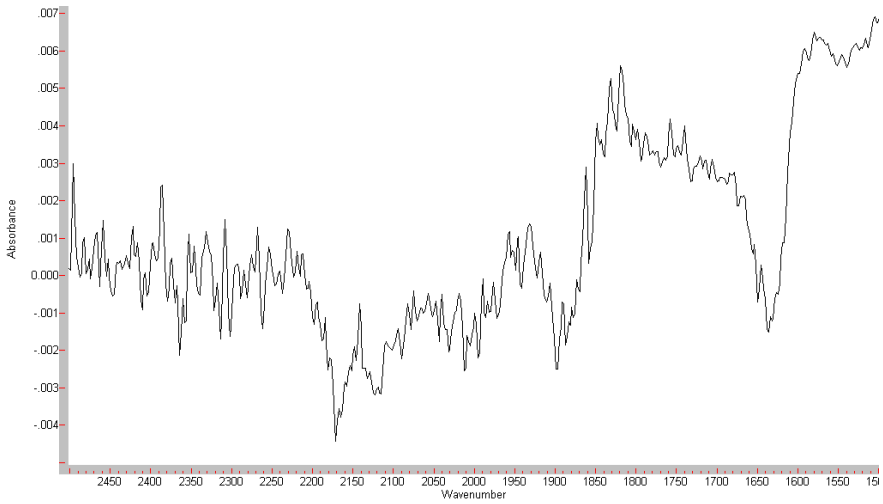

Figure 6.25: Infrared absorbance spectrum for CO and air over SiO_2 sample after 1.4 minutes

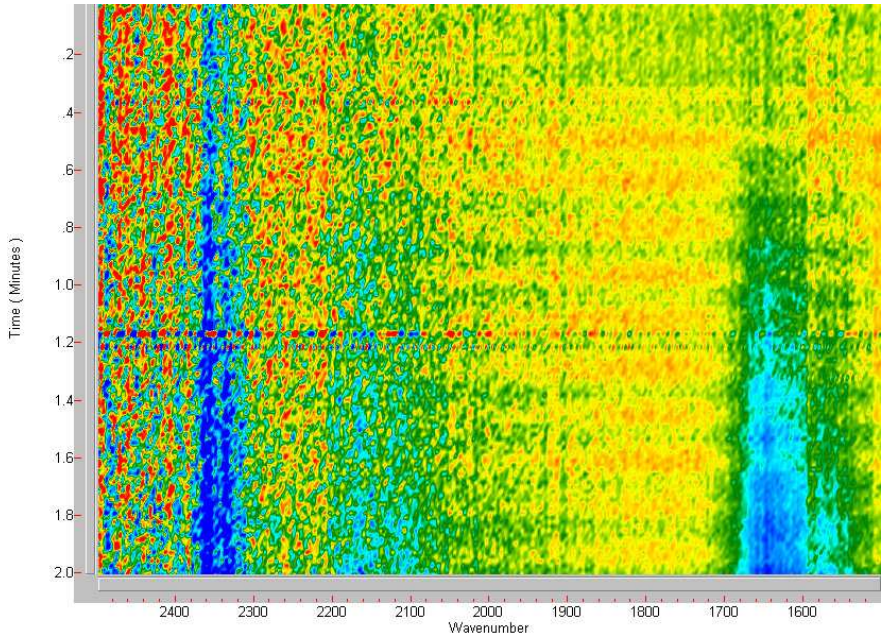

Figure 6.26: Oscillating microwave power infrared absorbance spectrum for CO and air over Al_2O_3 sample

has been previously noted in the conventionally heated experiments (Section 6.1.1). Whilst these effects are undesirable, the features due to the chemical species of interest are clearly distinguishable. Thus while it would be wise to keep these banding effects in mind during interpretation of the results, they do not prohibit the reaching of meaningful conclusions.

Alumina

The time resolved spectrum of alumina under microwave radiation is displayed in Figure 6.26 and shows a number of similarities to that recorded with the silica sample. The spectrum is stable before the initiation of microwave heating, which occurs at 0.3 min, after which oscillation in the background can be seen below 2000 cm^{-1}. No significant change in the carbon monoxide signal can be seen, and although there is a marked evolution of negative peaks due to CO_2, this is once again likely to be due to miscancellation. The major differences in the spectrum relative to the silica sample is the broad feature around 1630 cm^{-1} which develops as time progresses. This is due to the desorption of water adsorbed on the alumina surface, which will desorb as

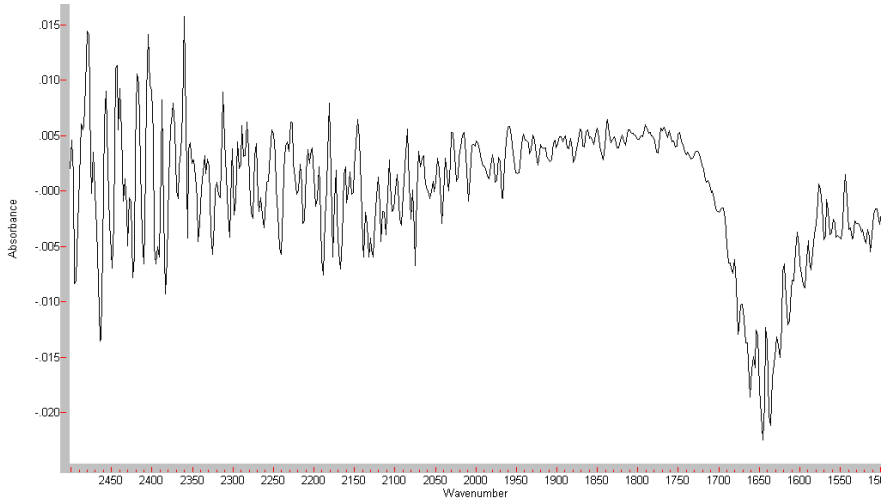

Figure 6.27: Infrared absorbance spectrum for CO and air over Al_2O_3 sample at 90 s

temperature rises. An individual spectrum extracted from the time resolved kinetics spectrum at 90 s into the data collection is shown in Figure 6.27 and displays the features described.

EUROPT-1

The results obtained for the heating of EUROPT-1 under CO and air are shown in Figure 6.28, which displays the time resolved transmission infrared spectrum. Before the application of microwave heating at 30 s, there are two features in the spectrum of note. Firstly, there is a very noisy region around 2079 cm^{-1} due to the terminally adsorbed CO. As virtually all the infrared light is absorbed by this species, a slight variation in absolute intensity at the detector can cause a significant response in the calculated absorption spectra. This feature hence shows both the maximum and minimum recorded values, leading to a small region which defies interpretation. The other feature of the spectrum before irradiation is the presence of weak positive CO_2 peaks which appear stable for the first 30 s of the data collection.

Upon the application of the oscillating microwave radiation, the CO_2 peaks increase rapidly, demonstrating an increase in the gas caused by enhanced oxidation of CO as the temperature rises. A decrease in the gas phase CO can also be seen, although the large linear adsorbed CO peak makes this hard to see. Consequently, this high

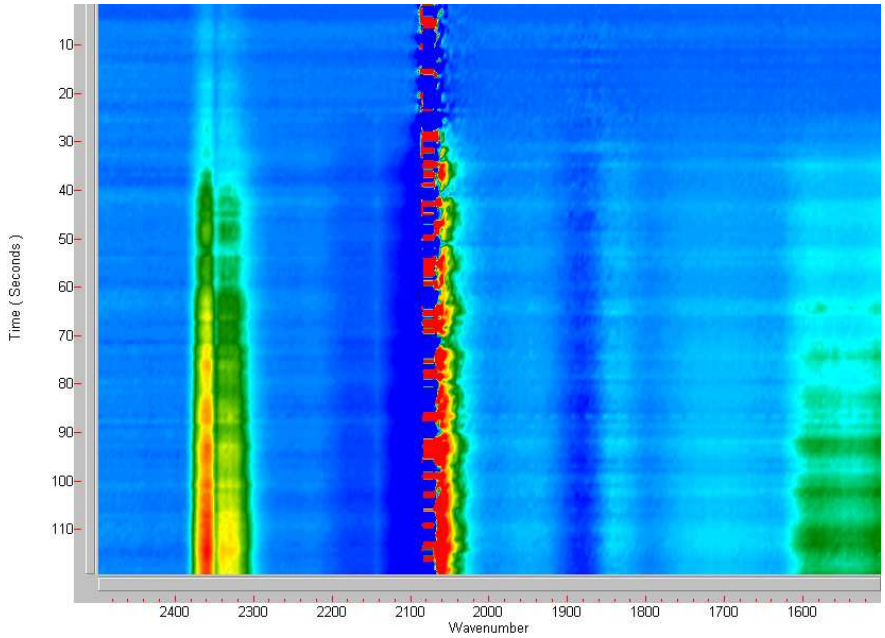

Figure 6.28: Oscillating microwave power infrared absorbance spectrum for CO and air over EUROPT-1 sample, full range

wavenumber region is expanded, and is shown in Figure 6.29. It is possible to see oscillatory character in both the CO and CO_2 peaks, although they are opposed in direction. This displays the interconversion of these gases in the oxidation reaction, as would be expected under these conditions.

To lower wavenumber of the adsorbed CO noise, there is more evidence of heating that can be obtained from the interaction of CO with the metal surface. Although there is a central region of the huge linear CO peak where interpretation is impossible, immediately to either side of this there are features which allow us to infer it is shifting in band position, and indeed oscillating. A positive oscillating feature appears in the spectrum to the right of the CO noise from 2060 cm^{-1} as time progresses. This increases in intensity and decreases in wavenumber as the experiment progresses. Similarly, there is a decrease in intensity to the other side of the noisy portion of the spectrum. This is slightly obscured by the gas phase peaks, but it is easily seen that the R-branch shows a lesser decrease in IR absorbance than the P-branch, where it overlaps with the linear CO feature. As the absorbance decrease at higher wavenumber and the increase at low wavenumber both appear to be oscillating at 0.1 Hz, it seems safe to imply

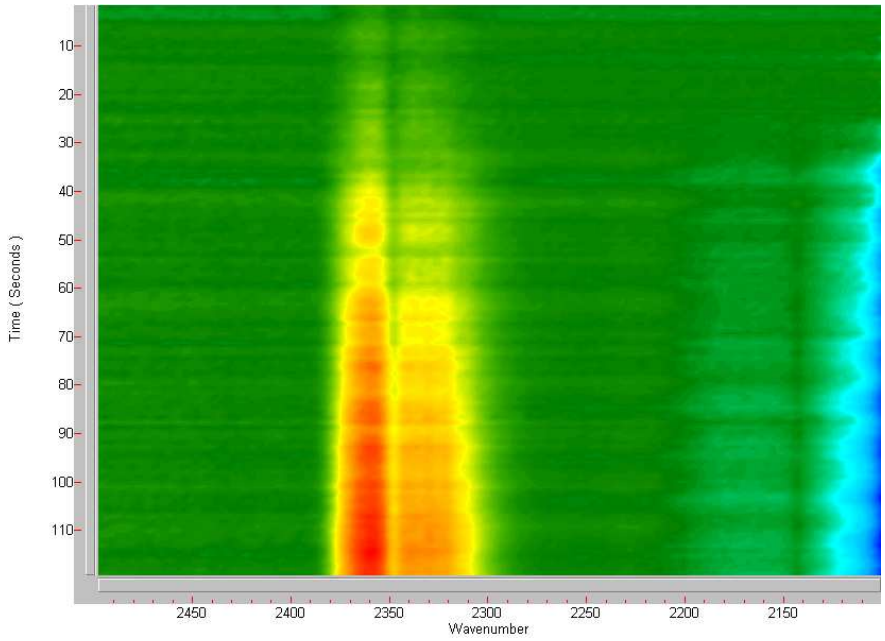

Figure 6.29: Oscillating microwave power infrared absorbance spectrum for CO and air over EUROPT-1 sample, high wavenumber

that the peak is shifting to lower wavenumber, and oscillating. As the linear CO has been shown to shift to lower wavenumber when conventionally heated in the previous experiments, this is not an unexpected result.

Other features at lower wavenumber to the adsorbed CO peak are shown in expanded view in Figure 6.30. The bridged species can be observed between 1870 and 1860 cm^{-1}, with a change in peak shape developing as heating occurs. The data shows a decrease in intensity at 1890 cm^{-1}, and an increase at 1840 cm^{-1} over the course of a run, which suggests that the peak may be shifting to lower wavenumber. However, a lower intensity negative peak also develops on the other side of the bridged CO band at 1795 cm^{-1}, which provides evidence that the peak is sharpening. The relative intensities of these features in addition to the liveliness of the baseline make a definitive interpretation of this behaviour difficult. A clear change is observed, but whether it represents a peak shift, or increasing definition and sharpness, is difficult to say. 0.1 Hz oscillations are also seen in these bridged features, indicating that they are linked to the microwave pertubation. It is possible to see the background oscillating at the frequency of the microwave power across the entire spectrum, with increasing severity

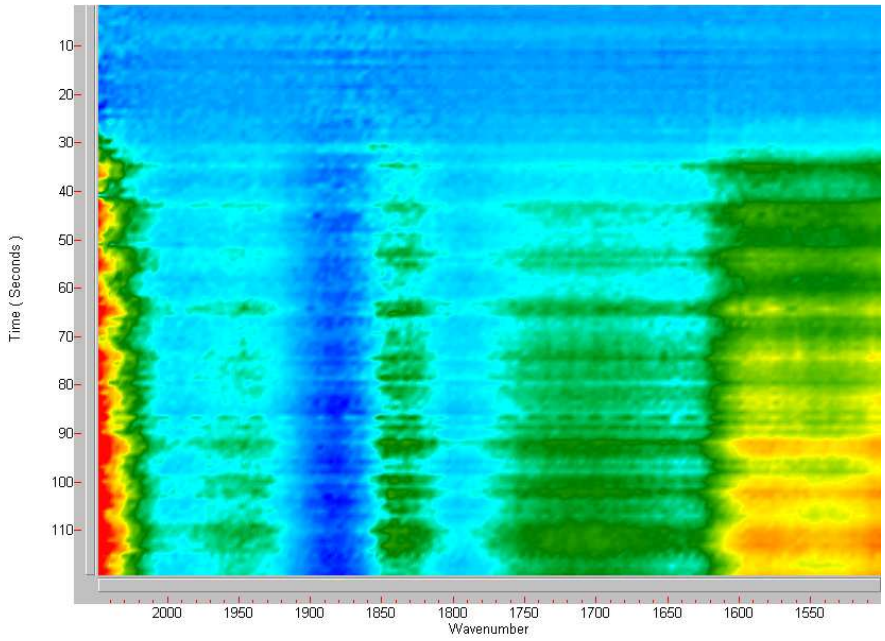

Figure 6.30: Oscillating microwave power infrared absorbance spectrum for CO and air over EUROPT-1 sample, low wavenumber

as wavenumber decreases. This is particularly pronounced below 1600 cm^{-1}, with a minimum at 1636 cm^{-1} suggesting evidence of water desorption from the support. An individual spectrum extracted from the time resolved data at 95 s is presented in Figure 6.31 to better display the relative strength of the peaks. The adsorbed CO peak is truncated to allow viewing of the other features.

EUROPT-3

The 0.3% Pt loading of the EUROPT-3 catalyst leads to much reduced features in the IR spectra due to adsorbed CO. The time resolved kinetics IR spectrum for the microwave heating of EUROPT-3 can be seen in Figure 6.32 and displays a number of features. The initial 20 s before the microwave radiation was applied shows a reasonable amount of experimental noise across the entire spectrum. After 20 s, under microwave power, features begin to develop which are caused by the microwave heating. The gas phase CO peaks show an oscillation of 0.1 Hz allied to an overall decrease. The origin of this effect may be either the thermal peak broadening previously discussed, or the oxidation of the CO to CO_2. Of the adsorbed CO species, only the linear form

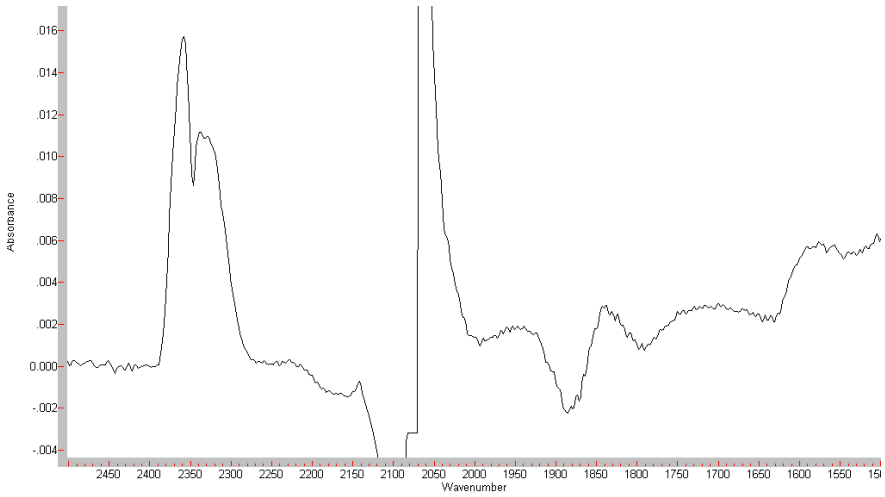

Figure 6.31: Infrared absorbance spectrum for CO and air over EUROPT-1 sample at 95 s

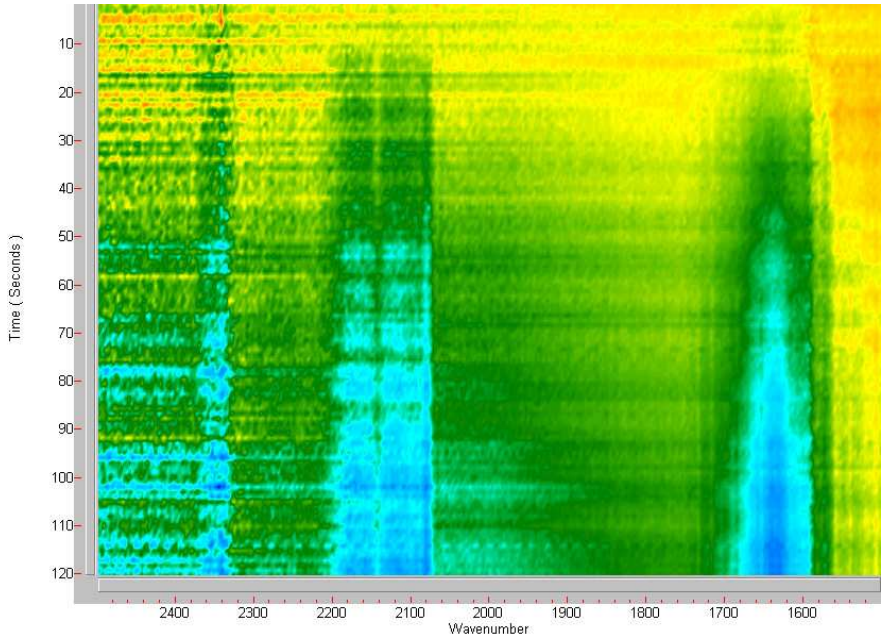

Figure 6.32: Oscillating microwave power infrared absorbance spectrum for CO and air over EUROPT-3 sample

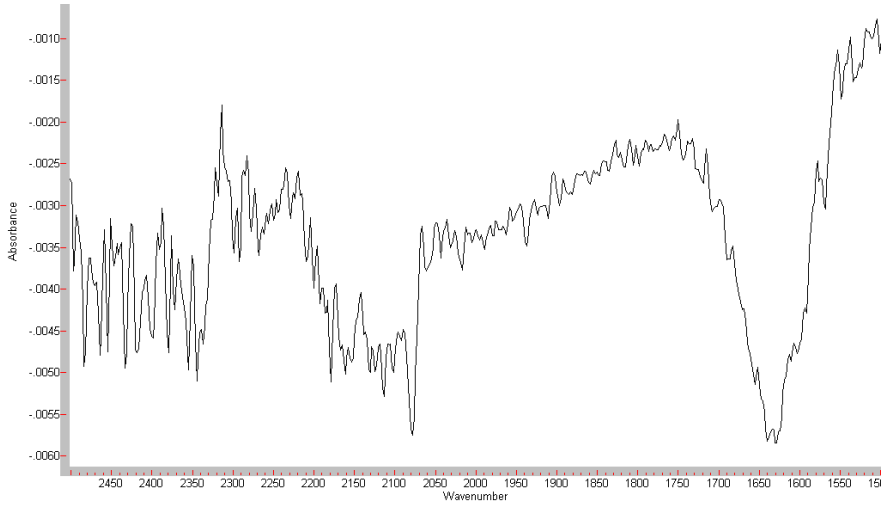

Figure 6.33: Infrared absorbance spectrum for CO and air over EUROPT-3 sample at 85 s

can be observed at 2080 cm^{-1} and this shows a decrease, although oscillations are not resolved in this feature. The spectrum also shows a minor negative doublet of peaks around 2340 cm^{-1} due to CO_2. The strength of these features are very weak, and due to potential miscancellation in the spectra at this point, do not bear further analysis.

The strongest peak in the spectrum appears at 1634 cm^{-1} due to the desorption of water from the alumina support. This peak is negative in character, and develops rapidly once the application of microwaves is begun. The previously seen carbonate shoulder can be observed at 1572 cm^{-1}. The background of the recorded spectrum also shows some oscillations at the frequency of the microwave pertubation leading to horizontal banding. This is more pronounced at lower wavenumbers, and can be seen increasing below the absorbed CO feature at 2080 cm^{-1}. A cross section through the time resolved kinetics data at 85 s is presented in Figure 6.33 and shows the relative magnitudes of these features.

6.2.2 Gas/Solid samples with stub tuner

The addition of a stub tuner to the transmission cell allows manipulation of the impedance of the cell to provide the optimum power transfer, and hence heating, to the sample. A greater heating effect should lead to increased spectral changes and thus a better understanding of the system.

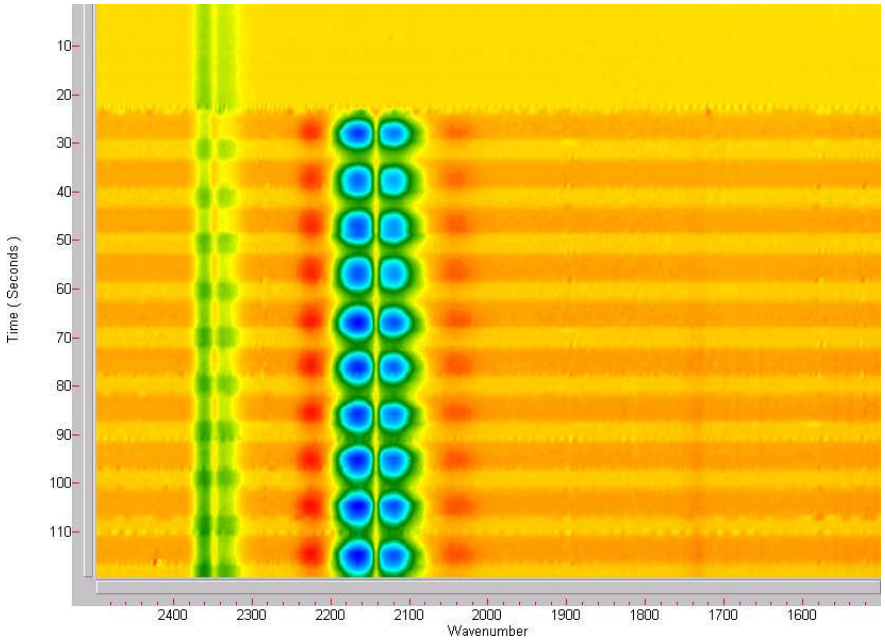

Figure 6.34: Time resolved kinetics infrared absorbance spectrum for CO

CO

The time resolved kinetics absorbance spectrum for the microwave heating of CO is shown in Figure 6.34 with blue denoting negative absorbance and red positive. Before the application of microwave power at 22 s the spectrum has only one feature, due to CO_2 miscancellation at 2348 cm^{-1}. The negative doublet of peaks remain steady throughout this period until the microwave power is enabled, when it begins to oscillate at 0.1 Hz. The entire spectrum demonstrates a banding which has a 10 s period, and is caused either by electronic interference with the detector, or through increased IR emission by heated parts of the cell. The temperature variation recorded with the thermocouple is presented in Figure 6.35 and shows a similar pattern to the previous microwave heating results shown in Figure 6.21 of Section 6.2.1.

The intensity of the CO_2 oscillation is identical to the strength of the modulation in the banding across the spectrum, which suggests that the CO_2 peak variation is an artefact caused by the changes in the baseline. Therefore the overall change seen in the CO_2 peaks is likely to be a miscancellation effect, due to variation in the instrument purge, and not influenced by the application of the microwave power.

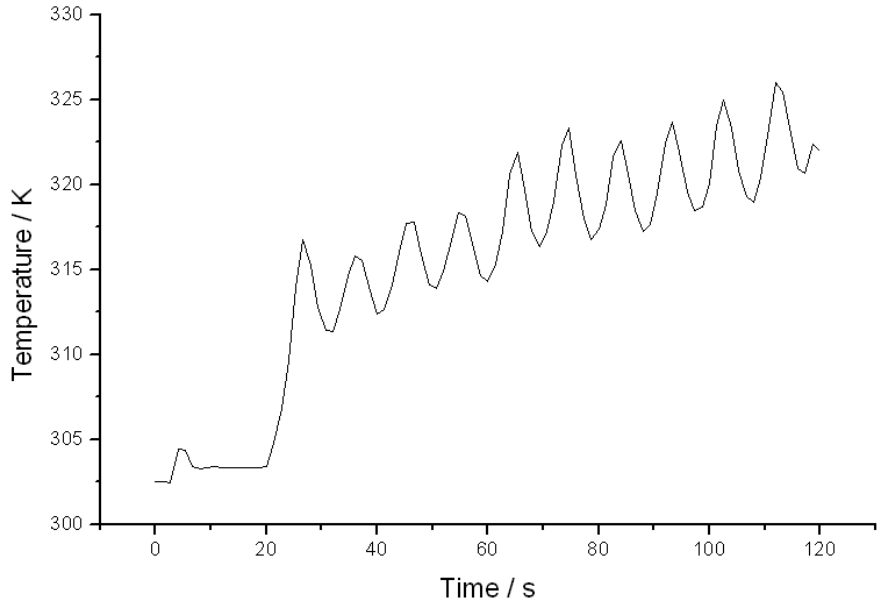

Figure 6.35: Temperature variation for CO under tuned microwave heating

After the initiation of the microwave heating regime, a series of negative features at 2123 and 2166 cm^{-1} can be seen oscillating with 0.1 Hz frequency corresponding to the maxima in the P and R branches of the gas phase spectra. Positive features outside these negative bands at 2235 and 2027 cm^{-1} indicate thermal broadening of the peaks, and thus heating of the gas phase is occuring. This band shape is clearly seen in Figure 6.36 which shows a spectrum extracted from the kinetics data at 90 s. The oscillations observed in the CO signal again display trends, with the positive peaks increasing, and the negative decreasing. The clarity of these features is however significantly enhanced from the situation without the tuner, and display a greater oscillation magnitude than the background modulation. Although there is a significant artefact from the mobile baseline in these results, the analysis of the species involved is eased by the clarity afforded by the more efficient application of the microwave radiation. A small peak, not observed for the experiment without the stub tuner, can be seen developing at 1740 cm^{-1} under irradiation. A peak at this position is commonly observed in small organic molecules which contain a carbon atom double-bonded to an oxygen, such as esters, carboxylic acids and aldehydes [76]. The origin of this peak is unclear, but it is possible that the cell has either become contaminated

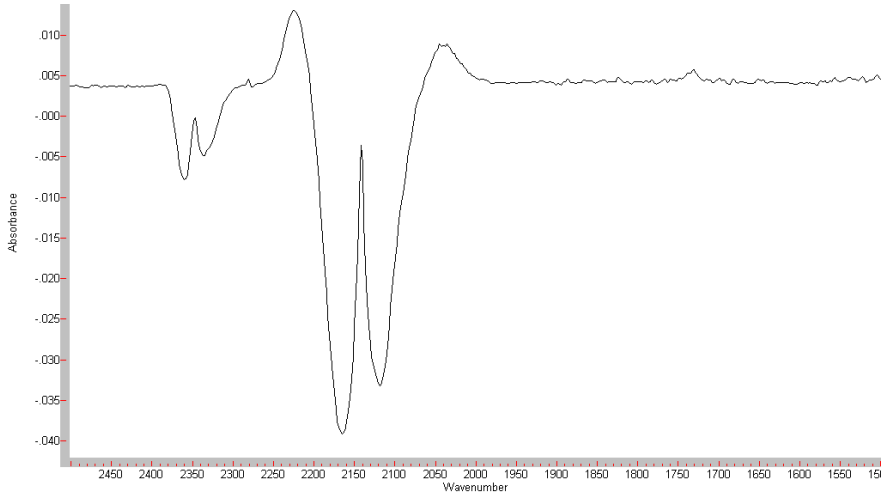

Figure 6.36: Infrared absorbance spectrum for CO at 90 s

with a moderately volatile organic species, or the high microwave power is causing evolution of such chemicals. This may be from such sources as decomposition of the o-rings, desorption of adsorbed solvent from the cleaning of the cell, or a number of other sources. The diminutive size of this peak illustrates that the effect is minor, and its position suggests it is not involved in the reaction of interest. As such, further interpretation is not attempted.

CO/Air

The time resolved kinetics data for the microwave heating of CO and air in the absence of a catalyst sample is detailed in Figure 6.37 and displays highly visible oscillations in absorbance. The cell is maintained at 303 K by conventional heating until 20 s, therafter a combination of conventional and modulated microwave heating is affecting the cell. No features are evident in the spectrum before 20 s indicating stable gas flow through the cell. Oscillating microwave power is applied at 20 s which again causes a negative band center flanked by positive peaks, which can be assigned to heating of the gas phase. This can be seen in Figure 6.38, which shows a spectrum extracted from the time resolved kinetics data at 85 s. The strength of these oscillations and the quality of the spectrum obtained is reduced from the pure CO sample, although it is still greater than when no impedance matching is used, as illustrated by the noise

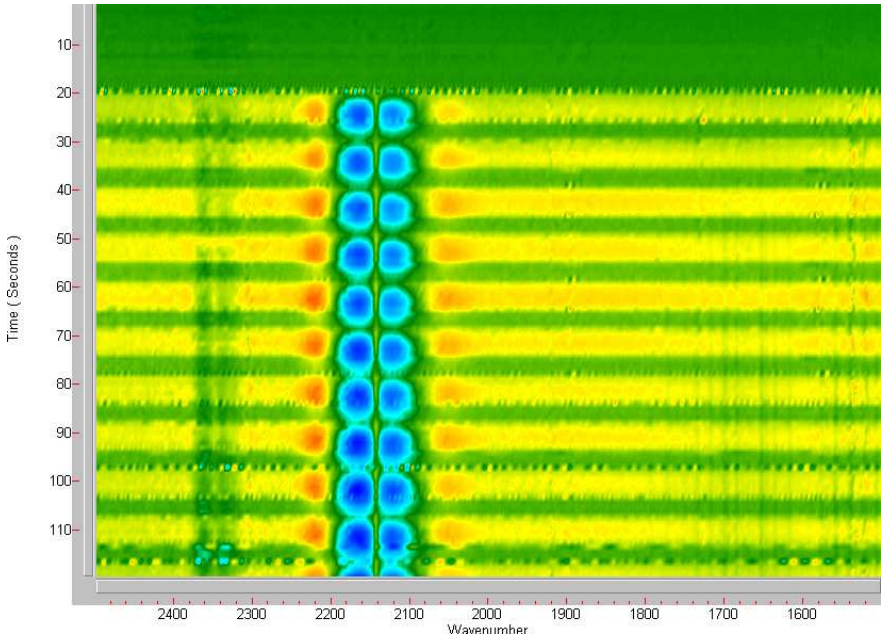

Figure 6.37: Oscillating microwave power infrared absorbance spectrum for CO and air

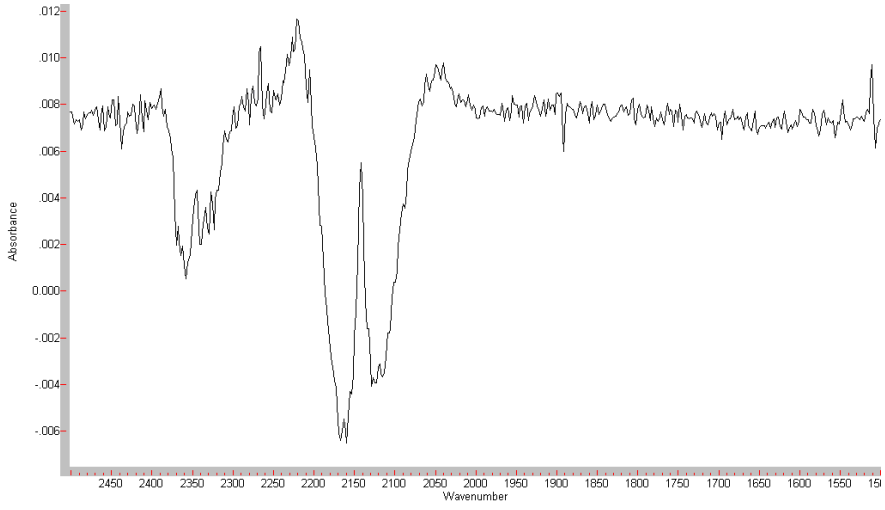

Figure 6.38: Infrared absorbance spectrum for CO and air at 85 s

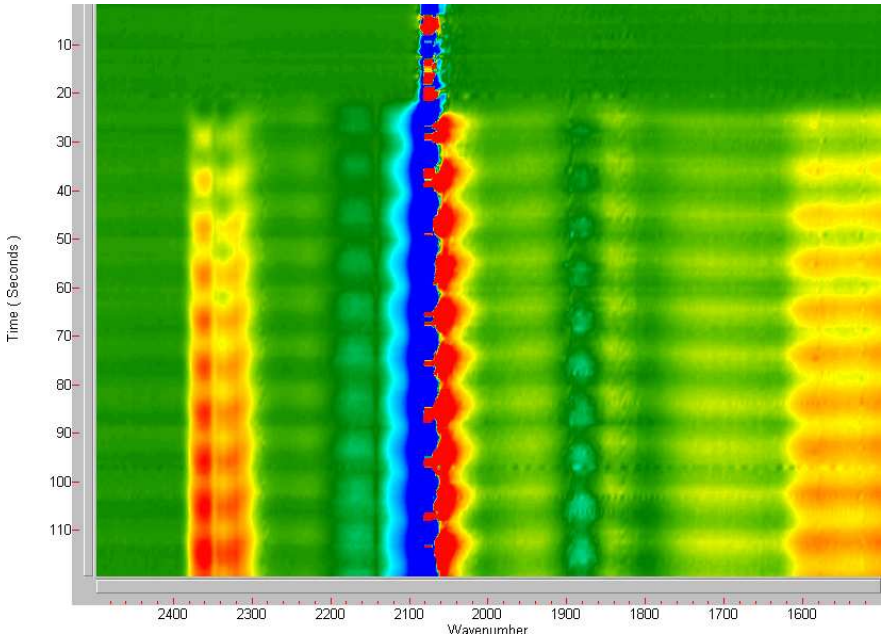

Figure 6.39: Oscillating microwave power infrared absorbance spectrum for CO and air over EUROPT-1 sample

level in the absorbance spectrum. The intense banding is again seen across the entire spectrum, although the legitimate changes in the spectrum are well resolved against it. Gas phase CO_2 and H_2O miscancellation features are seen in the results, becoming more intense with time as fluctuations in the system purge cause increased deviation from the background spectrum.

EUROPT-1

When plotting the time resolved kinetics spectra the linear adsorbed CO peak at 2038 cm^{-1} is so strong that small absolute changes in signal lead to large absorbance changes, resulting in a very poor signal to noise ratio around this feature, even before the application of microwaves at 20 s, as can be seen in Figure 6.39. The terminal CO peak around 2080 cm^{-1} shows clear oscillations at the applied frequency, and also exhibits an increase in intensity at lower wavenumber, and a corresponding decrease at high wavenumber over the course of the experiment. This demonstrates a shift to lower wavenumber under microwave heating. The shift to lower wavenumber under this heating regime therefore indicates a lowering of the CO coverage due to its conversion to

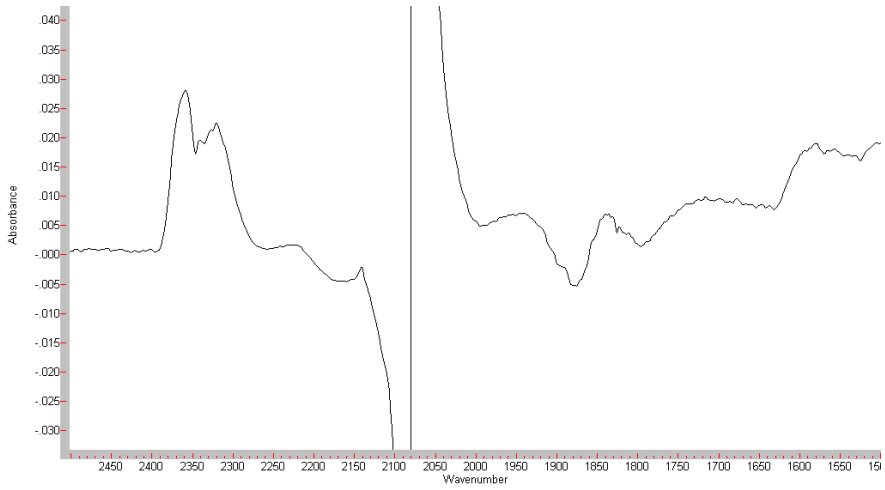

Figure 6.40: Infrared absorbance spectrum for CO and air over EUROPT-1 sample at 85 s

CO_2. The change in peak position is illustrated in Figure 6.40 which shows a spectrum extracted at 85 seconds from the time resolved kinetics spectra. There is a negative peak to the left of the noise, above 2083 cm^{-1}, and a corresponding positive peak at lower wavenumber to the noise, below 2067 cm^{-1}. The signal due to gas phase CO is dwarfed by the adsorbed species, but slight oscillations in the R-branch can be seen at 2166 cm^{-1}.

The bridged CO also oscillates at 0.1 Hz and shows a decrease at 1890 cm^{-1} and 1800 cm^{-1}, with a slight increase at 1840 cm^{-1}. This would suggest that the broad peak is becoming sharper, although oscillations in the baseline make interpretation difficult in this region. It is also possible that the bridged species is simply shifting to lower wavenumber. Oscillations are clearly seen in the CO_2 signal, which displays a doublet of positive peaks around 2343 cm^{-1}. The feature increases with time, as the oxidation of CO produces greater concentrations of CO_2.

The strength of the banding in the background appears to increase towards the lower energy end of the spectrum. This suggests that in this case the effect is caused by thermal emission from the solid catalyst, and it may be inferred from this that less microwave energy is being emitted from the reaction cell as more is being absorbed by the sample. Typical data obtained with the thermocouple during irradiation is plotted in Figure 6.41 along with the CO_2 pressure recorded by the mass spectrometer, and

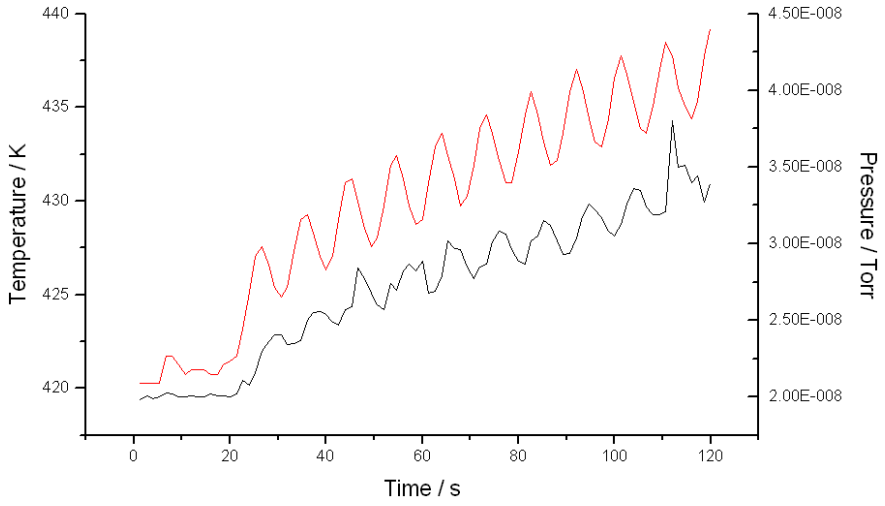

Figure 6.41: CO_2 pressure (black) and temperature (red) recorded under microwave irradiation

shows both signals oscillating at 0.1 Hz allied with a general rise throughout the course of the experiment. The temperature rise over the approximately 100 s under irradiation is circa 13 K, with a rise of around 2.5 K per cycle. The resultant conversion of CO to CO_2 under microwave heating is consistent with experiments carried out under conventional heating.

EUROPT-3

The time resolved kinetics spectrum obtained with an initial temperature of 399 K, is displayed in Figure 6.42 and shows similar behaviour to the previous experiments. Before the initiation of the microwave energy, the spectra are flat and steady. On the application of the radiation, strongly oscillating features are seen throughout the range under study. Gas phase CO shows a central decrease in intensity, with an associated positive side-band to higher wavenumber, demonstrating thermal broadening and thus heating of the gas. A sharp negative peak can be seen developing underneath the gas phase at 2080 cm^{-1} due to the terminally adsorbed CO on the Pt present. This is clearly seen in Figure 6.43, which shows a spectrum extracted from the kinetics results at 90 s. This feature can also be observed oscillating with the same amplitude as the gas phase species, which is significantly greater than the background fluctuation. The

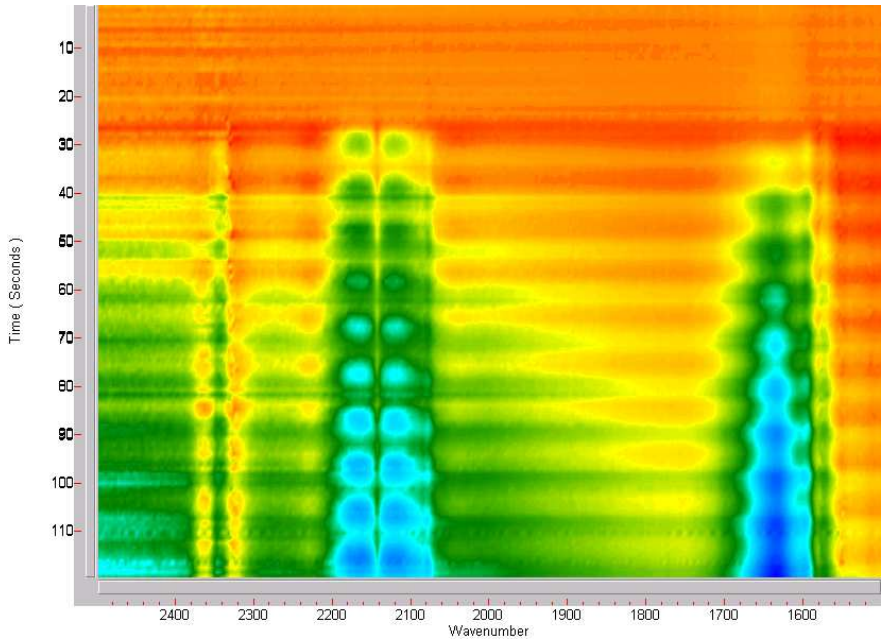

Figure 6.42: Oscillating microwave power infrared absorbance spectrum for CO and air over EUROPT-3 sample

Figure 6.43: Infrared absorbance spectrum for CO and air over EUROPT-3 sample at 90 s

presence of this negative peak may explain the lack of the thermal broadening side-peak on the right of the gas phase envelope. The CO_2 peaks remain at a reasonably constant value throughout the course of the experiment, although the rest of the spectrum shows a decrease, which suggests production of CO_2 through CO oxidation is occurring.

The strong negative peak at 1635 cm^{-1} is due to the desorption of water from the support, and shows two shoulders, one at 1574 cm^{-1}, and one at 1598 cm^{-1}. It is believed that both of these features are caused by the carbonate/carboxylate species previously described, and indeed the former peak has been observed in the other experiments. The development of the feature at higher wavenumber is restricted to this experiment, which may or may not be representative of the reactions on the sample. The increased heating effect obtained with the stub tuner may explain the absence of this peak, in the microwaved heated experiments that do not use it. However, the conventional heating experiment exceeds the heating caused by the tuned microwave without displaying this second shoulder. This initially suggests that the evolution of this second carbonate/carboxylate feature is enhanced with the application of microwaves. On closer inspection, the conventional experiments have shown that use of a single background for the absorbance spectra, over the extended heating range, causes the spectral baseline to shift and leads to aberrant spectra. It is possible that the second shoulder is obscured in the conventional heating results for this reason, and thus it can not be said whether this apparent increase is due to a microwave effect.

6.2.3 Liquid samples

The use of liquid solvents is unavoidable for many organic reactions, and their use in microwave synthesis is widespread [5]. A preliminary investigation into the influence of microwaves on the infrared spectrum of hexane (C_6H_{14}) and chloroform ($CHCl_3$) was therefore undertaken to assess the suitability of the microwave heated cell for the *in-situ* observation of liquid phase reactions.

The infrared absorbance spectra of the two solvents obtained in the microwave transmission cell are shown in Figure 6.44. The spectra show a number of strong absorbances due to the relatively large path length and saturation is seen for both liquids. Whilst the spectra have features widely spread across the spectrum, the do-

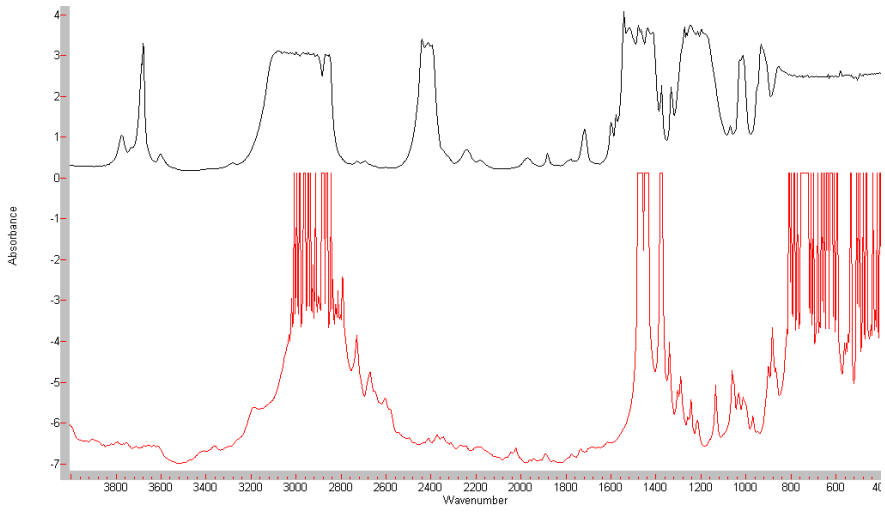

Figure 6.44: Full range mid-IR absorbance spectrum for hexane (red) and chloroform (black)

main between 2600 and 1600 cm^{-1} is relatively transparent for hexane, and chloroform displays only one moderately strong peak at 2420 cm^{-1}, between 2800 and 1620 cm^{-1}. It should not therefore be difficult to find an organic probe reaction that could be followed by IR spectroscopy in this region. The effect of heating on the pure solvents was examined in the same range as the gas and solid phase work, which encompasses much of the transparent region for these catalysts. Their spectra before irradiation are presented in Figure 6.45 to show the features in this region. Hexane shows weak peaks at 2015, 1894, 1777 and 1737 cm^{-1}, although these are close to the noise level. The absorbance significantly increases towards the right extreme of the spectrum, which is the lower portion of the CH_2 bending peak at 1472 cm^{-1}. The peaks contained within the region displayed correspond to incredibly weak absorbances, and vibrations that are not favoured. Consequently these are not generally assigned, as they account for only very minor features in the IR spectrum.

The chloroform shows a great deal more structure over the region under study, although most of these peaks are too diminutive to be of interest to the average spectroscopist. A saturated peak is visible at 2420 cm^{-1}, due to a C-H bending overtone, and a strong absorbance with its maximum at 1547 cm^{-1} is an overtone of the C-Cl stretch. This peak shows two shoulder peaks at 1580 and 1601 cm^{-1}, and these two large peaks bracket six unassigned peaks at 1721, 1781, 1884, 1973, 2181 and 2245

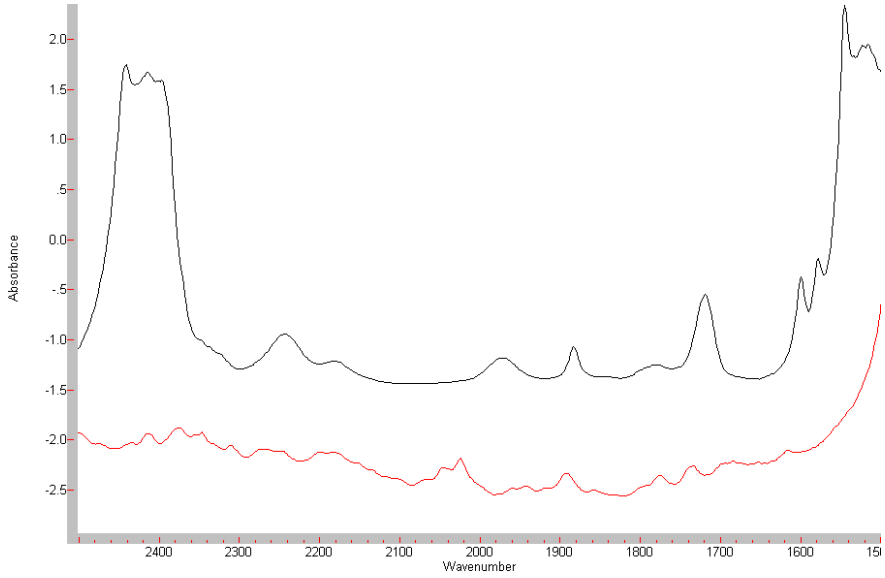

Figure 6.45: Working region IR absorbance spectrum for hexane (red) and chloroform (black)

cm^{-1}.

Hexane

The time resolved infrared spectrum of liquid hexane irradiated with the oscillating microwave power heating regime is displayed in Figure 6.46. The spectrum is steady and featureless before the application of microwaves at 25 s. When the sample is initially irradiated, noise develops across the spectrum as the absorbance signal becomes saturated, before dying away. The saturation recurs regularly, with a period of 10 s, according to the microwave power. Between the noisy sections when the detector saturates, it is possible to obtain spectra that have developed features which can be analysed. Spectra extracted from the time resolved data at 78 and 83 s are shown in Figure 6.47 and display the contrast between the noisesome and the placid spectra. The spectra shown are relatively noisy, but there are features that correspond to the peaks seen before irradiation, which demonstrate changes in the absorbances of these vibrations. There is a strong positive peak seen at 1737 cm^{-1}, and a two weakly positive peaks at 1777 and 1894 cm^{-1}. The other peak seen in the hexane spectrum of Figure 6.45 at 2015 cm^{-1} appears shifted to around 2031 cm^{-1}. The quality of the

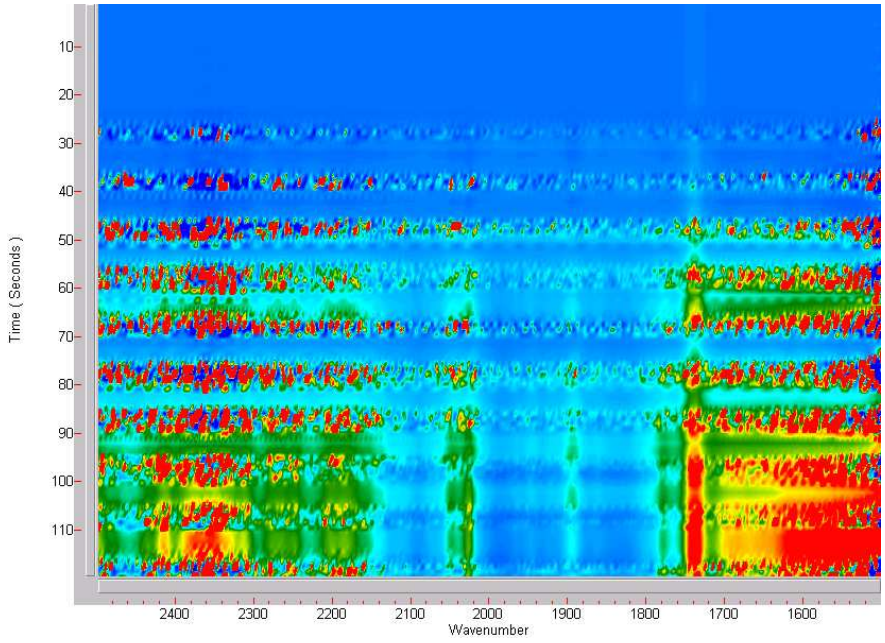

Figure 6.46: Oscillating microwave power IR absorbance spectrum for hexane

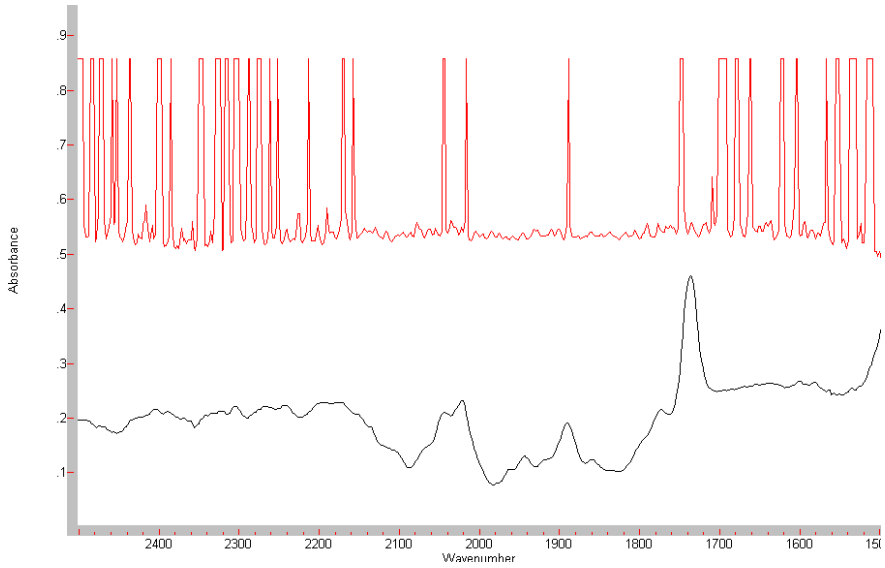

Figure 6.47: IR absorbance spectrum for hexane at 78 (red) and 83 s (black)

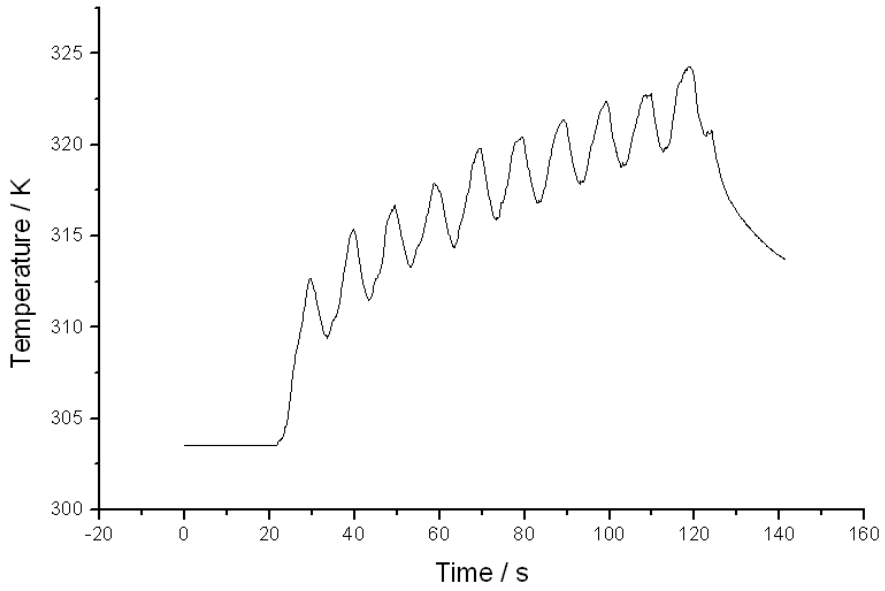

Figure 6.48: Recorded temperature for hexane under irradiation

spectra obtained prevent accurate measurements to be made, and the only phenomenon that may be confidently stated is the peak at 1737 cm^{-1}, which shows an increase in absorbance under microwave heating that is not replicated by the other peaks. It is possible that the peak at 1737 cm^{-1} is related to the peak observed at 1740 cm^{-1} for the tuned microwave heating of the CO sample. If there is a labile organic species which may be evolved under microwave heating, contact of the solvent with the cell interior may enhance this. It would appear that the microwave heating under these conditions is causing a leaching of some component into solution, or reacting with some contamination present in the cell.

Although the spectrum is very noisy, clear oscillations at 0.1 Hz frequency can be observed, with the region between 2150 and 1800 cm^{-1} being relatively transparent. The temperature recorded for this experiment is displayed in Figure 6.48, where the application of microwave energy can be seen initiated at approximately 20 s and ceased at 120 s, after the infrared data collection is complete. The character of the oscillating temperature profile is similar to that seen for the solid and gas experiments, with an oscillation allied to a general rise over the course of the experiment. A normal rising edge heats the sample *circa* 5 K, although there is a marked difference in the

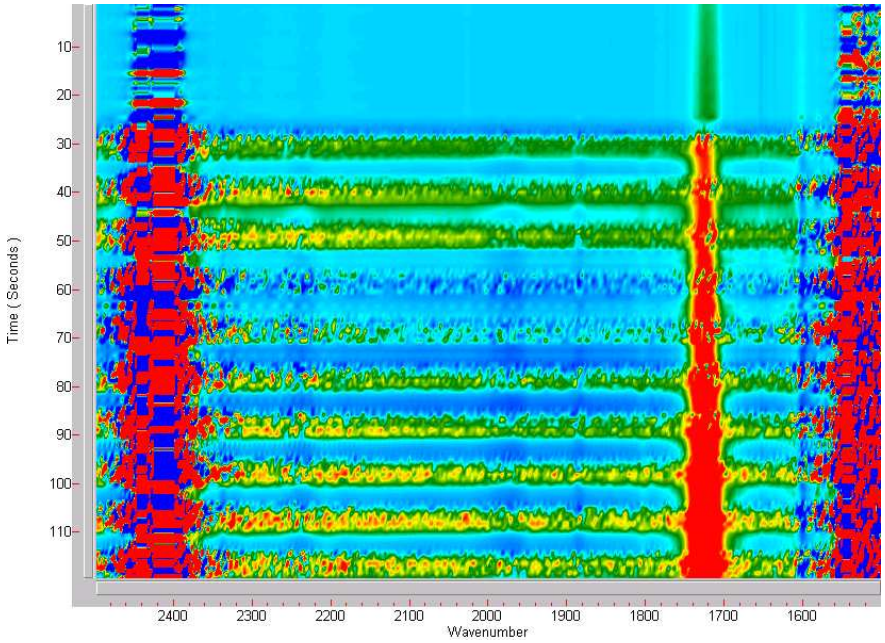

Figure 6.49: Time resolved IR absorbance spectrum for chloroform under irradiation

first rising edge when the microwave is initially applied. The temperature recorded by the thermocouple jumps around 10 K when the microwaves are enabled, and when the microwave power is cut at 120 s, the temperature shows an apparent exponential decay. This form suggests that there is no electrically induced effect with the thermocouple, as it follows a natural exponential cooling curve. Assuming this is true, the temperature jump when the radiation is enabled suggests that the microwave apparatus gives a power surge when generation is initiated. The peak temperature obtained for hexane was 324 K, showing a maximum 21 K rise during the experiment.

Chloroform

The time resolved kinetics IR absorbance spectrum obtained with chloroform can be seen in Figure 6.49 and exhibits similar 0.1 Hz oscillations to the hexane sample across the spectrum. The large peaks in the absorbance spectrum around 2420 and 1520 cm^{-1} cause a large amount of noise in the spectrum, even before the application of microwaves. The peak at 1721 cm^{-1} is also visible, but is stable for the first 25 s. The heating caused by microwaves results in growth of the peaks in these three positions,

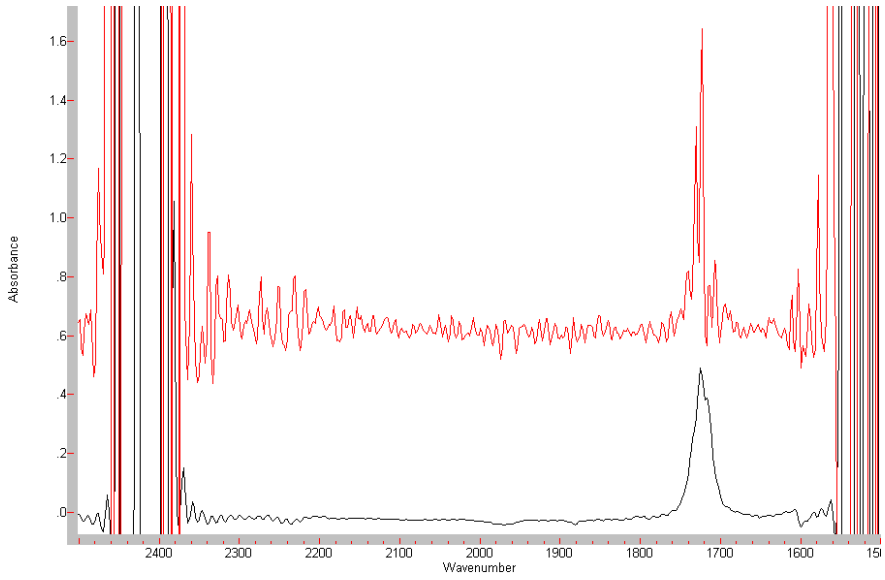

Figure 6.50: IR absorbance spectrum for chloroform at 78 (red) and 83 s (black)

with the two outer peaks causing a wider saturated region as the experiment progresses. The peak at 1721 cm^{-1} also becomes larger, but does not become noisy, showing a similar effect to the 1737 cm^{-1} peak in the hexane, although much stronger. It may be that the peak due to the suggested leaching or contamination product is shifting due to the different chemical environment of the solvent, or causing a different product in its reaction with the solvent. Whatever the reason for the peak shift, this effect is much greater in the chloroform than the hexane, suggesting that the process occurs more efficiently with this solvent. The rest of the spectrum shows oscillation across the entire range, which provides a relatively clear region for examination of compounds in solution between 2300 and 1800 cm^{-1}. Absorbance spectra extracted from the time resolved kinetics spectra at a peak (78 s) and a trough (83 s) are shown in Figure 6.50 and display this flat baseline clearly.

The temperature profile recorded is similar to hexane, as can be seen in Figure 6.51. The temperature gain on each rising edge is much greater than for hexane, with *circa* 10 K each cycle. The peak temperature of 336 K is also higher than obtained with hexane, showing an overall temperature rise of 33 K. This demonstrates that the chloroform couples more effectively with the microwave radiation at 2.45 GHz, the microwave frequency under study. This result is in keeping with the measured dielectric loss

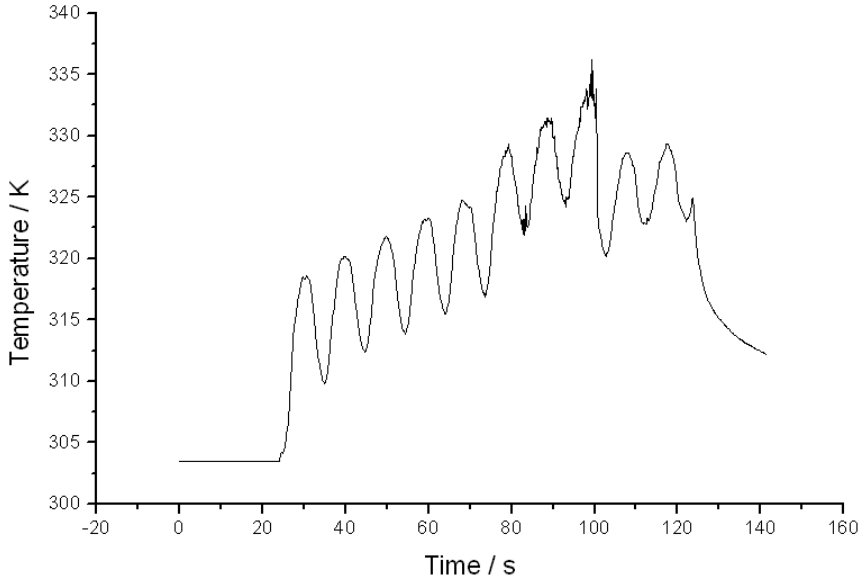

Figure 6.51: Recorded temperature for chloroform under irradiation

($\tan\delta$) of the solvents, with chloroform having a value of 0.091, and hexane, 0.020 at room temperature and 2.45 GHz [77].

6.3 Conventionally heated emission IR

A body in equilibrium with its surroundings which is absorbing infrared radiation will also be emitting it, and with the same wavelength [65]. The spontaneous emission of infrared radiation from materials may be collected and analysed to obtain spectroscopic information in a similar manner to transmission measurements. In addition, the strength of emission is strongly temperature dependent and may be used as a method of thermometry.

6.3.1 CO

As materials emit in the infrared spectrum at temperatures above absolute zero, the collection of emission spectra is theoretically possible at virtually any temperature. However, collection of spectra is usually carried out under heating to avoid interference by radiation that is emitted from the surrounding environment at ambient temperature. In the experimental setup used for these experiments, the data is complicated by

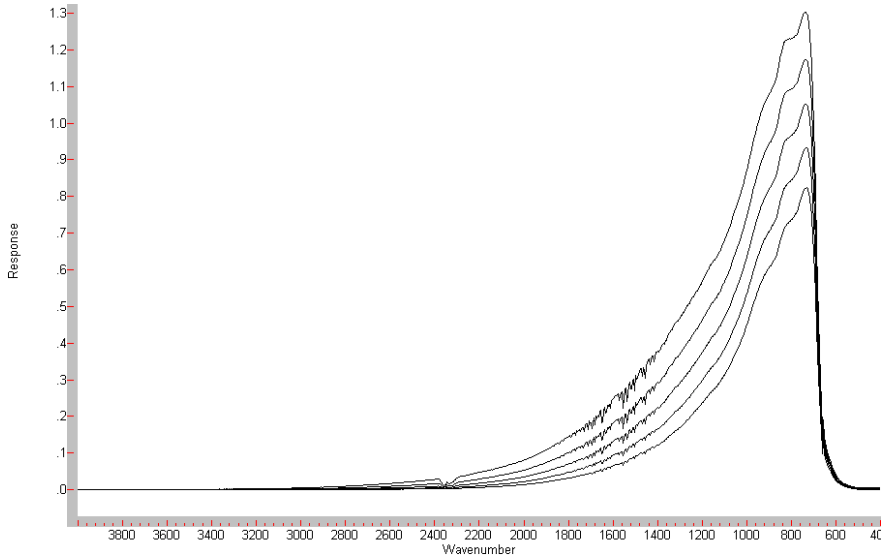

Figure 6.52: Emission IR spectra obtained for CO between 323 and 423 K at 25 K intervals

surrounding the sample of interest with the other heated elements that make up the cell body. A series of single beam spectra of CO in the transmission cell obtained at 25 K intervals between 323 and 423 K, are shown in Figure 6.52. The spectra show an increase in intensity and a shift to higher wavenumber in the peak maximum as heating occurs, but this is not as great as would be expected. What these changes do demonstrate however, is that heating is occuring and that it is possible to observe this with the spectrometer and emission optics. Figure 6.53 displays calculated spectra for a black body over the same temperature range as the sample, and demonstrates the differences caused by the ambient temperature background, the emission from the heated cell and the non-linearity of the detector. Whilst vibrations due to CO are not immediately obvious in the collected emission spectra, it is possible to observe features due to gas phase CO_2 and water. As these peaks appear negative, these features are due to the species absorbing IR, and not emitting. The genesis of these peaks is the purge gas in the spectrometer absorbing the light emitted by the cell. The beam path through the spectrometer is approximately 2 m, which results in strong absorbances for these atmospheric features. The optical path through the cell is 3 mm, thus dramatic variations will need to occur within the cell to appear this strongly in the emission spectrum. To maximise the emission features due to the species of interest, back-

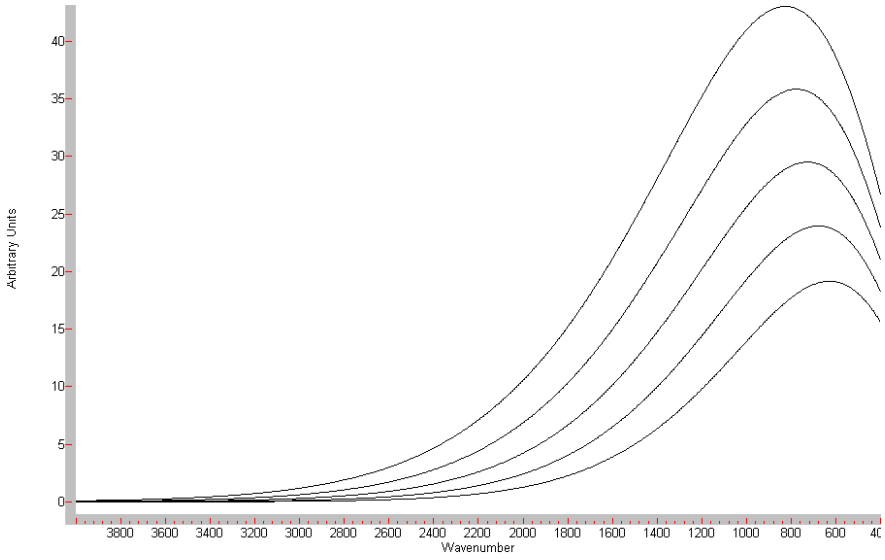

Figure 6.53: Calculated black-body spectra between 323 and 423 K at 25 K intervals

ground spectra are obtained with the same sample, at the same temperature, in a helium atmosphere. This unfortunately leads to a significant time difference between the sample and background spectra, but this method was found to have the greatest sensitivity. Consequently spectra are plotted as an absorbance function, in which any absorbance occurring will give positive peaks, whilst emission at a point will lead to negative features.

Figure 6.54 shows the spectrum obtained for CO at 423 K using this method, as maximum signal to noise ratio is obtained at the highest temperature due to the increased emission. A doublet of negative peaks appear in the spectrum centred at 2142 cm^{-1} which increase with temperature due to the IR emission from the CO stretch. There is also some variation of the peaks due to CO_2 at 2348 cm^{-1}, which is probably due to variation of atmospheric CO_2 in the body of the spectrometer or accessory.

6.3.2 CO and Air

When air is added to the flow through the reaction cell (Figure 6.55), the features due to CO_2 present in the air flow are immediately obvious, with well defined negative peaks present. This could be due either to the CO_2 in the cell emitting, or due to the purge gas variation. Towards the left of the feature at 2382 cm^{-1} a positive peak

Figure 6.54: Emission IR spectrum for CO at 423 K

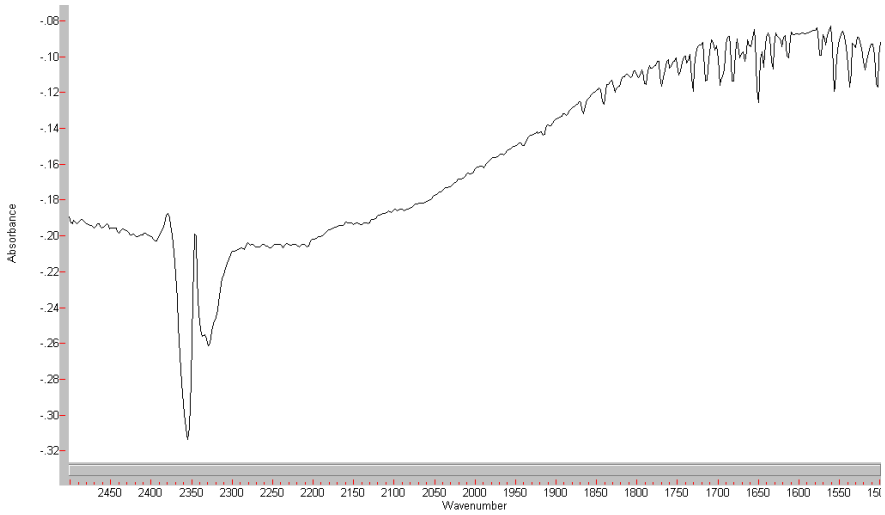

Figure 6.55: Emission IR spectrum for CO and air at 423 K

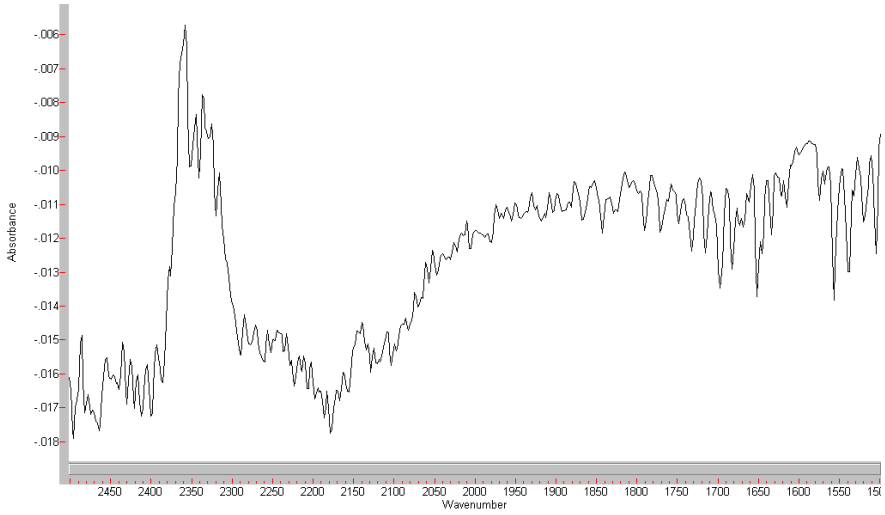

Figure 6.56: Emission IR spectrum for CO and air over silica at 423 K

has formed. This may suggest thermal broadening, but this characteristic shape would only appear if the background showed CO_2 peaks. As CO_2 is obviously present in the purge gas, this would not be an unreasonable interpretation, were it not for the fact that this postive peak does not appear on the other edge of the peak structure. The P-branch does show an unusual peak shape, suggesting that the positive feature is due to a miscancellation effect, rather than peak broadening. The carbon monoxide doublet is also present, but shows weak positive peaks, suggesting that the CO is acting as a net absorber of IR. The light that is detected is being emitted from a number of places, and whilst the optics should maximise the collection of light from the sample, it cannot be guaranteed. The gauze covering the windows will emit radiation, and for the light emerging from the gauze furthest from the spectrometer bench, this will have travelled through the sample cavity in the cell. The CO inside the sample cavity has absorbed the wavelengths of light that correspond to the CO stretching vibration, thus this shows as an absorbance in the spectrum, rather than an emission.

6.3.3 Silica

The spectrum obtained with the presence of a silica disc in the emission apparatus is shown in Figure 6.56 and appears to show the inverse of the results obtained when no solid sample is present. The CO shows negative peaks, which suggests that the sample

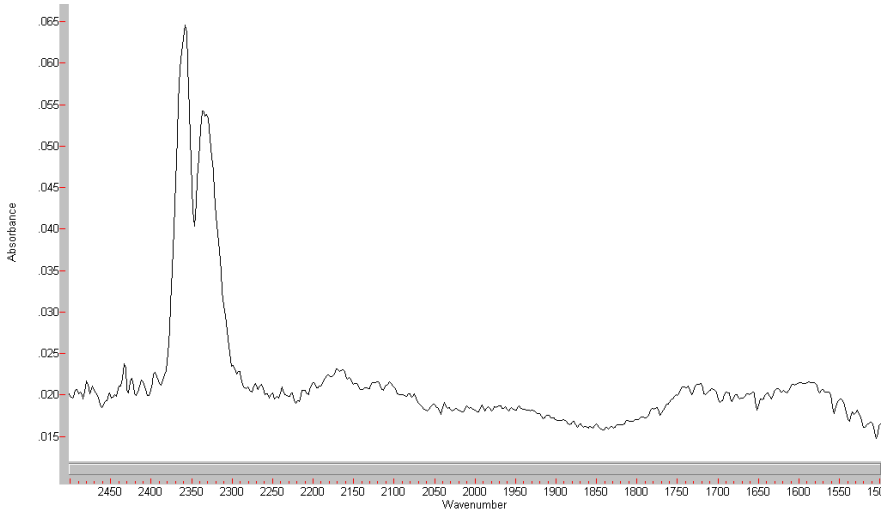

Figure 6.57: Emission IR spectrum for CO and air over Al_2O_3 at 423 K

is emitting, and the CO_2 has positive peaks. The peaks due to CO are only visible at high temperatures, which is further evidence that the CO peaks are due to emission from the gas, whilst the CO_2 peaks are visible at all temperatures and are likely to arise from miscancellation in the purge. It should also be noted that the effective path length of the cell has significantly decreased with the addition of the solid. Emission is only likely to be detected from the solid surface of the catalyst facing the detector, and the gas phase also on this side of the disc. Light emitted on the other side will be absorbed by the catalyst wafer, and not reach the detector.

6.3.4 Alumina

A spectrum obtained with the alumina sample present is shown in Figure 6.57 and displays strong positive peaks for CO_2 and weaker positive peaks for CO. The fact that both of these peaks are positive indicate that the gases are absorbing the light emitted by the solid sample. The lack of emission observed from the gas phase illustrates the difficulties in using this technique to obtain spectral information, as whether a species appears to absorb or emit does not seem to fit any pattern. The limitations of the experimental set up mean that the optimisation of the cell position and alignment to achieve the highest signal strength does not always coincide with the signal from the sample under study.

Figure 6.58: Emission IR spectrum for CO and air over EUROPT-1 at 423 K (red) and 378 K (black)

6.3.5 EUROPT-1

EUROPT-1 shows an interesting change in peak structure when heated, as can be seen in Figure 6.58. Below 378 K strong positive peaks from CO_2 are present, but no CO peaks are visible. Above this temperature, negative peaks due to both species develop. This behaviour is interesting as it shows the reversal of the peak direction of the CO_2. The change in direction suggests that there is an increasing CO_2 pressure, which would be expected if the CO oxidation was occuring. Although this clearly fits in with experience and the IR data collected in transmission, the noise associated with the emission method prevents unequivocably assigning this effect to CO oxidation, although the postulation that this has been observed is reasonable.

6.3.6 EUROPT-3

The behaviour of the EUROPT-3 system is presented in Figure 6.59 and shows similar results to those obtained from the EUROPT-1 catalyst. At low temperature the only species apparent is CO_2, showing large positive peaks. As the temperature rises, these peaks decrease in intensity, and negative peaks due to CO become visible. This decrease in the CO_2 absorption suggests that the oxidation is occuring. Furthermore, the CO_2 peaks do not become negative for the EUROPT-3 experiment, which suggests that

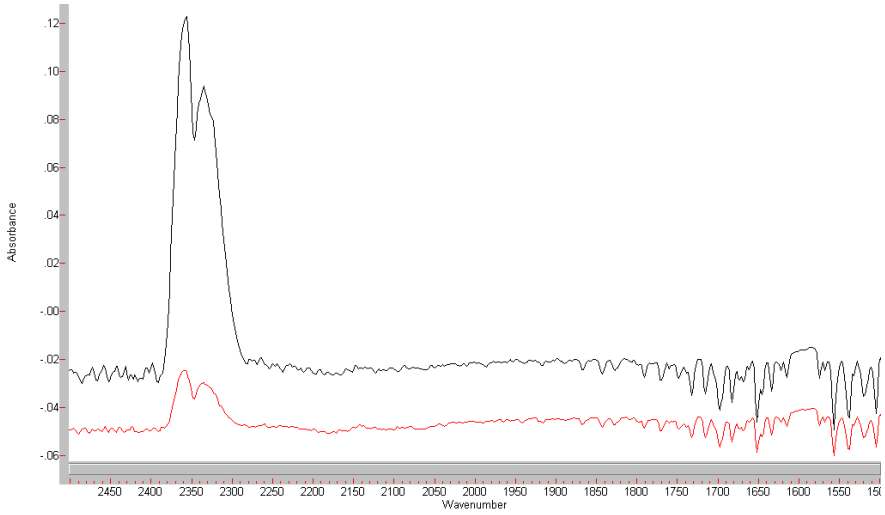

Figure 6.59: Emission IR spectrum for CO and air over EUROPT-3 at 423 K (red) and 378 K (black)

the magnitude of CO oxidation is reduced over the catalyst containing less platinum. Although this interpretation fits with the expected data, it is presented tentatively due to the low signal to noise available using the apparatus in this configuration. Decreases in absolute peak strength, whether absorption or emission, only occur in the platinum containing catalysts. For the other samples, increases are associated with increased temperature, which are presumably due only to the increased light intensity reaching the detector. The presence of features over the active catalysts which show a decrease under heating adds further evidence that these effects are legitimate rather than artefacts.

6.4 Microwave heated emission IR

To maximise the response in the time resolved microwave heated spectra, a background spectrum was collected under the reacting gases immediately before the application of the microwave power. This gave the greatest sensitivity to any changes and allowed the observation of weak peaks.

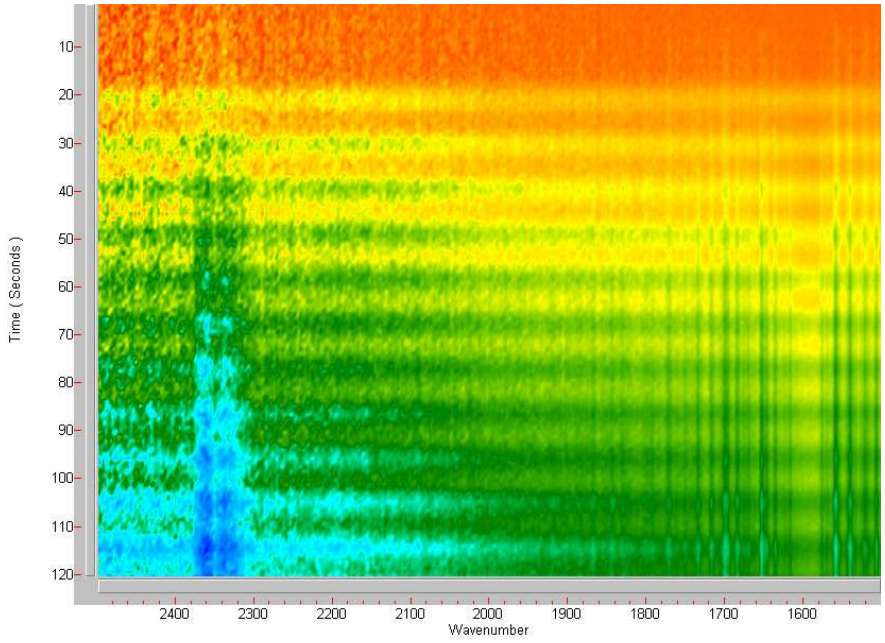

Figure 6.60: Oscillating microwave power infrared emission spectrum for CO

6.4.1 Carbon monoxide

It would be expected that the only feature observed when CO was passed through the cell would be due to the CO stretching vibration at 2143 cm^{-1}. However, this is not what occured with the emission spectra collected, as can be seen in Figure 6.60. The absence of features in the first 20 s of the spectrum shows that the system is stable before the application of microwaves. Once the irradiation is enabled, the intensity of the spectrum can be seen to oscillate with the applied microwave power across the entire spectral range. The oscillations increase in amplitude as the wavenumber decreases and the emission intensity increases, as shown by the decreased baseline values. This emission increase demonstrates that at least some part of the apparatus is heating, although it is not clear where the increased emission detected is originating. The fact that the increased emission shows oscillations at 0.1 Hz suggests that whatever the emitter is, it can gain and lose heat rapidly enough not to significantly damp the temperature modulation. The source of the emission is therefore not likely to be the applicator plates, but may be for example, the Ni gauze covering the windows. Deviations from the banding across the spectrum are visible due to CO_2 at 2349 cm^{-1}

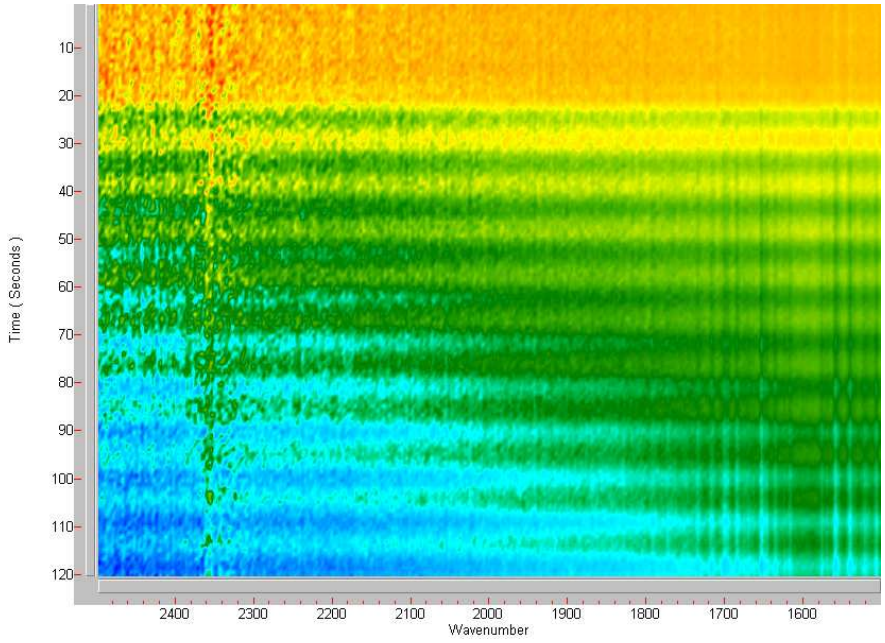

Figure 6.61: Oscillating microwave power infrared emission spectrum for CO and air

and the rotational structure of water centered around 1596 cm^{-1}. These can be seen becoming more intense as time elapses after the microwaves have been applied. The amplitude of the oscillations within the carbon dioxide and water peaks is the same as that seen in the background, with the downward trend over time appearing unconnected. The slight change in these species is likely to result from variation in the purge gas and serves to highlight the diminutive scale of the legitimate changes that occur in the spectrum. Whilst the spectral features are similar across the range of temperatures studied, the emission signal increases with temperature, resulting in a better signal to noise ratio as the experiment progresses.

6.4.2 Carbon monoxide and air

The spectra obtained when air is added to the gas flow are similar to those obtained with pure CO. A representative spectrum is shown in Figure 6.61 and oscillation across the entire spectrum is again seen, interrupted by features due to CO and H_2O. The oscillations are again obviously due to the microwaves, as the spectrum is featureless before their application at around 20 s. The variation seen in the purge gas is reduced

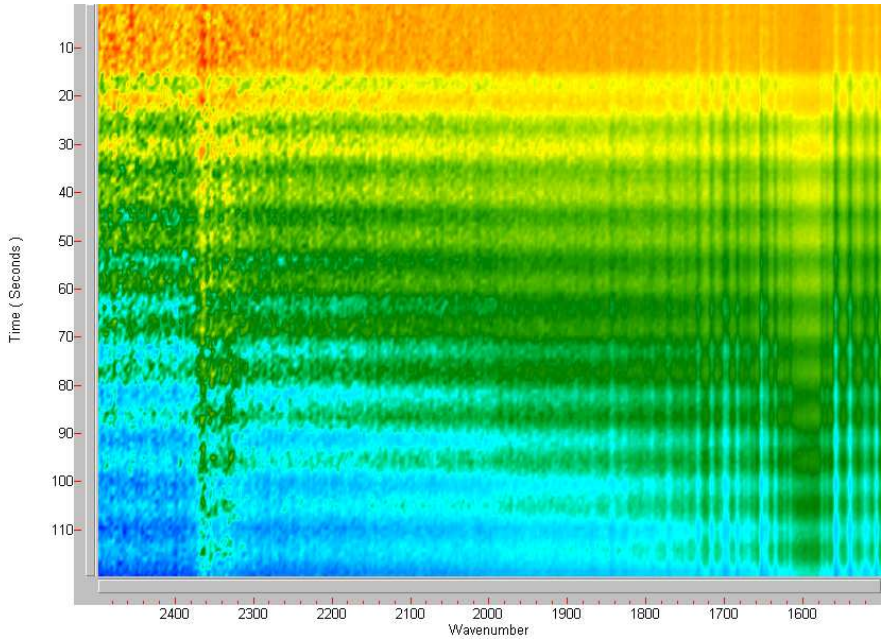

Figure 6.62: Oscillating microwave power infrared emission spectrum for CO and air over SiO_2

in this experiment, with reduced CO_2 and H_2O influence in the infrared spectrum.

6.4.3 Silica

The introduction of a solid sample to the cell presents a more efficient IR emitter in the sample position. The results obtained show a much higher overall signal detected which suggests that the emission accessory is reasonably effective at collecting radiation from the sample cavity. The quality of the collected spectra is not significantly increased however, with similar results to the pure gas samples. This can be seen in Figure 6.62, which shows the time resolved kinetics spectrum for the microwave heating of SiO_2. The spectrum again shows 0.1 Hz oscillations once the microwave power is enabled, with noise due to CO_2 and H_2O present.

6.4.4 Alumina

The alumina sample (Figure 6.63) shows the strong oscillation across the spectral range common to the previous samples, and a particularly pronounced emission increase in the CO_2 signal. This is once again likely to be associated with the purge variation, as

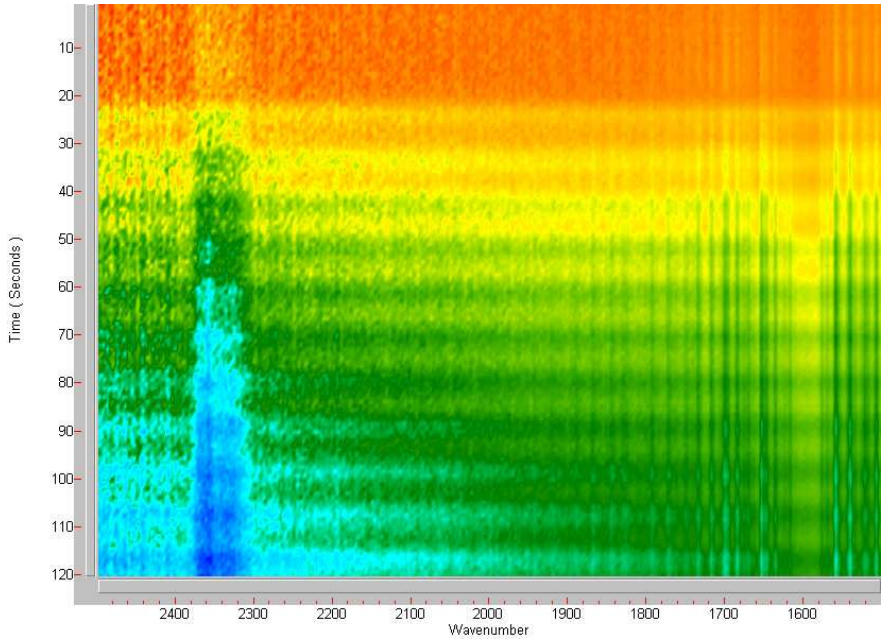

Figure 6.63: Oscillating microwave power infrared emission spectrum for CO and air over Al_2O_3

the oscillation amplitude is similar to that of the baseline, and no Pt is present for the catalytic reaction to occur on. The gas phase water signal shows a similar response, further suggesting that these features are linked through the purge atmosphere and are independent of the applied microwave power.

6.4.5 EUROPT-1

The EUROPT-1 sample shows similar results to those obtained with the other systems, with a typical spectrum shown in Figure 6.64. The EUROPT-1 sample shows a similar strong CO_2 emission increase to the alumina sample, which although could be attributed to the increased presence of CO_2 from the oxidation reaction, is likely to be due to the miscancellation gas in the environment. No loss of CO associated with the CO_2 oxidation is observed in the IR, which would be apparent if the spectra were representative of the environment within the cell. The water peaks are also showing an absorption decrease that correlates with the CO_2 loss, which further suggests the origin of the effect to be variation of the atmospheric gases in the beam path.

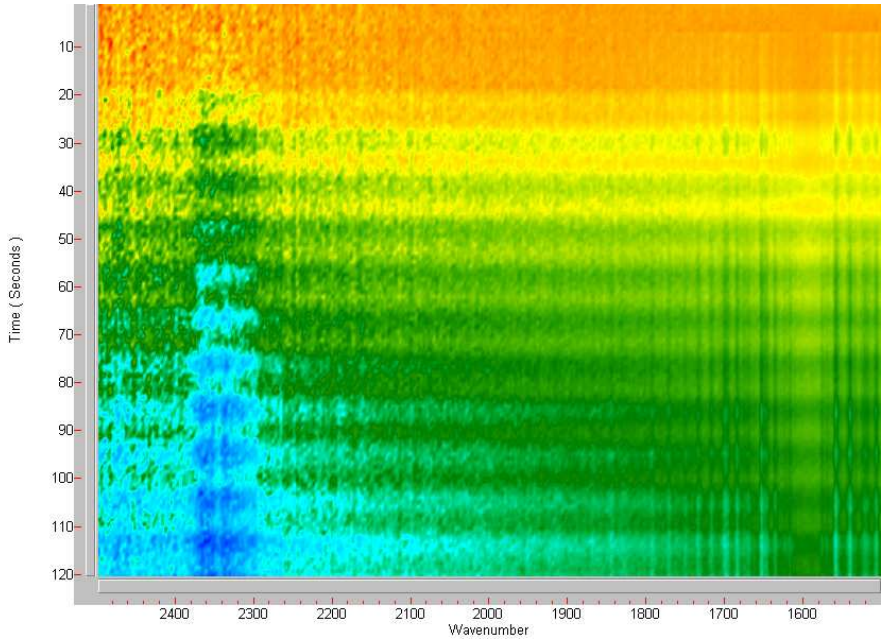

Figure 6.64: Oscillating microwave power infrared emission spectrum for CO and air over EUROPT-1 catalyst

6.4.6 EUROPT-3

The spectra obtained when EUROPT-3 discs are used in the emission accessory are consistant with those obtained with all the other materials, showing CO_2 and H_2O present with a strong oscillation across the entire spectral range. A sample spectrum is given in Figure 6.65.

6.5 Mass spectrometry

The mass spectrometry results obtained with the reacting gases by themselves and over the pressed disc samples heated conventionally and by microwave power are presented. Analysis of the gases exiting the cell provides information regarding the processes occuring within the microreactor. The results obtained with the mass spectrometer for the pure CO sample are not presented as the low flow rate associated with these experiments is not sufficient for accurate results. The spectrometer pumps gases from the intake capillary into the vacuum system and at low flow rates atmospheric gases are introduced in addition to the cell exhaust. This 'back-sampling', as it is known, presents

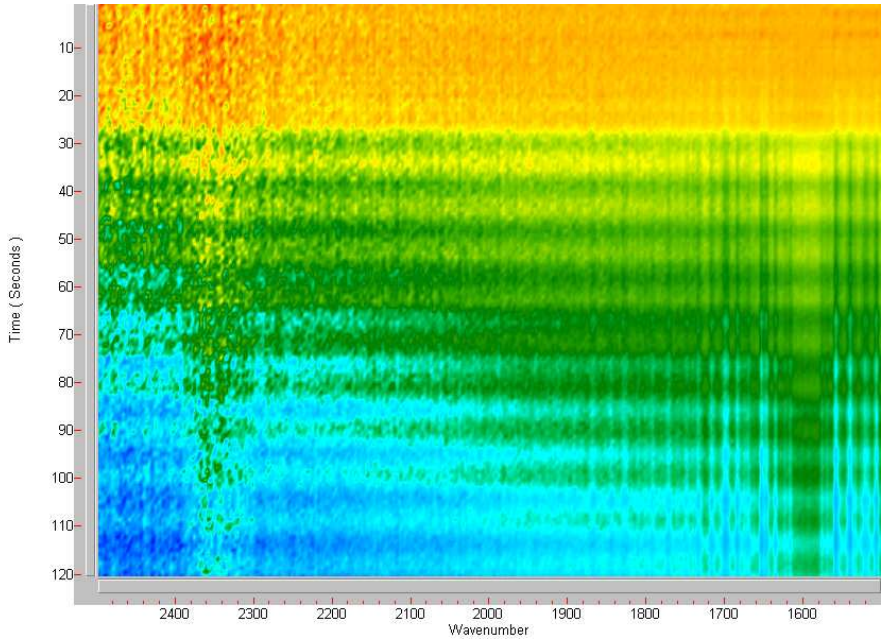

Figure 6.65: Oscillating microwave power infrared emission spectrum for CO and air over EUROPT-3 catalyst

wayward results for the pure CO sample, although the higher flow rates associated with the other experiments can supply the necessary intake rate the instrument requires.

6.5.1 Conventional heating

The mass spectrometry results obtained through conventional heating of samples in the transmission cell are presented in Figures 6.66 to 6.70 and are grouped by mass analysed.

The variation of mass 18 is shown in Figure 6.66 and shows that the detection of water as the experiment progresses is similar for all the samples. Both a heating and cooling phase are presented, with a sharp initial increase followed by a reduction with increasing temperature and time. This can be interpreted as the desorption of water from the samples, which would display the profile shown. Initially a rise in pressure is seen as the increased temperature desorbs water from the solid, resulting in the presence of more gas phase water. Above 330 K, a decrease in pressure is seen as the rate of water evolution from the sample drops below the rate of water exiting the cell in the gas exhaust. The CO/air sample shows the smallest decrease in pressure as the

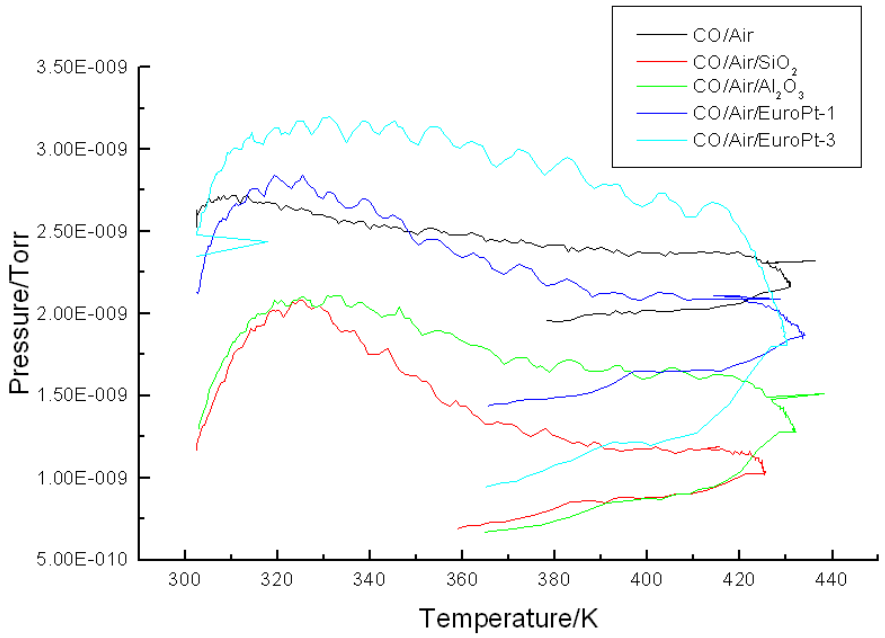

Figure 6.66: Variation of mass 18 under conventional heating

water present is only desorbing from the cell walls. Some oscillatory character can be observed in some of these traces, which is believed to be due to the method of heating, where temperature was not smoothly ramped, but the voltage to the electrical heaters was periodically raised. All samples show a continued decrease on cooling, showing irreversibility as the lost water is not regained.

Due to the nature of data collection by the spectrometer, the results of the variation of mass 28 displayed in Figure 6.67 are rather noisy. It should be remembered that mass 28 represents both the CO reactant and the N_2 in the air used as oxidant. It would not be expected that the level of inert nitrogen would change during the reaction, hence any change in the trace should be due to variations in CO pressure. All of the experimental traces show an slight increase over the course of an experiment, even after cooling is initiated, demonstrating either an irreversible change occuring, or drift in the experimental results. This is much more pronounced for the solid samples of SiO_2, Al_2O_3 and EUROPT-1. The fluctuation within an experiment is significantly lower than the variation between experiments, and not much greater than the noise level. In addition to this, the mass 28 signal is considerably larger than the change expected,

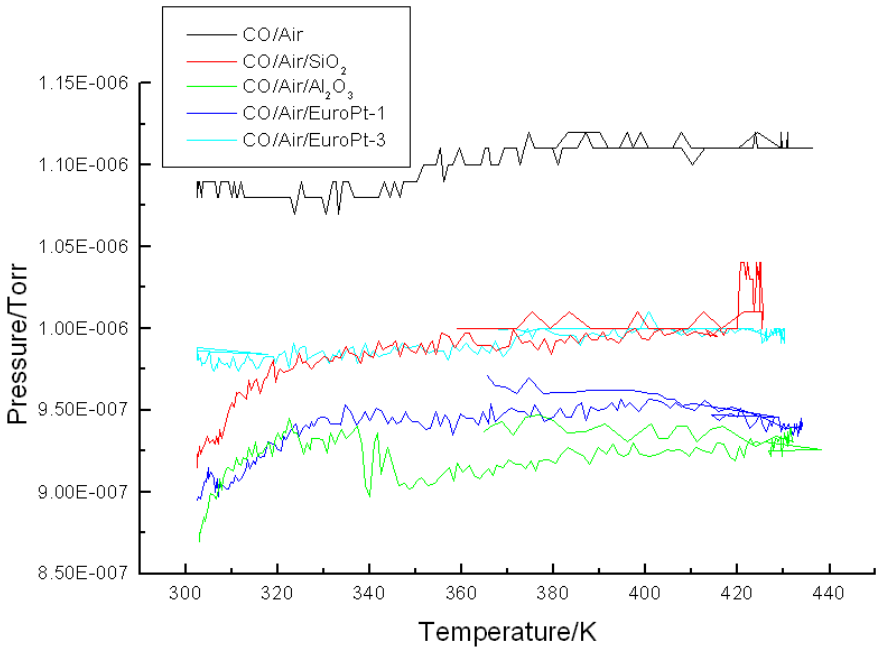

Figure 6.67: Variation of mass 28 under conventional heating

such that the difference is a vanishingly small fraction of the overall peak. It would therefore be difficult to assign any change in the CO pressure with confidence.

The mass 32 results can be seen in Figure 6.68, which shows similar trends to those seen in the mass 28 traces. All samples except EUROPT-1 again show an irreversible increase in signal, with a significant early increase when the solid present is SiO_2, Al_2O_3 or EUROPT-1. The general trend is barely above the noise level present, and does not warrant further discussion. There is however, a marked decrease present at higher temperatures in the mass 32 trace over EUROPT-1. This decrease is presumably due to its consumption in the oxidation reaction. A similar decrease was not seen for mass 28 as a much greater absolute change would need to occur to give the same proportional change, and the nitrogen from the air masks this.

Since the reaction being studied is the oxidation of CO to CO_2 in air, it would be expected that the greatest difference between catalysts would be observed in the production of CO_2. This is indeed the case, as can be seen in Figure 6.69. The EUROPT-1 with its high Pt loading is by far superior to the other samples as its CO_2 trace dwarfs that of the other samples. The oxidation reaction occurs on the Pt

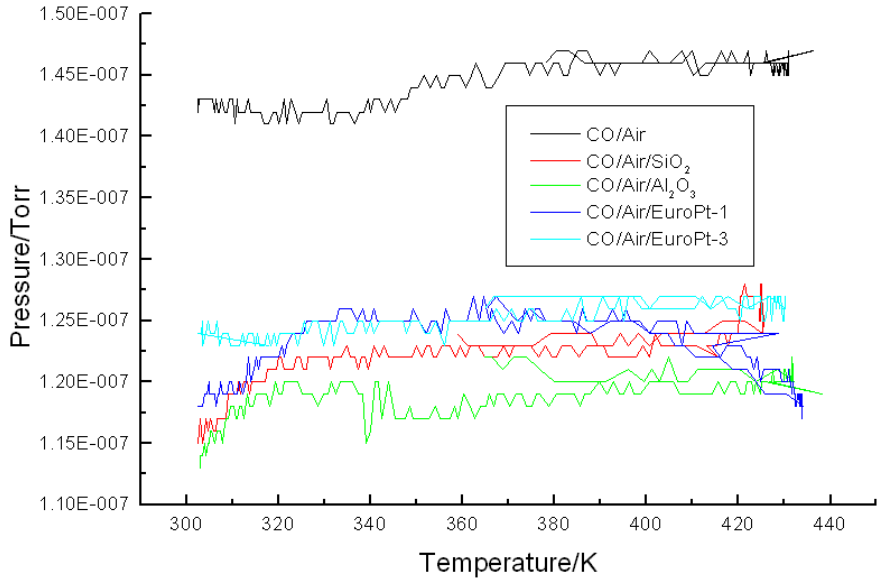

Figure 6.68: Variation of mass 32 under conventional heating

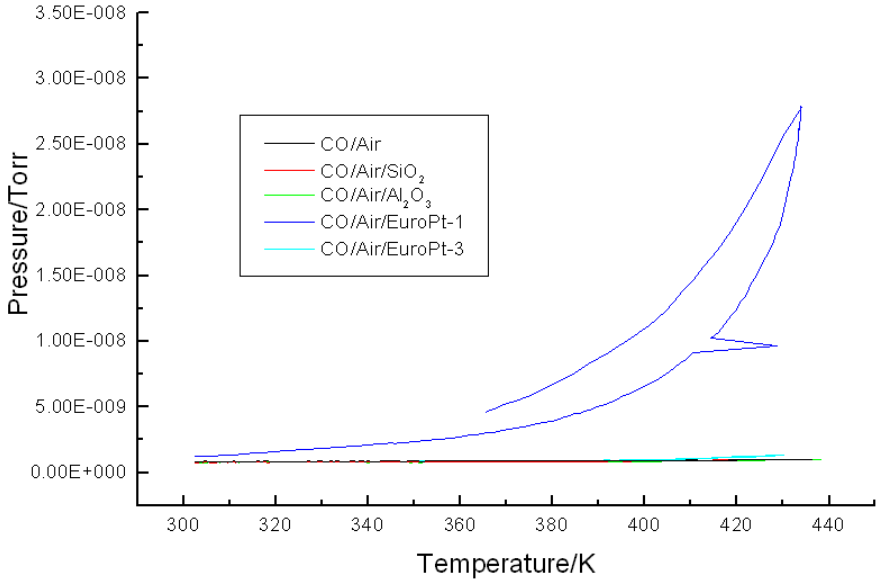

Figure 6.69: Variation of mass 44 under conventional heating

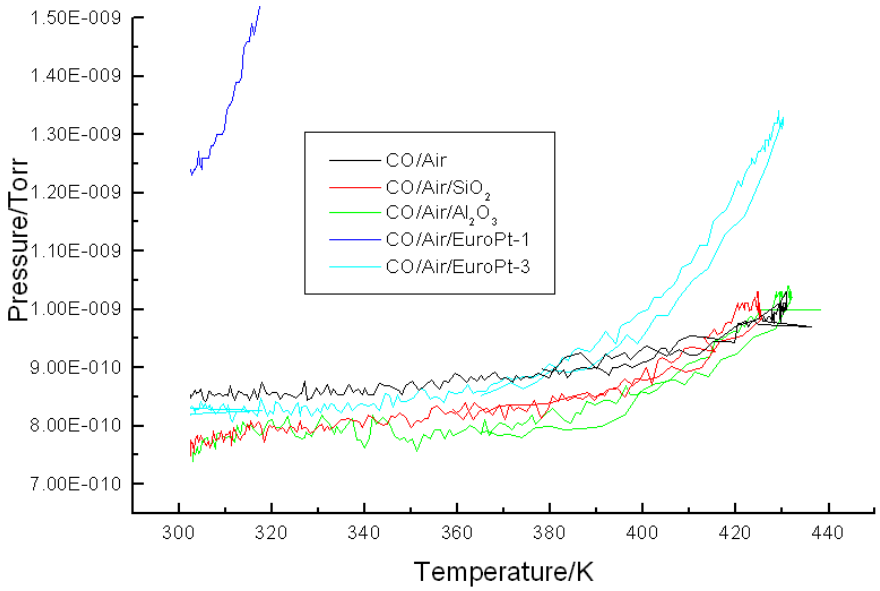

Figure 6.70: Variation of mass 44 under conventional heating (expanded view)

surface, thus the greater Pt loading gives a greater area for the reaction to occur on. An anomolous data point appears on the heating cycle for this trace, and higher activity is seen upon cooling. This hysteresis is due to the exothermic reaction sustaining the increased CO_2 production as the sample cools. An expanded view to analyse the CO_2 production from the other samples is presented in Figure 6.70. EUROPT-3 shows the second greatest CO_2 production, whilst the CO_2 production over the support materials and when no solid is present is similar for the reacting mixture. Although some CO_2 is produced when there is no Pt present in the system, the amount is not dependant on the presence of a solid sample in the cell. This confirms that the reaction is occuring on the Pt of the catalytic materials and not on the SiO_2 or Al_2O_3 supports. The CO_2 produced when no Pt is present is likely to be occuring at a hot surface, either on the Ni gauze covering the windows of the cell, or the walls of the cell body exposed to the reactant flow.

6.5.2 Microwave heating

Each individual experiment under microwave heating was carried out over a much reduced time and temperature range compared to the conventional heating, although a

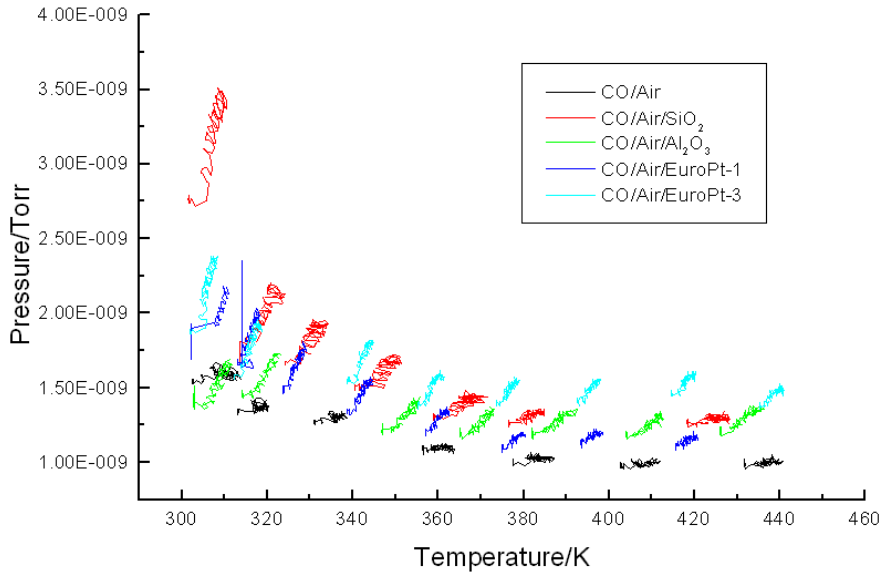

Figure 6.71: Variation of mass 18 with temperature under microwave heating

number of initial temperatures were used for each sample studied. This allows analysis of the gases evolved both within each two minute run under the oscillating microwave power and between these runs to be made. The results obtained under microwave heating of the reaction are presented in two sections, with those using the stub tuner separate from the experiments without impedance matching. Analysis again focusses on the differences between the samples and is grouped by mass signal.

Without stub tuner

Figure 6.71 shows plots of the mass 18 traces obtained for all samples under microwave heating without impedance matching. Each cluster of points represents a two minute time span under oscillating microwave power, and each colour represents a different sample in the apparatus. All samples demonstrate similar behaviour, although of varying strength. Where the trend is downward with conventional heating, the microwaves cause an increase, which results in the best-fit line followed by each cluster deviating significantly from the overall trend line.

The first few data points in each trace are collected under isothermal conditions, to ensure that the sample is stable, before the microwave pertubation is introduced. The initiation of irradiation causes a rise in both temperature and the partial pressure of

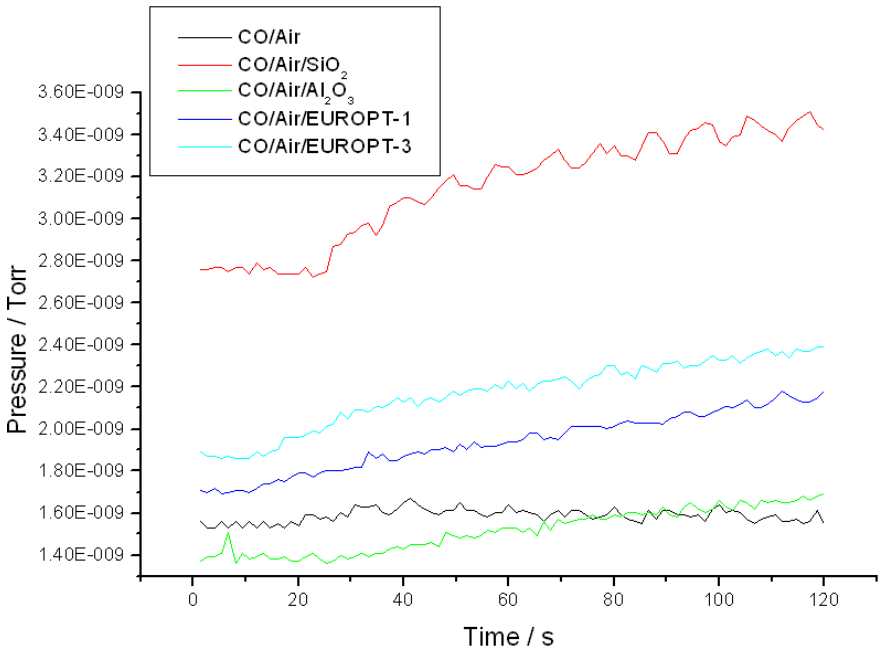

Figure 6.72: Variation of mass 18 with time under microwave heating

water, as the heating causes desorption of the water present. The greatest pressure rises are seen at the lowest temperatures, which correspond to the earliest experiments, and much less pronounced increases are seen at higher temperatures, as the water on the solid surfaces has been depleted by the previous treatment. The CO/air sample again shows the lowest pressure rise due to the absence of the water contained in the pressed wafer samples. The conventional heating trend, represented by the data collected before irradiation, shows a downward slope for all samples. This shows that the pressure of water is reduced in subsequent runs, due to its depletion under microwave heating, in addition to the loss of pressure seen conventionally.

A sample of the results obtained for each two-minute microwave experiment is shown in Figure 6.72 which shows the evolution of the mass 18 signal for all samples at the lowest recorded temperature. All samples show an increase when placed under the influence of microwaves. The solid silica sample has the highest water signal and shows strong oscillations at 0.1 Hz. The other samples also show suggestions of some oscillatory character.

The results obtained from following mass 28 for all samples are displayed in Fig-

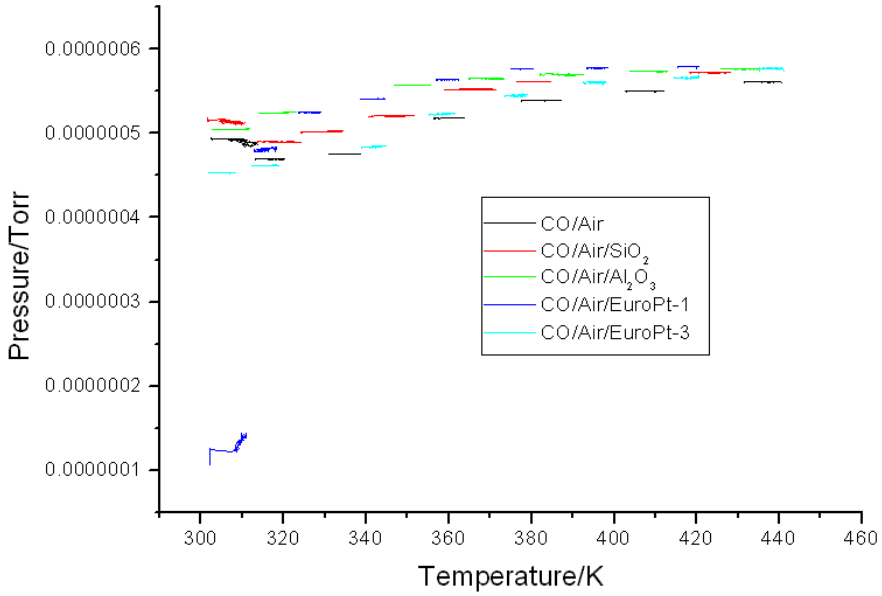

Figure 6.73: Variation of mass 28 with temperature under microwave heating

ure 6.73. For all of the samples the variation both within and between clusters is relatively slight. A small increase can be seen between clusters due to conventional heating, although the overiding trend within the clusters themselves is flat, resulting in only a minor difference in angle between the in-cluster trend and the between-cluster trend. This shows that any changes in mass 28 caused by the reaction are masked by the relatively high pressure of N_2 and CO.

The pattern shown by mass 32 is similar to that displayed by mass 28, as can be seen in Figure 6.74. The samples show minimal variation in mass 32 under both conventional and microwave heating, although the change under conventional heating again appears greater than that seen within each microwave cluster. The low conversion obtained for these experiments means that any decrease in mass 32 is below the threshold of observation.

The production of CO_2 can be followed by monitoring the pressure of mass 44 as displayed in Figure 6.75. The data from EUROPT-1 shows that the microwave and conventional heating show similar effects, as both the in- and between-cluster trends have the same gradient at each point. As previously, the EUROPT-1 result overwhelms the other data, and an expanded section of the lower portion of this plot

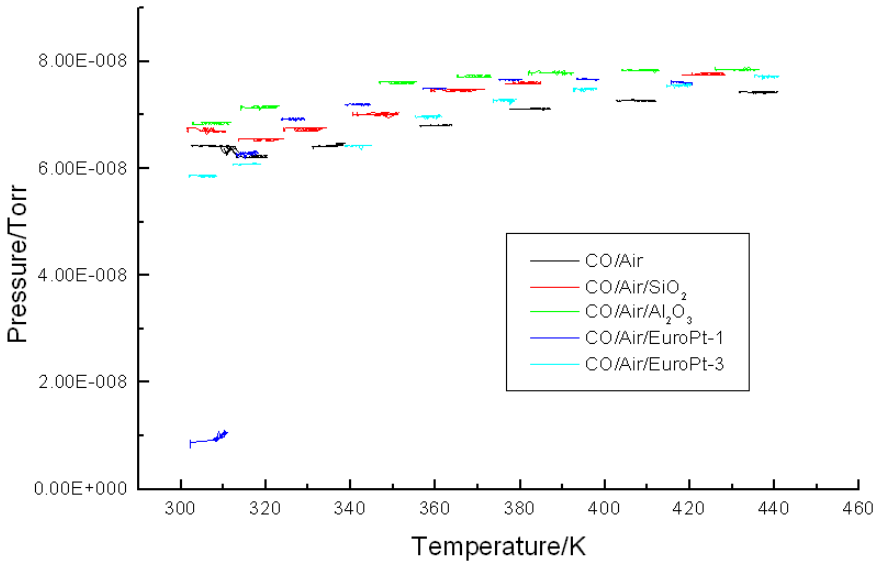

Figure 6.74: Variation of mass 32 with temperature under microwave heating

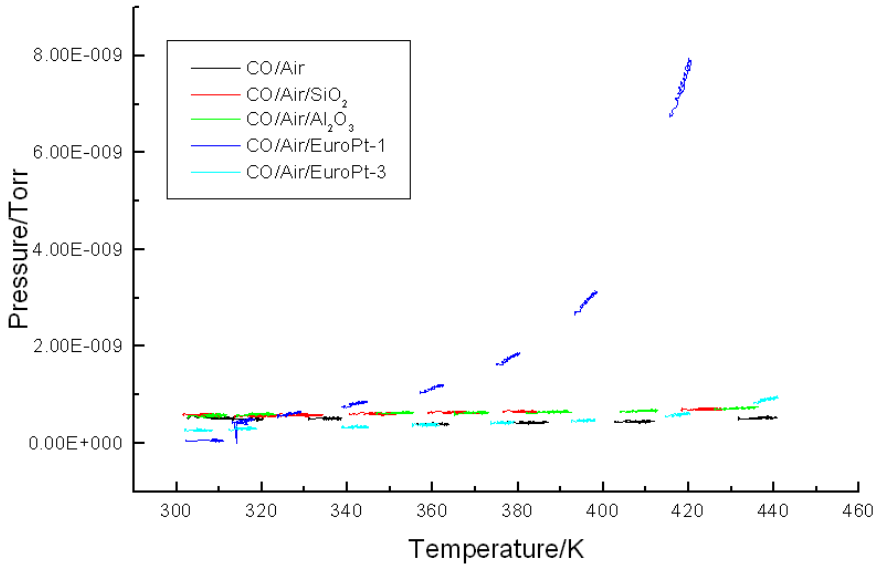

Figure 6.75: Variation of mass 44 with temperature under microwave heating

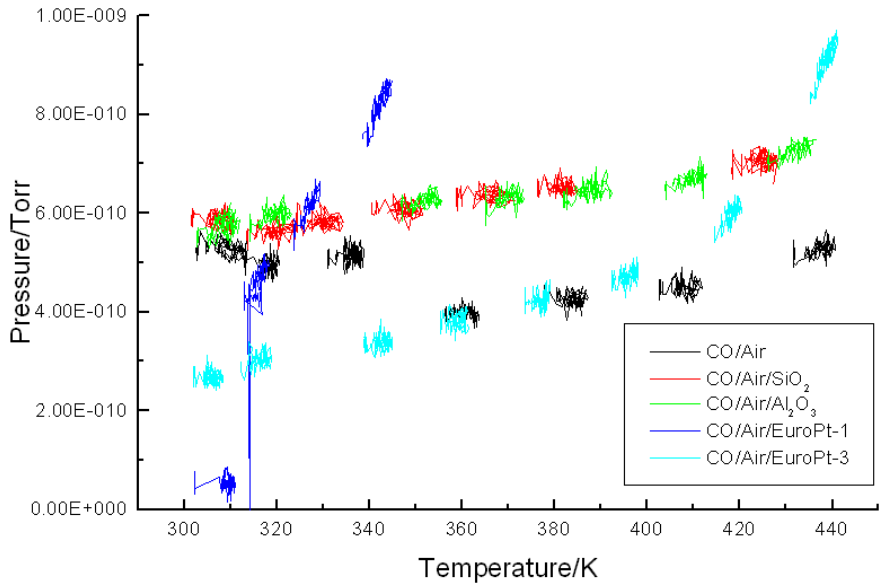

Figure 6.76: Variation of mass 44 with temperature under microwave heating

is shown in Figure 6.76. The SiO_2, Al_2O_3, EUROPT-3 and CO/Air results all show good agreement between the two heating regimes, with a significant upturn around 400 K apparent for the EUROPT-3 sample, and a gentle increase seen with SiO_2, Al_2O_3 and CO/Air. The good agreement between the conventional and microwave heating results suggests that the CO oxidation reaction is independent of the heating method.

With stub tuner

Figure 6.77 shows the behaviour of mass 18 under microwave heating with the stub tuner optimised for energy transfer. All of the samples show a pronounced oscillating increase when irradiated, especially at low temperatures and high vapour pressure. The EUROPT-1, EUROPT-3 and CO/air experiments show a steady decrease in the trend between clusters due to conventional heating. The increase in water signal observed is considerably larger for the solid samples than the CO/air, indicating desorption from the catalyst discs. The overall form observed is very similar to the results obtained with no impedance optimisation.

The variation in the mass 28 pressure for these experiments is shown in Figure 6.78, and again shows significant similarities to the non-optimised results. There are no sig-

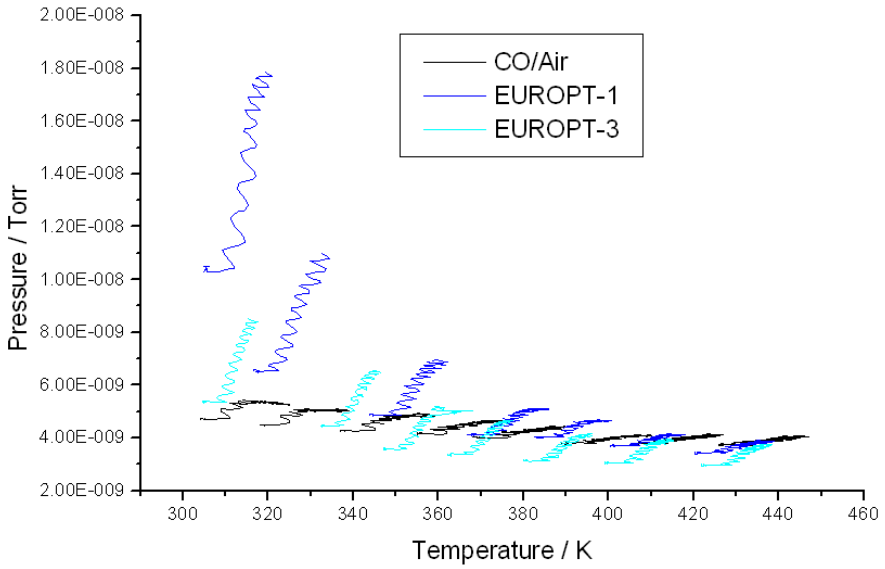

Figure 6.77: Mass 18 traces for samples under tuned microwave heating

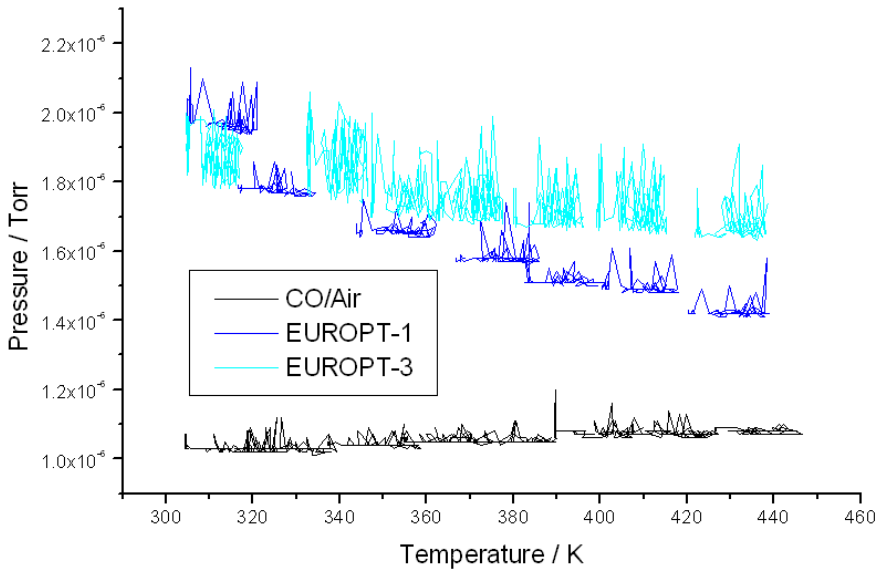

Figure 6.78: Mass 28 traces for samples under tuned microwave heating

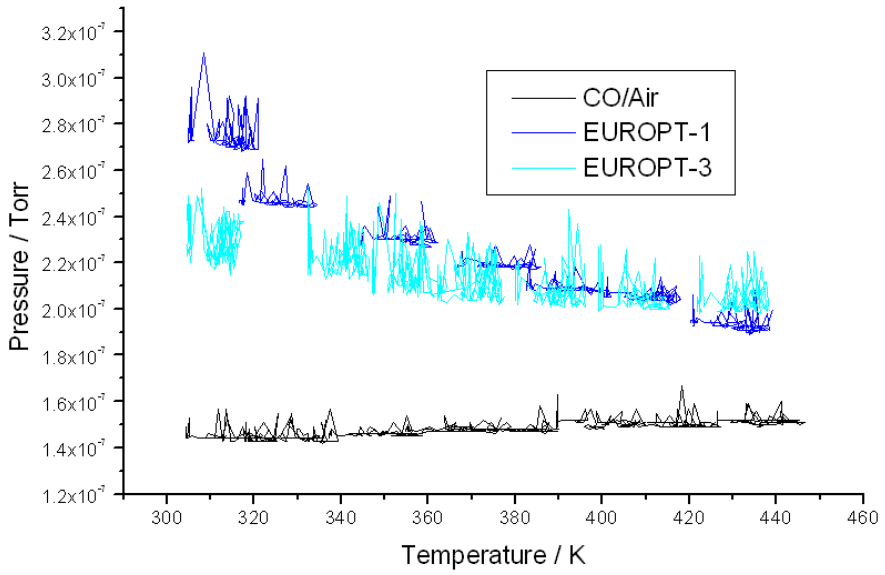

Figure 6.79: Mass 32 traces for samples under tuned microwave heating

nificant variations in mass 28 pressure seen for any of the samples under microwave radiation. There is also little change observed for the conventional heating, between-cluster trend for the purely gaseous sample, although both of the EUROPT samples show a drop in mass 28 at higher temperatures. These traces appear abnormally high compared to the other samples at low temperature, and show no periodic features associated with the microwave modulation. Both these factors suggest that the observed decrease is caused by poor flow rate control rather than the reactive oxidation of CO.

Figure 6.79 displays the mass 32 variations associated with the change in partial pressure of O_2. The partial pressure due to O_2 does not vary much under microwave heating for the EUROPT or CO/air experiments. The EUROPT samples show decreases in mass 32 pressure with conventional heating that are similar to the mass 28 response. The pressure is anomolously high at low temperature, yet drops at higher temperatures. This is again unlikely to be due to the CO oxidation, as oscillations are not observed in the traces.

The CO_2 production over EUROPT-1 dominates the mass 44 results displayed in Figure 6.80. The CO_2 pressure rise corresponds to that seen before, both in conventional and microwave heating modes. The oxidation over EUROPT-3 is also occuring in a comparable manner to that seen without the tuner present. The CO/air sample

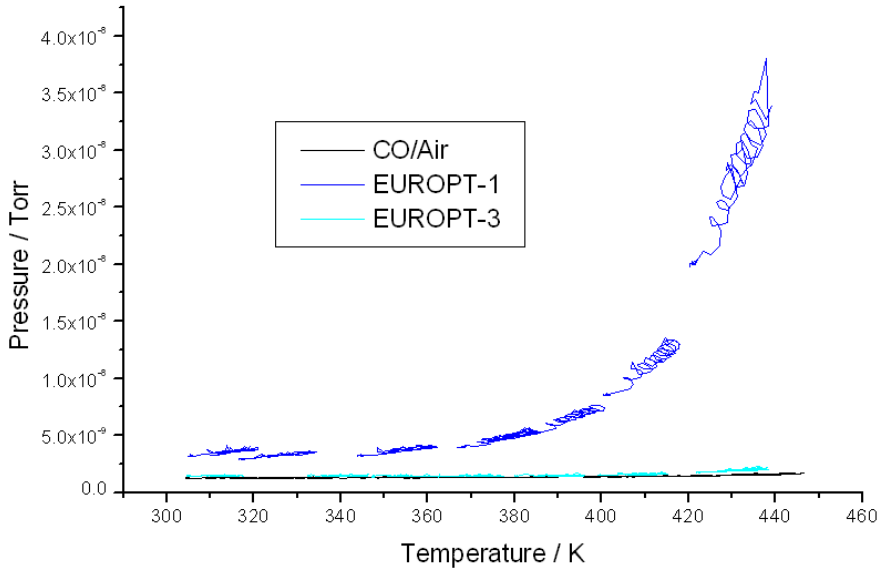

Figure 6.80: Mass 44 traces for samples under tuned microwave heating

shows minimal oxidation when compared to that over the catalysts, although a conventional increase is shown if the results are replotted on a more appropriate scale, as shown in Figure 6.81 which displays the CO_2 pressure obtained with and without the EUROPT-3 sample.

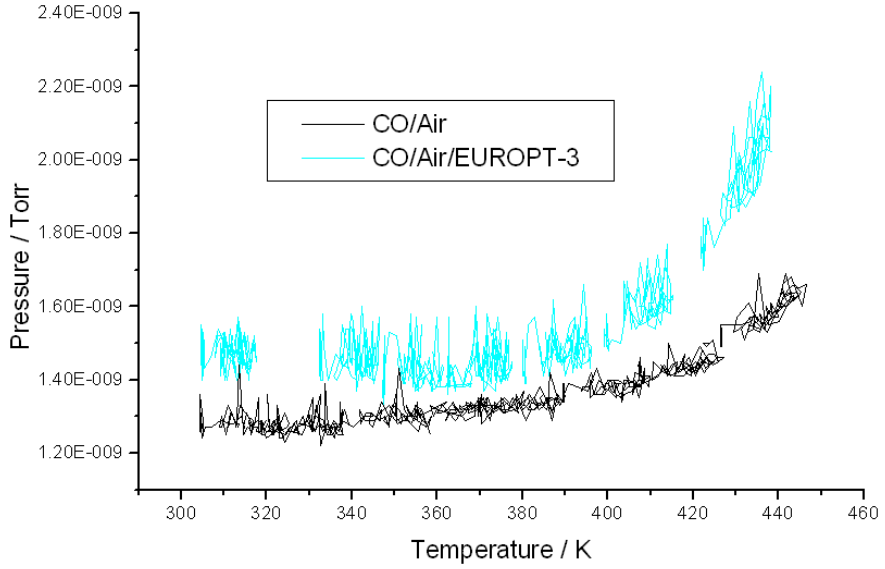

Figure 6.81: Mass 44 traces for CO/air (black) and EUROPT-3 (cyan) samples under tuned microwave heating

Chapter 7

DRIFTS cell experiments

The CO oxidation reaction over the two Pt-containing catalysts was followed in the DRIFTS cell using conventional and microwave heating. The use of the catalysts in powder form also simplifies loading the cell and allows gas to more freely diffuse around the sample.

7.1 Conventionally heated DRIFTS

7.1.1 EuroPt-1

A typical DRIFTS spectrum for the reaction gases over the EUROPT-1 catalyst is shown in Figure 7.1. The gas phase CO doublet is readily apparent, and the adsorbed species shows itself as a maximum at 2085 cm^{-1}, although the strength of this feature is relatively weak for such a strong chromophore. The limitations of DRIFTS in general and the microwave cell in particular allow only relatively poor spectra to be obtained, which is demonstrated by the relative strength of the miscancellation defects of CO_2 and H_2O, being as intense as the CO species of interest.

Figure 7.2 shows the development of the infrared features under the conventional heating regime. Features due to CO_2 and H_2O observed against the background can be assigned to variation in the spectrometer purge, as these features show little change and do not correlate with the temperature. The background itself demonstrates a significant rise in absorbance intensity under heating, which is reversed upon cooling. The form of the background rise is different to that seen in the transmission spectra,

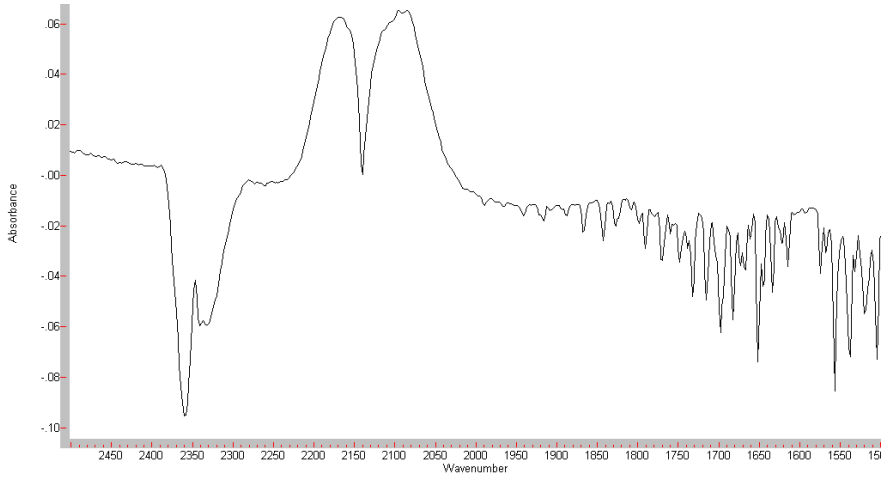

Figure 7.1: DRIFTS spectrum for reaction gases over EUROPT-1

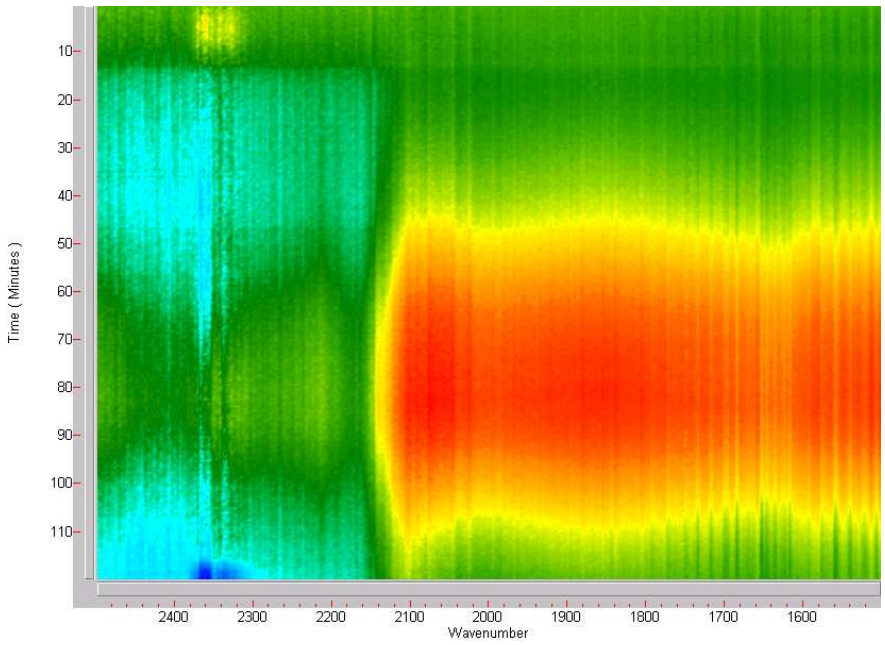

Figure 7.2: Conventionally heated time resolved DRIFTS spectrum for reaction over EUROPT-1

Figure 7.3: Extracted DRIFTS spectrum at 80 min for reaction over EUROPT-1

as it is not even across the entire spectrum. At 2100 cm^{-1} there is a significant step between the smaller increase to higher wavenumber, and a large increase to the lower side. This is illustrated by Figure 7.3, which shows a spectrum extracted at 80 minutes. Although this feature is the strongest facet of the spectrum, the noise level shows it to be very weak, and is purely due to a shift in the baseline due to heating. As DRIFTS spectra relate to the combination of scattering and absorbance they are sensitive to changes in the reflectance of the sample. Restrahlen bands occur at frequencies which display high resonance reflection, and it is possible that variations in the refractive index of the sample with temperature could cause such a step in the recorded spectra. This clear change presents itself at the same point in the spectrum as the gas phase CO peaks and is also potentially due to a poor background spectrum resulting in miscancellation of this strongly absorbing species.

7.1.2 EuroPt-3

Figure 7.4 shows a DRIFTS spectrum obtained for CO and air over EUROPT-3 before heating was applied. Gas phase CO is clearly present around 2143 cm^{-1}, although there are no visible features due to adsorbed CO. The low platinum loading of the catalyst and the poor optical efficiency of the DRIFTS cell are both likely contributors to this. CO_2 and H_2O again show strong peaks relative to the CO doublet due to the purge gas variation, indicating that the sensitivity to the system being investigated is

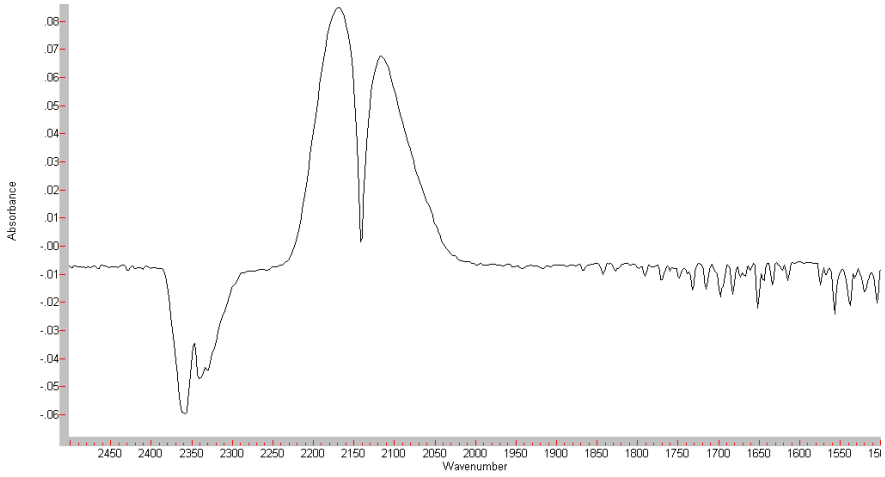

Figure 7.4: DRIFTS spectrum for reaction gases over EUROPT-3

fairly low. The EUROPT-3 is much more reflective than the EUROPT-1, appearing light grey instead of dark brown. This allows collection of better quality spectra from the EUROPT-3, as less of the incident light is absorbed, and a greater response is thus achieved at the detector.

Figure 7.5 displays the time resolved DRIFTS spectrum for EUROPT-3 obtained from the conventional heating experiment. The baseline of the spectra once again shows a pronounced increase in intensity upon heating, although in contrast to the EUROPT-1 DRIFTS results, this extends across the entire spectral range. The CO_2 and H_2O show peaks that become increasingly negative as time progresses. The fact that these peaks show similar behaviour to each other and appear unconnected to the temperature suggests that these features are caused by variation in the instrumental purge. There is evidence of the gas phase CO, with a negative doublet of peaks centred around 2143 cm^{-1} visible. The peak shape is more clearly illustrated in Figure 7.6, which shows a spectrum extracted from the kinetics data at 80 minutes. The negative carbon monoxide features are clearly visible, but there also appears to be small positive bands flanking these, suggesting thermal peak broadening as seen in the transmission experiments in Section 6.1.1. Whilst the magnitude of the positive peaks relative to the negative features is much reduced to that seen before, the overall weaker signal strength caused by the use of the DRIFTS cell may account for this. The decrease in signal at the peak center may also be caused by oxidation of the CO, which would be

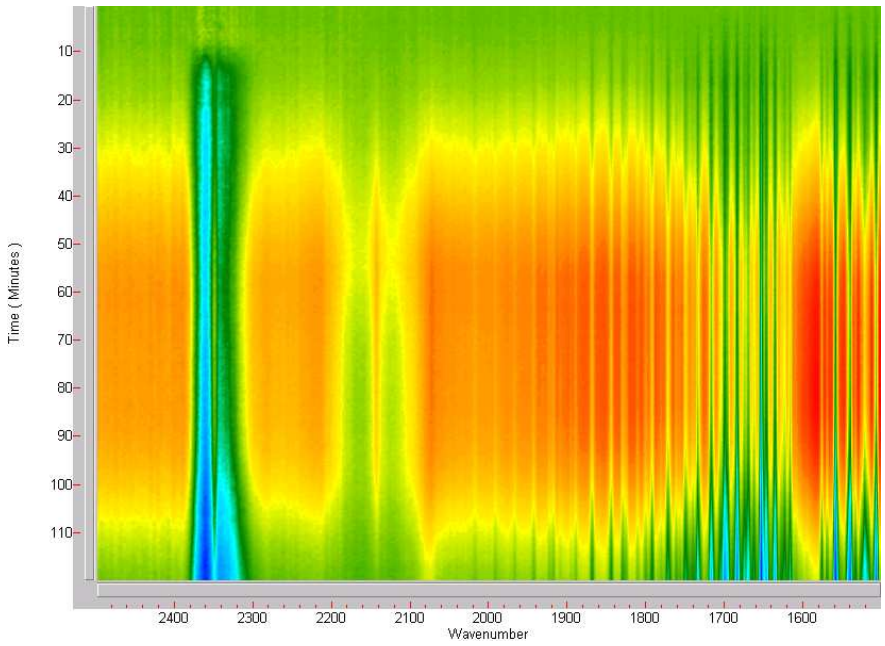

Figure 7.5: Conventionally heated time resolved DRIFTS spectrum for reaction over EUROPT-3

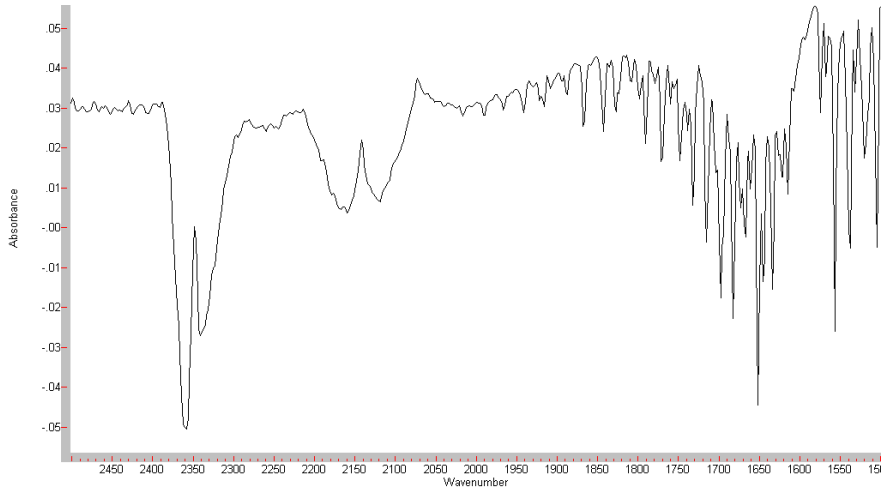

Figure 7.6: Extracted DRIFTS spectrum at 80 min for reaction over EUROPT-3

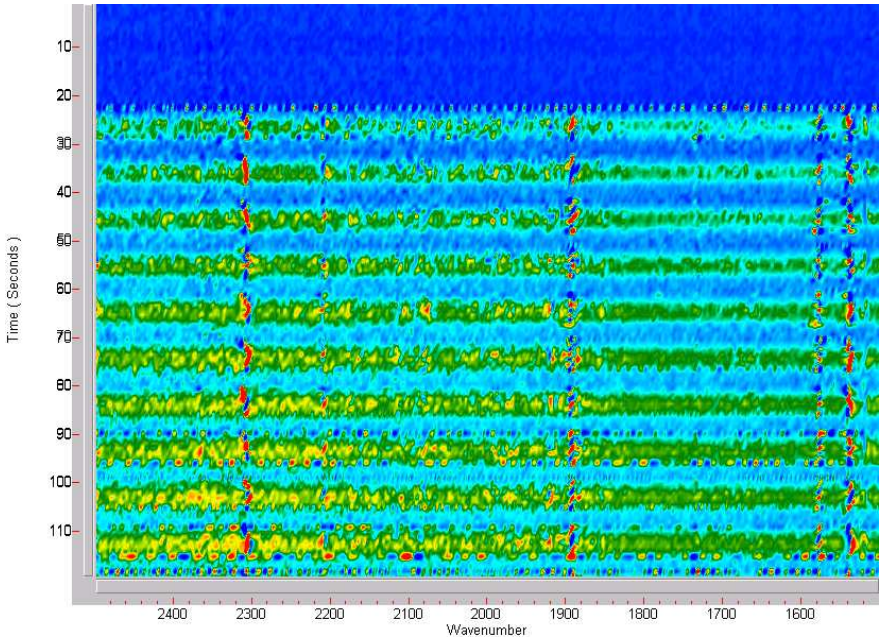

Figure 7.7: DRIFTS spectrum for microwave heated reaction over EUROPT-1

expected to give a corresponding increase in the CO_2 signal. As this is not seen, the reaction can not be significant if it is concealed by minor changes in the purge gas. The use of an optically unfavourable cell is limiting the acquisition of good data in preference to being able to obtain results under microwave heating. Unfortunately this comprimise leads to ambiguity in interpretation of results, and it is possible that both oxidation and thermal broadening are contributing to the peak structure.

7.2 Microwave heated DRIFTS

7.2.1 EuroPt-1

The time resolved kinetics DRIFTS spectrum for EUROPT-1 under oscillating microwave power is displayed in Figure 7.7. No features appear in the spectrum for the first 20 s, indicating that the system is stable before the application of microwaves. Once the irradiation begins, banding appears across the entire range of the spectrum with 0.1 Hz frequency. Peaks due to reacting species do not appear in the spectrum, as can be seen in Figure 7.8 which shows extracted spectra at 88 and 93 s, corresponding to

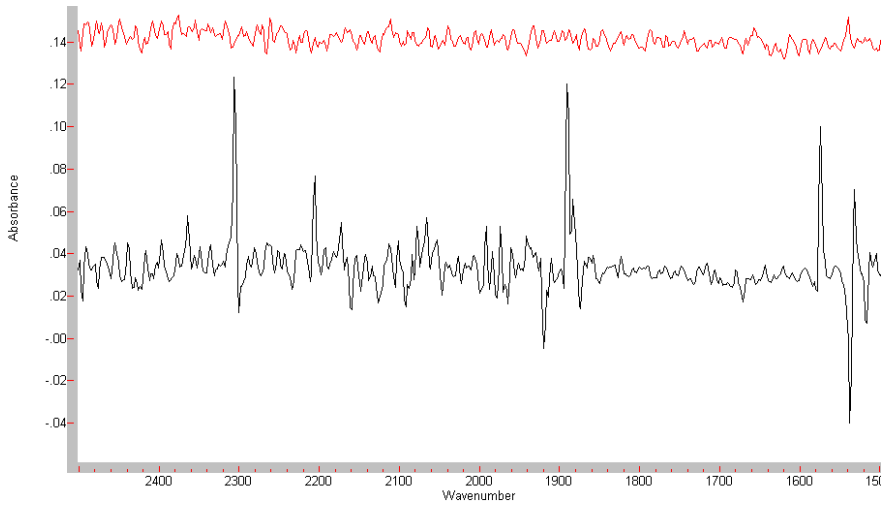

Figure 7.8: DRIFTS spectra for reaction over EUROPT-1 at 88 (red) and 93 s (black)

a minimum and maximum in the banded spectra. Sharp features at 2307, 2207, 1892, 1576 and 1533 cm^{-1} persistently appear at the band maxima and do not appear to correspond to chemical species present. Interference with the spectrometer electronics has been previously noted, and seems stronger with the use of the DRIFTS cell compared to the transmission cell. Some individual spectra display obvious artefacts, in Figure 7.7 examples can be seen at 22, 90 and 96 seconds. Figure 7.9 shows the extracted spectra at 22 s, which shows a signal not unlike a standard interferogram that would be obtained when collecting data. Regular oscillations and beat frequencies are visible, which suggests that some oscillating signal is interfering with the spectrometer electronics and causing this malfunction in the resultant spectra. The increased noise level and the lack of spectral features due to the materials being studied unfortunately does not allow a meaningful interpretation of the DRIFTS results for EUROPT-1 to be made.

7.2.2 EuroPt-3

The microwave heated time resolved kinetics spectrum for EUROPT-3 obtained with DRIFTS is displayed in Figure 7.10. The system appears steady before the application of the microwave energy after 20 s, although there appears to be the merest hint of a signal due to CO_2 miscancellation between 2370 and 2320 cm^{-1}. The initiation of the

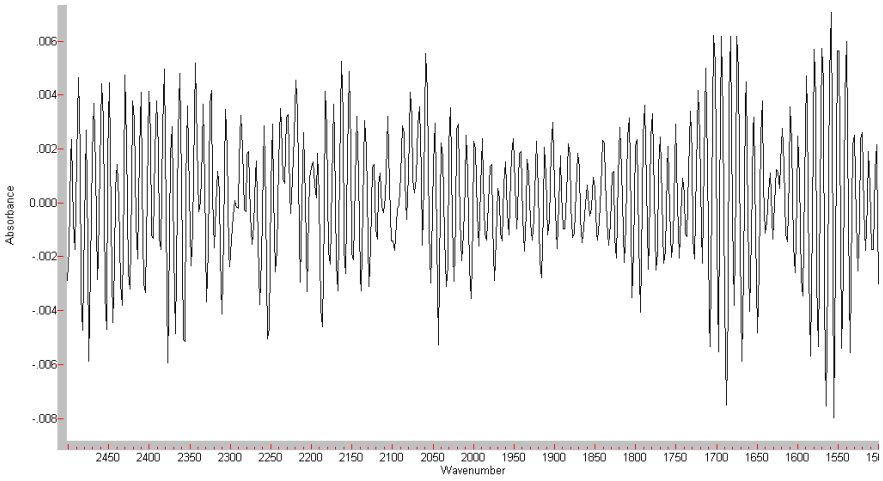

Figure 7.9: DRIFTS spectra for reaction over EUROPT-1 at 22 s

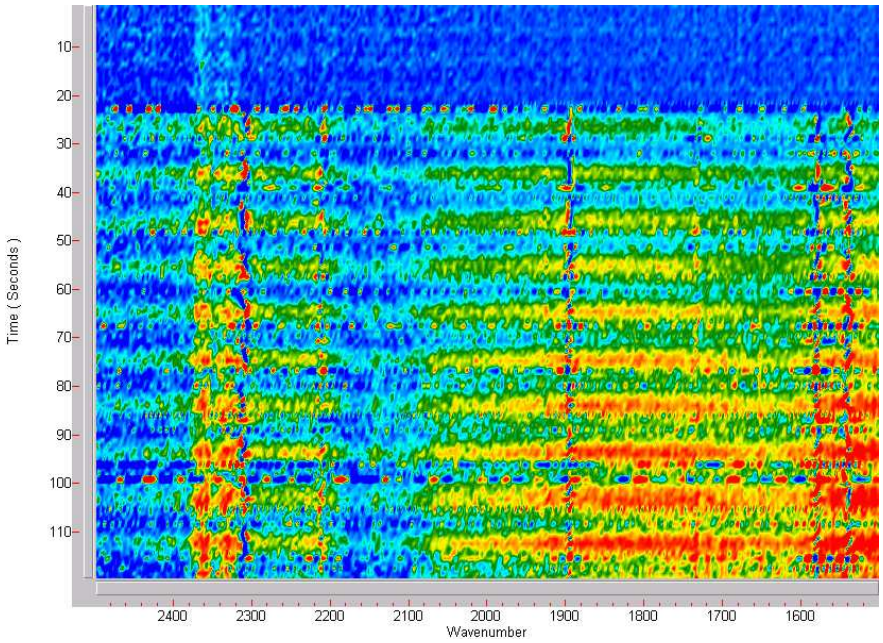

Figure 7.10: DRIFTS spectrum for microwave heated reaction over EUROPT-3

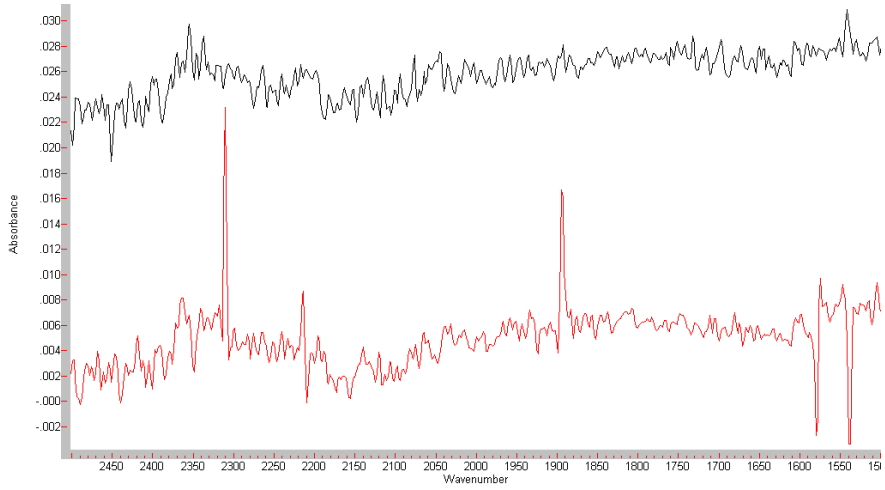

Figure 7.11: DRIFTS spectrum for microwave heated reaction over EUROPT-3 at 83 (red) and 88 s (black)

microwave perturbation at 22 s brings forth the familiar banded pattern dominating the spectra. The intensity of this oscillation appears weaker between 2190 and 2070 cm^{-1}, denoting that there is an opposing effect at this point in the spectrum. This position corresponds to the gas phase CO peaks, thus it can be concluded that there is a decrease in the CO concentration upon microwave heating. The CO_2 region shows the opposite effect, with an increased oscillation magnitude around 2348 cm^{-1}. When both of these features are taken into account, it would be sensible to assume that the oxidation of CO to CO_2 is occurring and thus the microwave DRIFTS cell is a viable piece of apparatus.

The time resolved kinetics spectrum again shows the development of some features assumed to be noise as can be seen in Figure 7.11 which shows spectra extracted at 83 and 88 s. Negative CO and positive CO_2 features may be seen at 2350 and 2145 cm^{-1} above the general noise level and the background oscillation artefact. These spectra also display sharp spikes which occur at the same points as in the EUROPT-1 experiment. This suggests that there has been the introduction of yet another artefact, as the position of these features does not appear to correspond to any chemical species present. These features appear to be due to the interference of the microwave with the spectrometer electronics, as they appear at times that coincide with high microwave power. Calculations show that if these artifacts are being introduced before the Fourier

transform is occuring, they will have a frequency between 450 and 800 Hz, which corresponds to extreme low frequency radio transmissions as are used to communicate with submarines. As interference is not seen for the other experiments at these frequencies, this seems highly unlikely. Rather it would seem that the spectrometer electronics are creating artefacts in a different part of the signal processing path.

Chapter 8

Discussion

The results presented previously demonstrate various facets of the reacting system. Greater insight may be achieved by viewing the system holistically, and demonstrating the relationships between the techniques. Further manipulation of the data can also result in a greater understanding of the processes occuring. The variation of the activity of a catalyst with temperature is of fundamental importance, thus in an unconventionally heated system a detailed treatment of the heating produced is needed.

8.1 Temperature

The challenges associated with measuring temperature reliably in a microwave system have been discussed in Section 1.5. Analysis of the data collected to assess the validity and scope of the measurements is undertaken here.

8.1.1 Thermocouple measurement

For every material used in the experiments, a heating curve was obtained with temperature measurement by the thermocouple, for each run under microwave irradiation in the transmission cell. These were truncated to ensure there were no spikes due to beginning or ending the collection, and plotted as a scatter graph. The data for CO and air with no solid, are presented in Figure 8.1 and show a similar form to the graphs obtained from the other materials investigated. A line of best fit was calculated by linear regression to give values for the average temperature rise over the period studied,

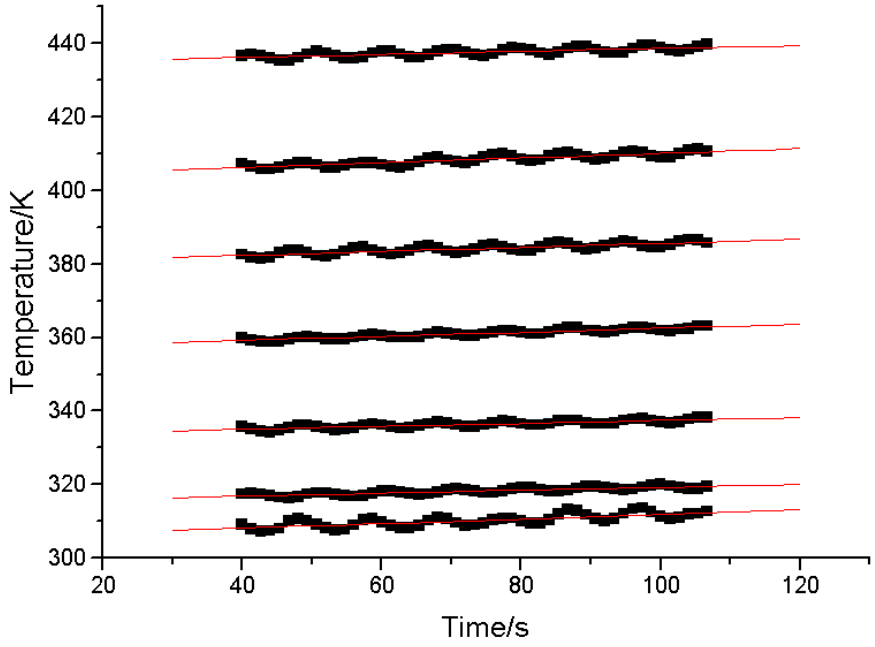

Figure 8.1: Thermocouple temperature data for CO and air under microwave heating

at each initial temperature. There was little variation seen in the gradients produced, showing that the heating rate was independent of the initial temperature. The average power input of the microwaves was constant in each run, for each sample, and at each temperature. This led to a relatively constant temperature ramp rate under the influence of irradiation for each run, independent of initial temperature. The temperature gradients for each sample were then averaged and the results are presented in Table 8.1.

The samples all show a significant positive gradient indicating that heating is occuring, with the values obtained using the stub tuner greater than double that of the

Table 8.1: Average temperature rise calculated from thermocouple data

Sample	**Average heating rate/ Ks^{-1}**	
	Untuned	**Tuned**
CO	0.047 ± 0.003	0.107 ± 0.006
CO/Air	0.051 ± 0.002	0.149 ± 0.004
CO/Air/SiO_2	0.045 ± 0.004	-
CO/Air/EUROPT-1	0.042 ± 0.001	0.110 ± 0.004
CO/Air/Al_2O_3	0.060 ± 0.002	-
CO/Air/EUROPT-3	0.034 ± 0.001	0.102 ± 0.003

untuned system. This shows that greater power dissipation through the cell and sample is occuring, resulting in increased heating, when the system is optimised in this manner. The observed oscillations in the temperature data vary in amplitude, although the gradient does not appear to be significantly affected by this. The heating rates obtained with and without the stub tuner show minor variations between samples which are possibly due to the experimental conditions. Factors such as placement of the catalyst wafer in the cell, tuning optimisation, and the quality of the contact of the thermocouple with the sample are all likely to lead to such discrepancies. The data collected for each reacting system should be internally consistent however, and it is clear that there is a legitimate oscillatory heating effect allied to the overall temperature ramp for all of the samples.

By positioning the transmission cell thermocouple within the microwave cavity, it was hoped to obtain the temperature of the solid through intimate contact of the thermocouple with the sample. In addition, however, the thermocouple will also be in contact with the gas phase, (particularly important in the absence of a solid!) and the ceramic sample holder.

The peak to peak height for the thermocouple data has been seen to vary considerably, sometimes during the collection of data. Figure 8.2 shows the temperature variation recorded for carbon monoxide and air in the emission experiment, which corresponds to the experiments in Section 6.3.2. The sudden and significant change in the amplitude of the oscillations causes problems in assessing the temperature rise where the amplitude changes during data collection, as can be seen from the best fit lines displayed. However, an amplitude change between irradiation cycles does not affect the gradient, as can be seen in Figure 8.3, which shows the temperature variation recorded for alumina in the emission experiment presented in Section 6.3.4. Here the gradual temperature rise seen is consistent across the experimental runs, and produces a consistent overall heating result. Thus only experiments without variation in the oscillation amplitude were used for the calculation of the average heating rate. The changes in the magnitude of the oscillation suggest the presence of an undesireable effect. Four phenomena could be the cause of this amplitude change; instability of the microwave power supply, electrical discharge, electrical pick-up by the thermocouple

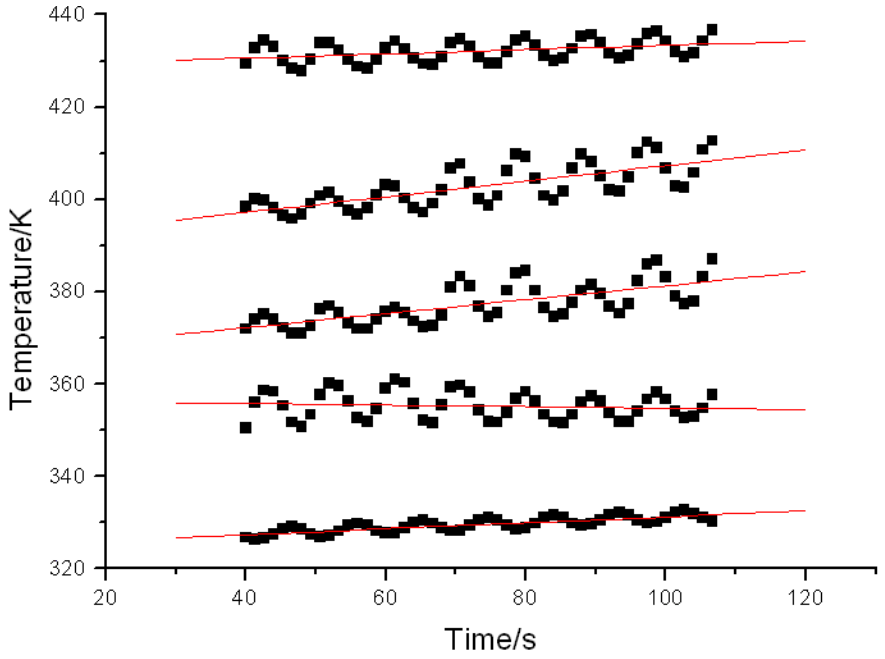

Figure 8.2: Temperature variation recorded for carbon monoxide and air with the thermocouple

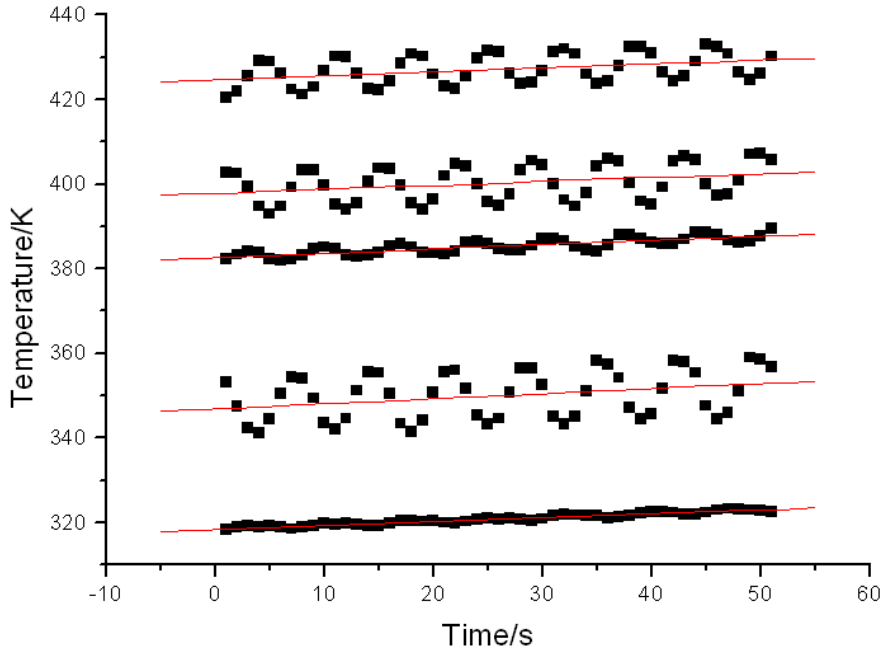

Figure 8.3: Temperature variation recorded for Al_2O_3 with the thermocouple

wires and localised heating.

Although an initial surge in power has been previously suggested on enabling the microwave power, it is unlikely that the instrument would develop an unstable power output that would correspond to the changing magnitude seen. If the power output did vary, a change in the average heating rate would likely result, and affect the temperature gradient seen.

The parallel plate applicator relies on the maintenance of an oscillating potential difference between the two plates. The concentration of the microwave field at the thermocouple tip may have lead to an electrical discharge, which would interfere with temperature measurement. It is likely however, that if this were the case, infrared emission would also be enhanced and be visible as a baseline shift when the discharge was in effect. Furthermore, electrical discharges usually require either very high voltages or low pressures, neither of which are present in the system.

Electrical pick-up through the thermocouple was known to be a potential problem when the experiment was designed. In keeping with this, the thermocouple assembly chosen was a model housed within a metal sheath, which was embedded and soldered into the ground applicator of the cell. The metal sheath should act as a Faraday cage and prevent any interference at the thermocouple junction. However, the sheath terminates 100 mm from the tip, where unshielded wires are attached. It is therefore possible that interference could result from this section of the cabling, although it would expected that if this were occuring, its strength would not vary significantly.

The position of the thermocouple quite obviously distorts the microwave field in its vicinity, which is likely to lead to a greater microwave intensity, and therefore heating, at this point. There is also the possibility that transient hot-spots occur spontaneously in a homogeneous field [29], and their presence around the thermocouple position could explain the increased heating effect. Thus an increase in the oscillation amplitude could be explained by the proximity of a hot spot to the thermocouple, and the variation seen can be attributed to the mobility of these phenomena. The form of the temperature profile suggests that the localised temperature increases caused in this manner are not maintained, as the overall temperature gradient is independent of the oscillation magnitude. Thus when power is reduced, the hot spots reach thermal equilibrium with

their surroundings as the heat is conducted away.

Thermometry within a microwave field is a well known problem, and the results presented have illustrated some of these difficulties. As such, quantification of the oscillation magnitude is problematic. However, the overall temperature rise detected with the thermocouple is completely reproducible and allows a measurement of the influence of the microwave heating to be made. Furthermore, it is certain that oscillatory heating is occuring, and the oxidation of carbon monoxide over the platinum catalysts shows good agreement with the measured temperature.

8.1.2 Infrared emission measurement

If it is assumed that the only radiation detected in the emission experiments is originating from items in the optical axis of the cell, a number of possibilities present themselves. The windows, the gauzes covering them, and the sample are obviously in the beam path, and the tip of the thermocouple also projects into this space. The emission detected may therefore originate from any of these sources, and further complications arise if the temperature is not uniform across these species. This may simply mean that the gauzes exhibit a different temperature from the catalyst wafer, or that hot-spots exist within the catalyst disc. There is also the possibility that the Pt particles within the catalyst have a different temperature to the support.

The presence of the gauze covering the windows will attenuate any emission from the sample in the cell and also emit itself. Ideally, with the gas samples in the cell, observable emission would only be expected from the CO and CO_2 present. The collected spectra however, show an increase across the spectrum, suggesting that there is a significant black-body contribution from other parts of the cell. Oscillations at 0.1 Hz observed across the spectrum intimate that the temperature of the Ni is modulated, and that this is in phase with the temperature recorded by the thermocouple. This is demonstrated in Figure 8.4, which displays the variation of the emission strength at 1350 cm^{-1} with the recorded temperature from the thermocouple obtained for the silica sample. The absence of observable gas phase peaks in the time resolved emission spectrum under microwave heating is disappointing, although the low concentration of matter in the gas phase compared with the solid sample and cell components is the

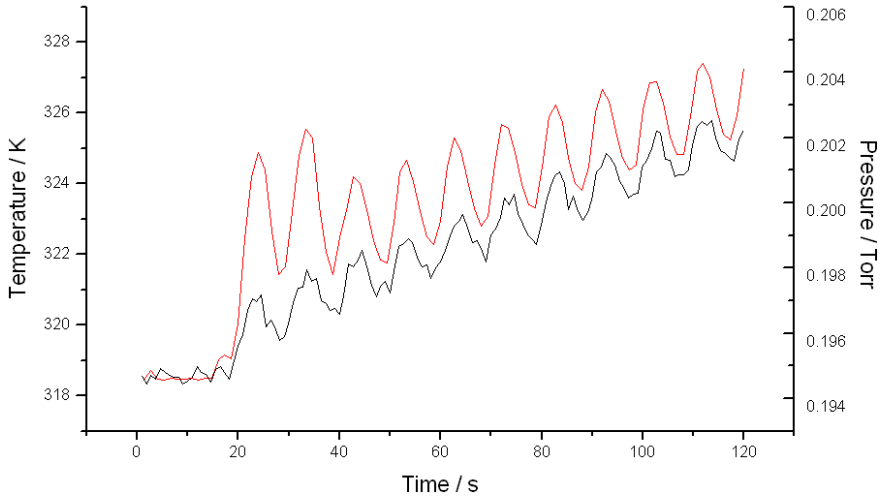

Figure 8.4: Variation of emission intensity at 1350 cm^{-1} (black) and temperature (red) with time for SiO_2

likely cause. It should also be remembered that although gas phase peaks are seen in the conventionally heated emission experiments, the background for these are obtained at the same temperature. The design of the microwave heating experiments dictates that the same background scan is used for the two minute data acquisition period, so that as time progresses and the sample heats, the background becomes less and less relevant.

Whilst small peaks in the emission IR due to the species of interest have been detected, the majority of the radiation detected appears to be of black-body character. This suggests that the source of the detected radiation must be either the body of the cell or the Ni gauze covering the windows. As no aperture was used to collimate the beam, it is not altogether surprising that the spectral information may be overwhelmed. However, the emission data obtained can be of considerable use in the determination of the gas phase temperature. The window gauzes are in intimate contact with the gases within the reactor, and are likely to be in thermal equilibrium with them. Thus it is reasonable to assume that the temperatures calculated from the IR emission data are representative of the gases present in the cell.

The emission of infrared radiation is strongly temperature dependant and can therefore act as a measurement of temperature. The emission spectra of silica under helium

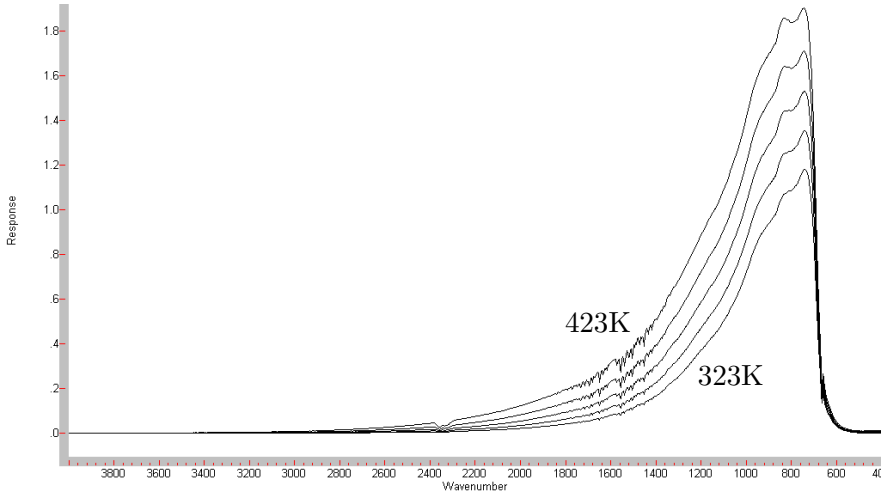

Figure 8.5: Single beam emission spectra for SiO_2 under He

at 323, 348, 373, 398 and 423 K are shown increasing in Figure 8.5. It can be seen that the position of the maximum at 746 cm^{-1} does not significantly vary, and the intensity markedly increases with temperature at all wavelengths. The form of the detected emission profile is partly determined by the characteristics of the detector, which has a cut-off at around 680 cm^{-1}. It should also be noted that whilst the CaF_2 windows are mostly transparent in the IR, their transmittance decreases sharply at low wavenumber, losing transparency around 1000 cm^{-1}. This can be seen in Figure 8.6, which shows the transmission spectra of CaF_2. As the windows are transparent above this value, they will neither absorb or emit the more energetic frequencies. At wavelengths where the transmittance is not 100%, the material can emit and absorb radiation. Thus any emission detected below the window's cut-off is unlikely to originate from inside the cell, and instead is due to the thermal emission from the window material itself. This effect precludes the use of the emission maximum for the measurement of the sample temperature within the cell, and thus a value at lower wavenumber must be chosen. To gain the best signal to noise ratio it is desireable to use the greatest signal strength which occurs at low wavenumber, hence the emission at 1350 cm^{-1} was monitored, which is within the transparent region of the windows.

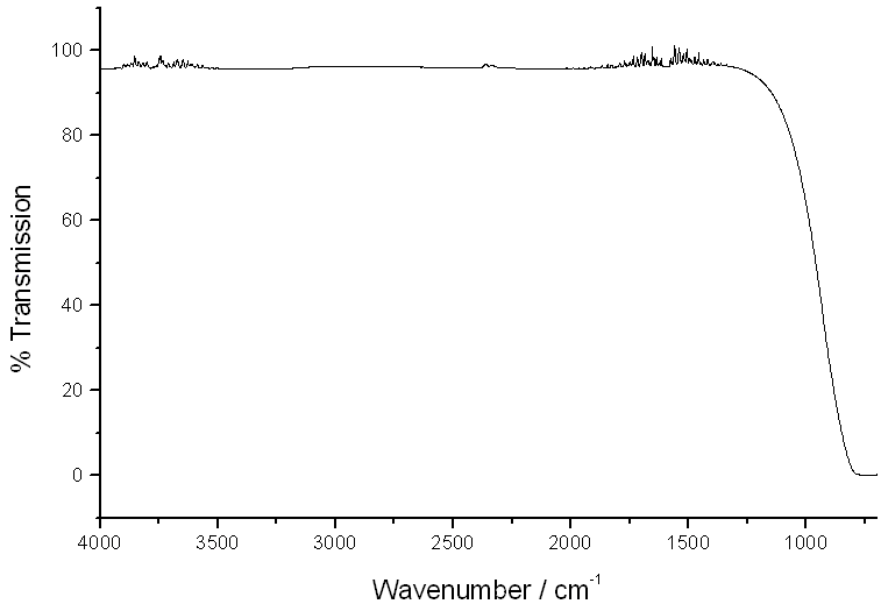

Figure 8.6: Transmission spectrum of CaF_2

Planck's law can be expressed:

$$I = \frac{2h}{c^2} \frac{\nu^3}{e^{h\nu/kT} - 1} \tag{8.1}$$

Where I is the emission intensity, T the temperature, c the speed of light, ν the frequency of radiation and h and k are Planck's and Boltzmann's constants respectively [78]. For a given wavelength therefore, a plot of $\ln I$ against $1/T$ should yield a straight line. Figure 8.7 shows this plot for SiO_2 under the reacting gases at 1350 cm^{-1} with conventional heating, and displays reasonable linearity.

For each sample under microwave heating, calibration graphs of $\ln I$ vs. T were obtained at 1350 cm^{-1} using the infrared emission values before the microwave radiation was applied. Using the emission values under irradiation, temperature values could thus be calculated for the portion of each experiment under microwave heating. This allowed plots of temperature similar to those obtained using the thermocouple data to be plotted. The data for silica under CO and air at an initial temperature of 319 K is presented in Figure 8.8 and shows strong similarities with the graphs obtained from the thermocouple data.

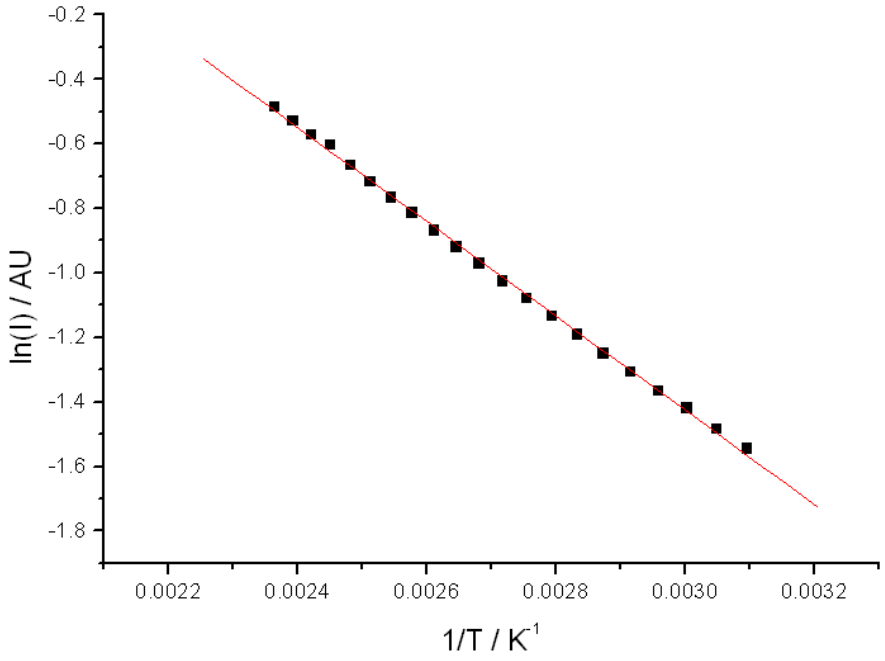

Figure 8.7: Infrared emission variation with temperature at 1350 cm^{-1}

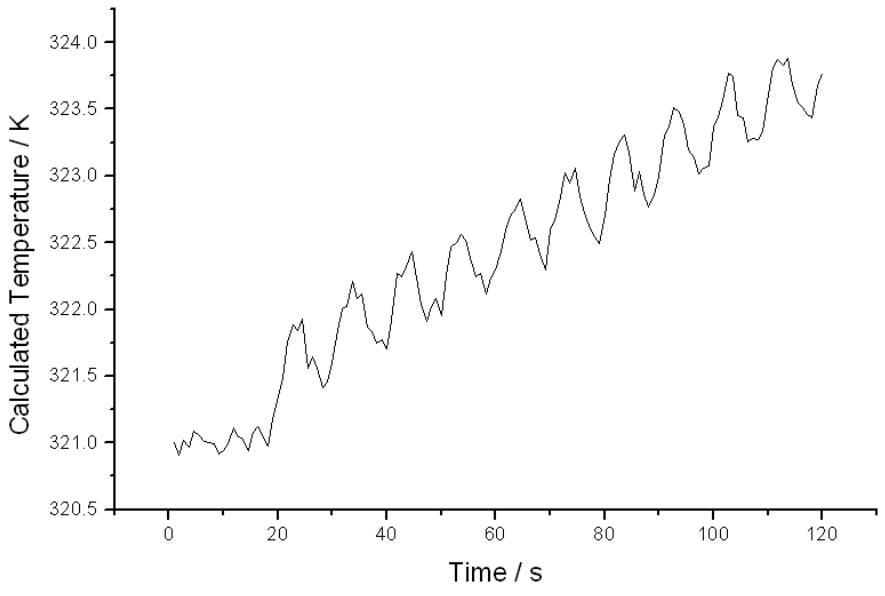

Figure 8.8: Calculated temperature for CO and air over SiO_2 under microwave heating

Table 8.2: Average temperature rise calculated from infrared emission data

Sample	**Average heating rate/ Ks^{-1}**
CO	0.036 ± 0.003
CO/Air	0.036 ± 0.004
CO/Air/SiO_2	0.034 ± 0.003
CO/Air/EUROPT-1	0.041 ± 0.003
CO/Air/Al_2O_3	0.045 ± 0.002
CO/Air/EUROPT-3	0.033 ± 0.003

Table 8.3: Average temperature rise calculated using both methods

Sample	**Average heating rate/ Ks^{-1}**	
	Thermocouple	**Infrared**
CO	0.047 ± 0.003	0.036 ± 0.003
CO/Air	0.051 ± 0.002	0.036 ± 0.004
CO/Air/SiO_2	0.045 ± 0.004	0.034 ± 0.003
CO/Air/EUROPT-1	0.042 ± 0.001	0.041 ± 0.003
CO/Air/Al_2O_3	0.060 ± 0.002	0.045 ± 0.002
CO/Air/EUROPT-3	0.034 ± 0.001	0.033 ± 0.003

The initial temperature rise on enabling the microwave is larger than that seen for subsequent leading edges, which was also seen in the thermocouple data. Whilst not as great as that observed for the thermocouple results, this initial jump suggests that there is an increased effect on initiation of the microwave power. Clear oscillations at 0.1 Hz are also observed allied to a general rise in temperature over the course of the experiment. The overall rise is *circa* 4 K, with each rising edge about 0.5 K in height. To obtain the heating rates for each sample, best fit lines were calculated with a truncated data range as before, and the results are presented in Table 8.2.

8.1.3 Comparison

Table 8.3 shows the a comparison of the heating rates calculated from IR emission with those obtained using the thermocouple, for all samples under untuned microwave heating. The agreement between the methods of calculating the values is reasonably good. The untuned thermocouple readings appear similar to the calculated infrared values, although slightly higher. Two factors may account for this apparent discrepancy, although the meagre size of the differences may only be due to experimental

variation.

It has previously been mentioned that the thermocouple may enhance heating around its tip. If such a localised heating effect exists, readings obtained by the thermocouple would be anomalously high. It is also possible that there exists an artefact causing the infrared measurement to appear low. The IR radiation detected in the emission experiments is unlikely to originate purely from the gauzes covering the windows. Radiation detected from the external surfaces of the cell could could lower the calculated temperature, as these parts are likely to show a temperature lag compared with the contents of the cell.

Good agreement is seen in overall heating rates of the samples, showing that both methods may be used to measure the reaction temperature within the cell. Both methods clearly also show that the oscillating microwave power induces temperature modulation, which is echoed in the oscillating reaction seen in both the transmission IR and the mass spectrometry results. Differences in the magnitude of this oscillation are observed in the thermocouple results, although the possibility that this is caused by mobile hot-spots would explain this observation. Such hot-spots would also be unlikely to be observed in the emission results, which show a relatively uniform modulation strength.

8.2 Infared spectroscopy

Infrared spectroscopy *in-situ* allows investigation of the active species on the catalyst surface. A more detailed interpretation of the peaks obtained in the experiments is presented, with reference to their shape, position and intensity.

8.2.1 Peak shape

A large number of the spectra obtained show peaks accompanied by adjacent peaks of opposite intensity, *i.e.* positive peaks flanked by negative peaks, or negative peaks surrounded by positive ones. This form is almost certainly caused by a broadening of the peak envelope due to an increase in temperature. The vibrational bands due to gas phase components observed in the infrared have a specific width which is determined

by the rotational fine structure of the molecules present.

8.2.2 Simulated spectra

The infrared spectrum of a gaseous diatomic molecule depends strongly on the temperature of the gas. When in a gas, the quantisation of rotational energy levels can be observed in the spectrum. Whilst the individual rotational transitions can only be observed at high resolution, the band shape will vary as the different rotational energy levels are populated. A solution to the Schrödinger wave equation for a rigid rotating diatomic molecule gives

$$E_{rot} = J(J+1)\frac{h^2}{8\pi^2 I} \tag{8.2}$$

where h is Planck's constant, J is the rotational quantum number and I is the moment of inertia. This is a classical property of a rigid rotor, and is given by

$$I = \frac{m_1\, m_2}{m_1 + m_2} r^2 \tag{8.3}$$

where m_1 and m_2 are the atom's masses and r is the spacing between them. Each of the energy levels defined by J consists of $2J+1$ quantum states, so the degeneracy of level J is defined as

$$g_J = 2J + 1 \tag{8.4}$$

It is customary to express spectroscopic units in wavenumbers (cm^{-1}) and the properties of the molecule in terms of its rotational constant B (also in cm^{-1}), which is defined as

$$B = \frac{h}{8\pi^2 I c} \tag{8.5}$$

where c is the speed of light. The energy ε_J of a rigid rotor (in cm^{-1}) can then be expressed in terms of the rotational constant, B:

$$\varepsilon_J = \frac{J(J+1)hcB}{kT} \tag{8.6}$$

The rotational partition function when expressed in terms of the rotational constant gives:

$$Q_{rot} = \frac{kT}{hcB} \tag{8.7}$$

The fraction of all molecules n_J/N in energy level J is then given by the Boltzmann distribution:

$$\frac{n_J}{N} = \frac{g_J\, e^{(\varepsilon_J - \varepsilon_0)/kT}}{Q_{rot}} \tag{8.8}$$

or in terms of the rotational constant:

$$\frac{n_J}{N} = \frac{(2J+1)e^{\frac{-J(J+1)hcB}{kT}}}{Q_{rot}} \tag{8.9}$$

This allows a calculation to determine the population of the rotational energy levels at a given temperature from the B value to be performed.

The vibrational energies of an harmonic oscillator can be shown to be:

$$\tilde{\nu}_r = (\nu + 1/2)\tilde{\nu}_0 \tag{8.10}$$

where $\tilde{\nu}_0$ is the fundamental vibration energy of the oscillator and ν is the vibrational quantum number. In each vibrational state the molecule is also rotating, with a rotation constant that differs according to the vibrational energy level:

$$B_\nu = B_e - \alpha_e(\nu + 1/2) \tag{8.11}$$

Transitions can often be excited by infrared and visible light, and are associated with rotational transitions. Vibration-rotation absorption infrared spectroscopy generally follows the transition from the ground vibrational state to the first excited state. The associated vibrational transition has $\Delta J \pm 1$. By convention the higher vibrational energy state is denoted ν' and the lower state ν'', giving

$$\tilde{\nu} = \tilde{\nu}_0 = B'_\nu J'(J'+1) - B''_\nu J''(J''+1) \tag{8.12}$$

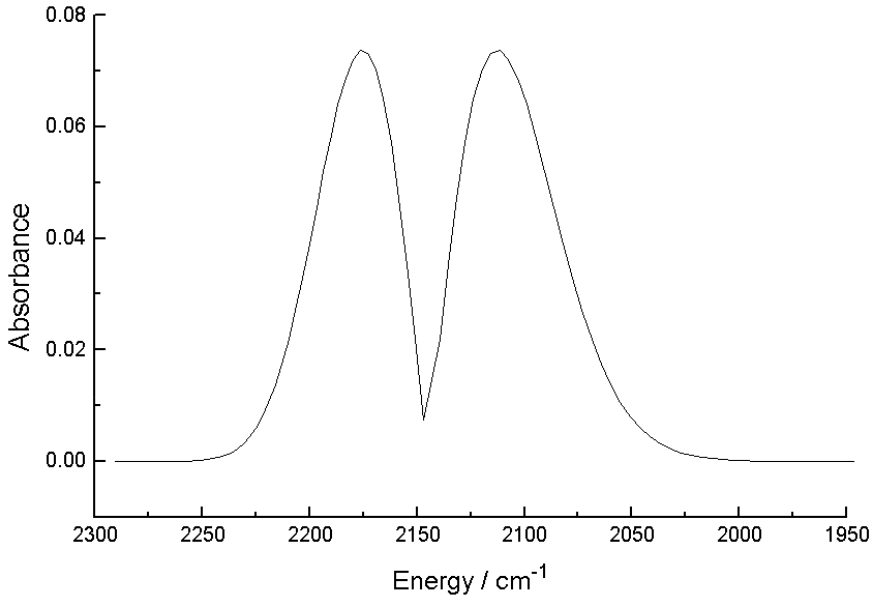

Figure 8.9: Simulated IR spectrum for CO at 373K

which can be rearranged to give

$$\tilde{\nu} = \tilde{\nu}_0 + (B'_\nu + B''_\nu)m + (B'_\nu - B''_\nu)m^2 \tag{8.13}$$

where m has the values $1, 2, 3\ldots$ for the positive rotational transitions ($m = J + 1$) and the values $-1, -2, -3\ldots$ for the transitions where $m = J - 1$. This gives

$$\tilde{\nu} = 2143.3 + 3.8274m - 0.0175m^2 \tag{8.14}$$

for the CO stretching vibration [79]. Whilst this gives the energy levels, the intensity of each of these transitions depends on the population of the initial rotational state which has been shown in turn to be a function of the temperature (Equation 8.9). By solving both Equations 8.9 and 8.14, it is possible to generate an estimate of the infrared absorption spectrum of carbon monoxide.

A simulated IR spectra at 373 K using these calculations is shown in Figure 8.9. If this spectrum is used as a background to convert another spectrum calculated at 378 K into absorbance using $A = \log(I_0/I)$, the resulting spectrum shows the familiar peak shape observed experimentally, as shown in Figure 8.10. The good agreement between

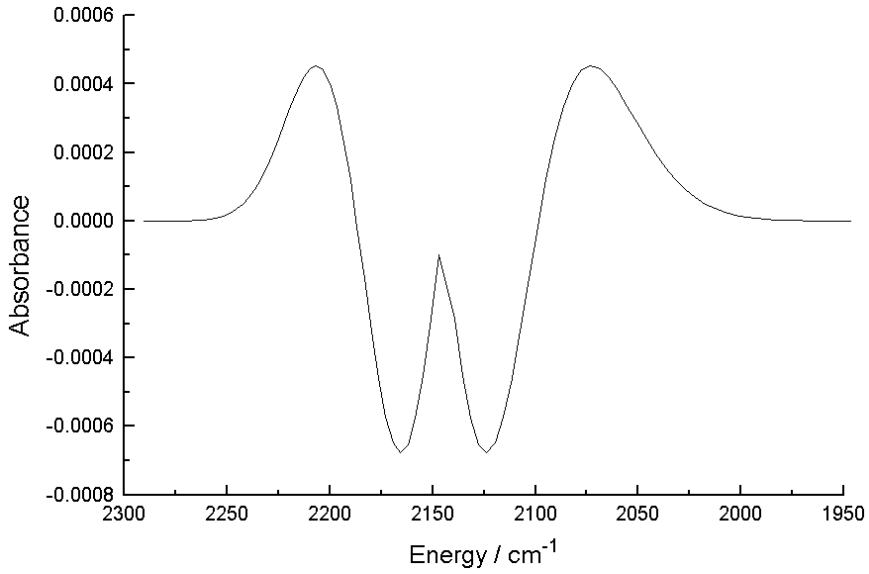

Figure 8.10: Simulated IR spectrum for CO obtained by using spectrum at 373K as background for that at 378K

theory and experiment demonstrates that at least a large proportion of the gas phase peak structure is due to thermal effects. That the CO peaks demonstrate this effect under most experimental conditions emphasises the heating effect of the microwave radiation.

8.2.3 CO Peak intensity

The intensity of the carbon monoxide peak oscillation in the spectra under microwave heating varies considerably, with the clearest results for the pure CO sample in transmission. These experiments show that the CO absorption intensity at the peak centre drops with an increase in temperature, as can be seen in Figure 8.11, which shows the IR absorbance intensity at 2170 cm^{-1} plotted in black, and the temperature in red. The time axes have been shifted to align traces on the initial leading edge. Three interpretations lend themselves to these data and are discussed below:

- Thermal peak broadening leads to lower intensity at peak centre
- Less CO physically present
- Increased IR emission due to increased temperature

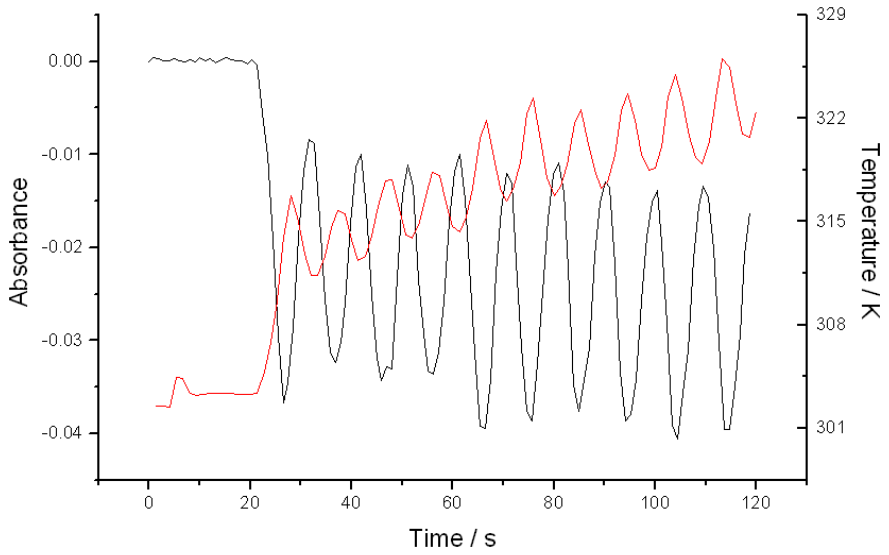

Figure 8.11: Temperature (red) and absorption intensity (black) changes under microwave heating for CO

Thermal broadening

Thermal broadening of the CO peaks results in the characteristic side peaks discussed above. Not all of the results obtained which show a loss in the peak centre demonstrate these associated features. Thermal broadening is clearly observed for the purely gaseous samples in the transmission cell, especially when utilising the stub tuner. The increased transference of energy to the sample using the tuner also allows broadening of the gas phase peaks to be seen over some of the solid samples. The experimental regime for the emission experiments under conventional heating would not show side-peaks, due to the use of a background under helium, rather than the reacting gases. For the microwave heated emission experiments, no variation is seen in these peaks.

Concentration

A decrease in CO concentration could be caused by a reaction occuring, or thermal expansion of the gas, assuming the pressure remains constant. The former is clearly apparent when CO oxidation is occuring, although this cannot explain the oscillation seen for the pure CO experiment. With the experimental set up used, the flow is against a constant external pressure and the gases are thus free to expand. This explains the

oscillations seen in the gas phase when the reaction is not occuring, as the gas handling apparatus will act as a pressure sink. Figure 8.11 also shows that the temperature and absorbance are completely antiphase, providing further evidence for thermal expansion. Furthermore, this effect is likely to be more efficient at low flow rates, which would explain the clarity of the peak oscillation for the pure CO sample.

Emission strength

An increase in infrared emission due to heating of the samples is observed in the spectral background under all conditions. This is much more obvious in the conventionally heated and emission experiments, but is also present in the other results. However, changes in the CO signal due to emission are weak under conventional heating, and not observed at all in the microwave emission experiments. This result suggests that any increase in emission due to the gas phase is minor when compared with that from other black-body sources, and is unlikely to cause the decrease in the CO peaks.

Effect strength

It is likely that all of these effects have some influence on the infrared spectra recorded in different experiments. Thermal broadening of the CO peaks is strongly observed in a number of the experiments undertaken, and it is possible that the intensity drop seen where no side peaks are observed is also due to heating of the gas phase. When the side peaks show a gain in intensity, they appear weaker than the loss at the peak centre. In cases where the sensitivity is low, it may be that only the strong loss is seen, and the weak gain is below the threshold of detection. The catalytic reaction under study will obviously deplete the reactant and lead to negative peaks. The fact that side peaks due to thermal broadening can be observed in the gas phase CO reacting over EUROPT-1 emphasises however, the strength of this effect. As such it is believed that in most cases the strongest effect will be due to the heating of CO. However, there are likely to be significant contributions to the peak profile from the other processes occurring simultaneously.

8.2.4 Carbon monoxide peaks

The position of a peak in the infrared spectrum is determined by the amount of energy absorbed or emitted in transitions between vibrational energy levels. These levels are determined by the masses involved, and also by the strengths of bonds between them. An interaction which alters the bonding between vibrating atoms will often lead to an observable peak shift in the infrared spectrum and therefore betray information on its nature. The adsorption of carbon monoxide on metals affects the strength of the C≡O bond and leads to changes in the infrared spectrum that are of considerable interest to the catalytic chemist [71, 80].

The envelope of the gas phase CO appears with its center at 2143 cm^{-1}, although the position of the peak maxima and minima appear to vary under conventional heating. This effect is caused by the changing population in rotational states as described in Section 8.2.2. Under microwave heating, although the intensity of these features change, their position does not vary. The movement seen in the conventionally heated spectra is due to the collection of spectra over a wide temperature range, and the use of a single background spectrum. The results obtained under microwave heating use a different background spectrum collected at each initial temperature, and do not display this effect.

CO may adsorb onto a Pt surface in a number of ways. The linearly adsorbed CO on a single Pt atom predominates, and leads to a strong infrared peak, the position of which varies according to the coverage of the metal. When the metal surface is completely covered with the gas, the peak appears around 2080 cm^{-1}. At lower coverages however, the peak position shifts to lower wavenumber [71]. The second peak originating from the adsorption of CO on Pt corresponds to the CO bonding to two metal atoms in a 'bridged' configuration and may be seen around 1850 cm^{-1}. The peak obtained from the species bonding in this manner is broader than the linear CO peak, and has been reported to broaden as coverage increases [81].

In the results obtained, the adsorbed linear CO peak is immediately apparent as the strongest feature in spectra taken with EUROPT-1 present. The peak appears with a flat top around 2080 cm^{-1} under conventional heating at all temperatures, indicating saturation of the surface and spectral intensity. The position of the linear adsorbed CO

peak over EUROPT-3 for these experiments is approximately the same, although it is often partially or completely obscured by the gas phase CO. Under microwave heating, the linear CO peak on EUROPT-1 indicates an oscillating shift in position. This is not observed in the peak maximum, which remains saturated at 2080 cm^{-1}, but displays an adjacent loss and gain in absorption at high and low wavenumber respectively. This suggests a decreasing coverage of the metal, which is consistent with the modulation in the rate of oxidation of the CO in the CO/air mix over the Pt catalyst, associated with the temperature swing under microwave heating. No shift is seen in the position of the linear species of EUROPT-3, due to the low conversion allowing the surface to remain saturated.

The bridged CO peak can also be observed showing a peak shift under conventional heating, although relating the spectra to the physical phenomena occuring is more difficult. The peak shows an intensity loss to the high wavenumber side of the peak, with an increase just below the peak centre. Another decrease is apparent at the low wavenumber side, although this feature is weak. The peak thus seems to be shifting to lower wavenumber on heating, but with an associated sharpening, which suggests a decrease in coverage. The microwave heating experiments also duplicate this result, and show oscillations at 0.1 Hz that appear in phase with the linear peak shift and antiphase to the CO_2 production. This is shown in Figure 8.12, which shows the variation of the absorption intensity at 1846 (black) and 2361 cm^{-1} (red), corresponding to the minimum of the bridged CO and the maximum of the gas phase CO_2 peaks respectively. The position of the bridged CO peak between the strong features of the linear CO and the adsorbed water means that these species may have an effect on the spectrum at this point. In addition, the baseline shift due to increased emission from the solid further convolutes the spectrum. Although the minima in the bridged band show a slight downward trend in addition to the oscillation, the maximum of the band at 1846 cm^{-1} appears to oscillate around a fixed absorbance value. This curious behaviour may thus be explained as a complex interplay between a number of factors affecting the spectrum at this point.

An unexpected peak is also visible in the spectrum of CO when no solid catalyst is present. This is displayed at 2042 cm^{-1} and is consistent with the adsorption of CO

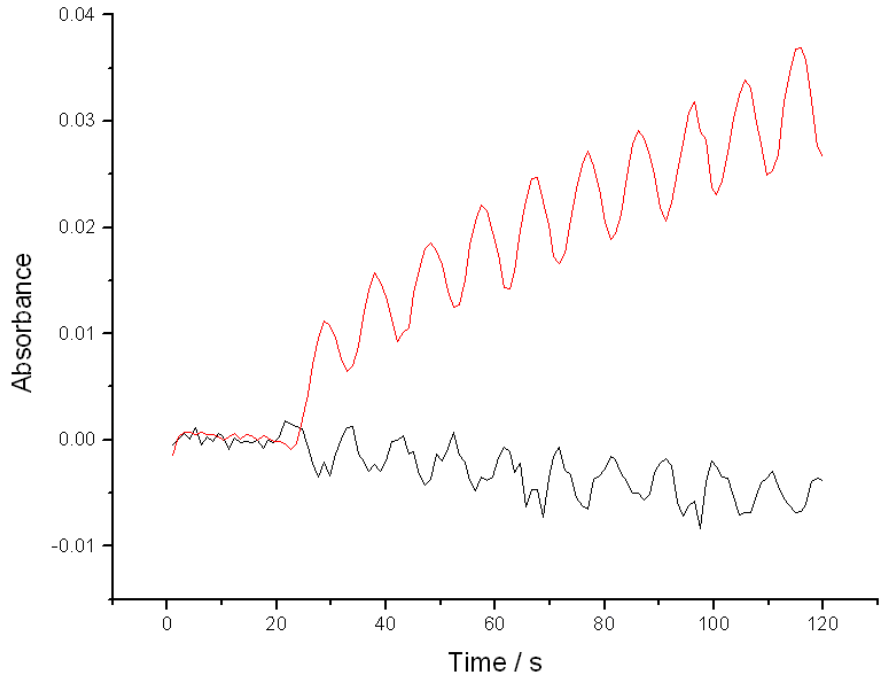

Figure 8.12: Absorption intensity changes under microwave heating for bridged CO (1886 cm^{-1}, black) and CO_2 (2361 cm^{-1}, red)

on Ni [71], which would be observed if the CO in the gas phase was adsorbing onto the nickel gauze covering the cell windows. However, nickel will also form $Ni(CO)_4$ under the right conditions, which has a strong IR absorbance at 2050 cm^{-1} [70]. This unfortunately means that with the results obtained it is not possible to determine whether the peak is due to the formation of nickel tetracarbonyl or adsorbed CO. Another peak appears at 1740 cm^{-1} under microwave irradiation of pure CO with the stub tuner, which suggests the presence of organic carbonyl containing species [76], possibly due to a compound leaching from the o-rings of the cell. This peak is also present in the liquid heating experiments and is further discussed later. As these two anomalous peaks are only present in the pure CO experiment, are vanishingly small and have no bearing on the CO oxidation reaction under examination, further interpretation was not undertaken.

8.2.5 Peaks arising in liquid reactions

The study of liquid samples in the transmission cell is hindered by the large path length that the IR beam must take through the solvent. This is a consequence of adapting the cell from the gas phase work, rather than the commissioning of a separate cell for the experiments. Across the mid-IR region, the spectra show strong absorbances that correspond to the major vibrations of the molecules, which absorb 100% of the light at their characteristic wavelengths. This unfortunately causes problems in the interpretation of the spectra, and so investigation was limited to the same range as for the gas and solid phase catalytic investigations of 2500–1500 cm^{-1}. This range appears reasonably clear of strong absorbances, and allows at least a small proportion of the light to be transmitted. Furthermore, this region contains the carbonyl stretching vibration, which is often important in the characterisation of compounds in organic synthesis. A number of small peaks appear in the recorded spectra which cannot be definitively assigned, and demonstrate an unusual response to microwave heating. The peak at 1721 cm^{-1} for chloroform and 1737 cm^{-1} for hexane increases under microwave heating. Were this purely a thermal effect, the other peaks in the spectra would show a similar absorption increase, however this is not the case. The fact that only one peak responds may be due to:

- A specific enhancement of one vibration mode
- Electrochemistry
- Selective heating
- An increase in concentration

The enhancement of a specific single vibration using microwave energy is highly unlikely. The 2.45 GHz microwave radiation energy used corresponds to 8.17×10^{-2} cm^{-1}, which is simply too small to excite vibrations. The apparent excitation of this single vibration mode is likely to be illusory, as the change in its associated features will be hidden under peaks already absorbing the entirity of the incident wavelength. As the two parallel plates have a varying voltage across them and are in contact wth the liquid, there is a small chance that electrochemistry may be occuring within the

solvent. The possibility of this occuring with the pure solvent is felt to be unlikely due to a lack of conductivity, although it cannot be totally ruled out. The two other causes suggested both rely on the presence of more than one species in the reaction cell. This may be due to impurities in the solvents, or the reaction of the solvent with the construction materials of the cell itself. A selective heating effect may cause one of these components to heat, and thus cause an absorption increase, as a materials infrared absorbance increases with temperature. However, if it is assumed that there is intimate contact between the two species, energy absorbed by one species would immediately be lost to its suroundings, due to the translational collisions occuring in the liquid. The final hypothesis is thus the most likely, and it appears that the heating resulting from the irradiation is causing leaching of material from the cell. This is likely to be either solvation of the O-rings, or the surface patina from either the applicator plates, or the sample holder. The presence of a similar peak in the gas phase experiments further adds credence to this explanation, although this is not an entirely satisfying result, as decreases in concentration are seen between peak maxima, suggesting that this is a reversible phenomenon. These decreases are relatively small when compared to the overall rise in absorption, and may be due to the thermal effects seen across the entire spectral range.

8.3 Mass spectrometry

The mass spectrometry results allow inference of the reaction pathway through study of the composition of the exhaust gas from the cell. Good agreement was seen between the two methods of heating.

8.3.1 Conventional heating

For all samples, the initial increase in the mass 18 signal seen previously in Section 6.5.1 under heating can be assigned to desorption of water. A comparitively small variation in the water signal is seen when no solid is present, as water can only desorb from the walls of the cell, and no water is introduced with the solid sample. Oscillations can be seen in the traces caused by the non-linear temperature ramp, which was effected by

periodically raising the voltage to the heaters in the cell.

The large initial increases in masses 28 and 32 seen for the reaction mixture over some of the solid samples can be interpreted as the outgassing of N_2 or CO, and O_2 from silica and alumina. This accounts for the great majority of the variation in these species throughout the course of the experiments. At elevated temperatures, a slight decrease can be seen for both masses over EUROPT-1. This is due to CO oxidation depleting both the carbon monoxide and oxygen.

The increases in mass 44 are easily reconciled as being the production of CO_2, and this is largely dependant on the presence of the metal, with the CO_2 produced over EUROPT-1 and EUROPT-3 being due to the reaction occurring on the Pt surface. Only these platinum containing catalysts show a significant rise in the mass 44 trace. The other samples show a minor CO_2 pressure increase of comparable magnitude to each other, when air is present, and no change is observed for the pure CO sample. Under these conditions it seems likely that the reaction is occuring either at the surface of the nickel gauze covering the windows, or the metal walls of the cell itself, although outgassing is also a possibility. If the reaction was enhanced by silica or alumina, a decreased activity would be observed for the reaction with no solid present, which is not the case.

8.3.2 Microwave heating

The microwave heated results from the mass spectrometer are a valuable tool in the interpretation of the reactions occuring. Whilst only minor changes can be observed in the reactant gases, (masses 28 and 32) the pressure variations in the water and the CO_2 present are of much greater interest.

Water desorption

The surface of a solid is an energetically unfavoured system, and thus will try to reduce its energy. Adsorption of a gas is one method to achieve a lower surface energy, and is thus generally exothermic. Physisorbed gases may be removed from a surface by heating, and this can be used as an analytical tool with methods such as temperature programmed desorption (TPD). This method relies on detecting the gases evolved

on heating a solid under a slow temperature ramp. This results in a maximum at the temperature of greatest desorption, with peaks resolved for energetically distinct species at different temperatures. The gas concentration in the cell is determined by the competition between gains and losses in the rate of supply of the gas, where the gains are the supply of the gas flowing into the cell, and the desorption of gas from the solid. The losses are due to the re-adsorption onto the solid studied, and loss out of the cell, as well as other losses, such as adsorption onto the walls of the cell, which may be considered negligible [82].

The water pressure during the conventional heating experiment reported in Section 6.5.1, shows a peak around 325 K for the solid samples, and the method is similar to a TPD experiment, although with a relatively unstable temperature ramp.

If the temperature is held at a constant value, desorption will occur with a gradually reducing rate until equilibrium is reached, and the rate of adsorption equals the desorption rate. The rate of desorption can be expressed as an Arrhenius equation of the form:

$$k_d = Ae^{-E_d/RT} \tag{8.15}$$

Where A is the pre-exponentional factor, E_d is the desorption energy, R is the ideal gas constant and T is the absolute temperature. Due to the form of this dependence, a small temperature increase will result in a large increase in the rate of desorption. For the microwave experiments, the temperature is approximately constant before microwave heating. The desorption rate decreases as the surface concentration depletes and the system tends to equilibrium. The temperature increase that results from the initiation of the microwave energy causes the desorption rate to rise, and the pressure of water in the gas phase thus increases. Over the limited time and temperature range that data was recorded under microwave heating, the rate of desorption is always greater than the loss of pressure through the gas flow. No peak maximum is therefore seen, as the system is always on the rising edge of the pressure curve, and rates appear enhanced at higher temperatures under microwave heating. The question is whether this is a microwave specific effect, or whether a similar temperature step after a period of stability would result in an analogous pressure rise for mass 18. To compare the results between the microwave and conventionally heated water desorption, it is therefore necessary

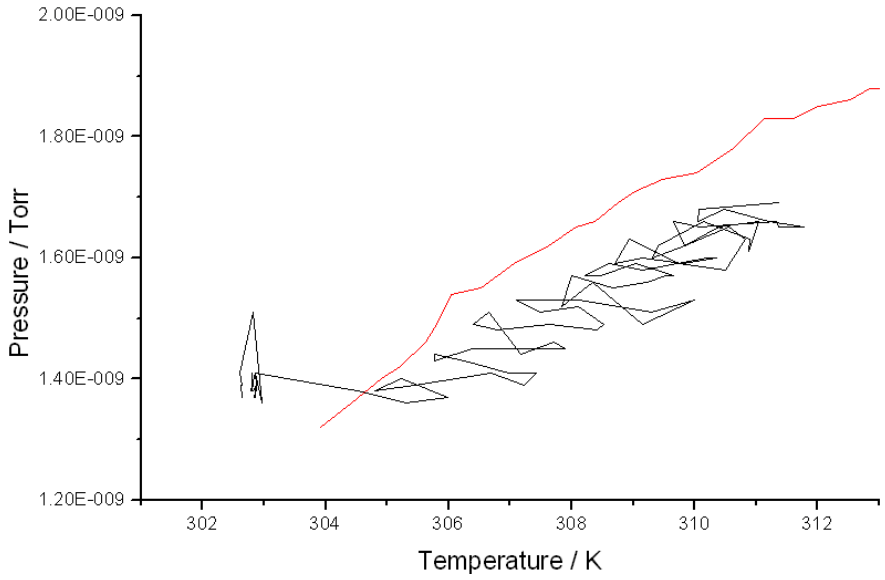

Figure 8.13: Initial variation in gas phase water under conventional (red) and microwave (black) heating over alumina

to study the initial rate of desorption of the conventionally heated experiments with that of the microwave results. When conventional heating is begun, the sample is in a stable state, and the high surface coverage results in an increase in desorption as the temperature rises. At higher temperatures,the coverage is depleted, and the ramping temperature present differences between the two heating regimes. Thus the conditions within the conventionally heated experiment are similar only for the first microwave run over a similar temperature range. Figure 8.13 shows the initial desorption of water from alumina under both microwave and conventional heating. The average gradients of the two traces over this temperature range are very similar, and thus suggest that, contrary to initial impressions, the desorption of water is not sensitive to the method of heating. The minor oscillations seen in the conventionally heated trace, (Figure 6.66 in Section 6.5.1) also demonstrate the increased desorption when temperature is increased from a system tending to equilibrium.

CO_2 production

The production of CO_2, as evidenced by the mass 44 pressure appears to follow a conventional temperature profile, as similar CO_2 pressures are observed in the con-

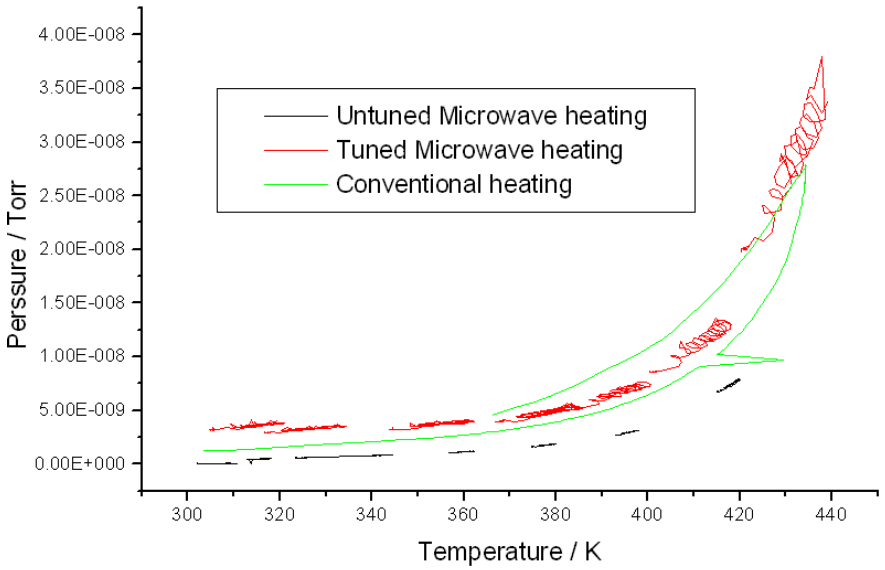

Figure 8.14: CO_2 production over EUROPT-1 under each heating regime

ventional and microwave heated results over all the experiments undertaken. This is shown in Figure 8.14, which shows the production of CO_2 over EUROPT-1 under each heating regime. The trends seen between and within clusters of data for the EUROPT catalysts are also virtually identical and thus it may be surmised that the temperature recorded by the thermocouple under microwave irradiation accurately reflects the temperature of the platinum. This conclusion implies that the temperature of the metal is equivalent to that of the support, which as the greatest solid phase will provide the bulk measurement recorded by the thermocouple, and is also presumably in reasonable thermal equilibrium with the gas phase. The origin of the heating of the support however, is not determined. The metal particles are likely to absorb the microwave energy in a much more efficient manner than the support materials used [2], and it would thus appear that the metal should be hotter than the support. Mathematical studies previously published have suggested that the possibility of a temperature gradient is either not possible [10], or only likely with metal particles of 40–80 nm [11]. The EUROPT-1 has Pt particles of 0.9–3.5 nm [83], with EUROPT-3 having Pt crystallites of less than 1.5 nm [84]. The small metal particle size and the intimate contact with the support show that if excessive heating is occurring within the metal, the heat is rapidly lost to the surrounding material through conduction, resulting in a homogeneous temperature

distribution. The temperature of the gas phase above the catalyst is also likely to contribute to the reaction rate observed. Spectroscopic evidence for the heating of the gas has been presented above, in terms of the peak broadening seen. However, if a temperature difference exists in the gas phase between the two heating regimes, the similarities in reactivity do not reflect this.

8.4 Assessment of reactions

The two cells designed for following the oxidation of carbon dioxide in air have yielded a body of work which allows interpretation of the reaction under microwave heating. The interpretation of these results, along with the less rigorous treatment of the heating of carbon monoxide, chloroform and hexane have resulted in an understanding of the processes occuring under irradiation.

8.4.1 Heating of carbon monoxide

The conventional heating of carbon monoxide in the cell showed that the higher rotational states of the gas phase become populated, which leads to broader bands in the vibrational spectra recorded. When microwave heating is used, the same pattern of peak broadening occurs, in agreement with the modelling study presented in Section 8.2.2. This demonstrates that the transmission cell is effective for microwave heating and changes induced by this may be observed in the infrared spectrum. Whilst it would be expected that the addition of air to the CO would decrease the heating effect seen, due to the loss of energy through collisions between the gases, this is not observed with the temperature measurements used. For all of the temperature measurements, the microwave power can be linked to the heating, as both oscillate at the applied frequency. It may therefore be concluded that the heating of CO using microwave power is rapid, and shows no unexpected non-thermal events.

8.4.2 Oxidation of carbon monoxide

The infrared spectroscopy of the adsorbed CO bands on the Pt surfaces of the EUROPT catalysts show similar effects under both microwave and conventional heating, albeit

with oscillations in the microwave experiments. The linear CO peak appears to shift to lower wavenumber when oxidation occurs. Although the peak saturates at its centre, a loss of intensity appears at higher wavenumber, with a corresponding increase at low values. Similarly, under both methods of heating, the bridged CO peak shows a minor red shift on oxidation, which is accompanied by a loss of intensity to either side of the feature, resulting in a 'sharpened' peak structure.

The production of CO_2 over the catalysts can be followed by both IR and MS. These methods show that the oxidation reaction is independent of the heating regime used. As expected, the production over EUROPT-1 is considerably larger than over EUROPT-3, although both catalysts are active for the reaction. The reaction also occurred to a limited extent when the support materials alone were used, although this limited conversion was possibly due to the Ni gauze covering the IR windows acting as a catalytic surface. This unfortunate effect was too small to be of major concern, and yet again no dependence upon the heating method was seen.

The desorption of the water from the solid catalyst samples occurs both in the conventional and microwave experiments, and can again be observed in both the MS and IR results. Whilst the form of the microwave traces appear to follow a considerably different path to the conventional heating method, this has been reconciled to show no significant rate enhancement or microwave effect.

It can thus be seen from these results that the CO oxidation is not sensitive to the heating method used. It appears that the platinum, the supports, the gas phase and the water impurity have a reasonably homogeneous temperature distribution. This result confirms the previous work carried out in this area [6, 10, 61] and shows that no 'microwave effect' is present for this reaction.

8.4.3 Heating of liquids

The work undertaken on liquid samples was not as successful as hoped, although it has provided a 'proof of concept', and is a fertile area for further study. Heating of the liquids was shown to occur effectively, and changes in the infrared region were observed. Design of a further cell with reduced separation of the applicator plates should allow *in-situ* IR observation of the many organic reactions which have shown enhanced rates

under microwave irradiation. This modification to the cell design will also permit the entire spectral range to be utilised for spectroscopy, and it is expected that this will produce a new insight into the mechanisms involved in this new synthesis tool.

8.5 Evaluation of cell design

The two cells which were created in the course of this study have displayed markedly different success rates. However, the use of the parallel plate design has shown itself to be successful in heating the samples, and spectra of adsorbed species have been obtained using both cells.

The infrared transmission cell design functions well for microwave heating of the sample and also allows easy collection of spectra. However, the cell also displays a few minor weaknesses. Firstly, the thermocouple, whilst providing a reasonable assessment of the bulk temperature, disturbs the homogeneity of the microwave field. This has been shown to lead to localised discolouration of the catalyst wafer under certain conditions. This is an unfortunate consequence of the need to measure temperature, and improvements would be achieved by using non-metallic temperature probes. The parallel plate applicators show deviations from flatness around the windows and o-ring grooves, which also distort the microwave field. Whilst elimination of some surface irregularites is possible, such as reversing the direction of screws that hold the applicator plates together and the elimination of o-ring grooves, the use of gauze to cover the windows is a comprimise that must be accepted. The gauze covering the windows may also contribute to the catalytic activity of the cell, in addition to its strong attenuation of the infrared signal, which decreases the cell's utility in less sensitive spectrometers. Unfortunately there does not appear to be any alternative that allows transmission of infrared light whilst being an electrical conductor. It should be possible however, to remove the applicator plates from contact with the sample by placing them outside the windows. This would prevent any catalytic reaction happening on the gauze, although separation of the plates is likely to increase with this construction. This would either result in a larger cell, or require the sample holder to become thinner. The sample holder is fragile, due to its ceramic construction, especially in its connections to the

tubing connections outside the field. Possible remedies exist, such as adaptations to the cell to allow reactant flows to enter through the applicator plate, as in the DRIFTS cell design. Use of other materials such as PTFE, which is more durable, may also alleviate this problem.

The width of the applicator plate, needed to ensure a homogeneous field around the sample, limited the angles of illumination and collection of the infrared light to the DRIFTS cell. In addition, the signal attenuation caused by the gauze covering the window, and the low sensitivity of the technique itself, lead to poor performance. Whilst a spectrum could be obtained for EUROPT-3 that showed the terminal adsorbed CO, changes in the surface species due to heating were not observed. The use of nylon screws to compress the o-rings in the cell also limited the heating range of the cell under microwave irradiation. Unfortunately, although the operation of the cell using mass spectrometry was confirmed, the optical limitations proved insurmountable to follow the reaction profile in the infrared.

The use of the stub tuner was necessary to observe any heating of the DRIFTS cell in the IR. The transmission cell, with its greater sensitivity allowed collection of data without the impedence matching, although the spectra collected with this addition show an increased heating effect and noticeably clearer features. The efficiency of transferring power into the sample is thus greatly enhanced and provides an increase in the magnitude for all measures of the reaction.

8.6 Conclusions

The microwave heated transmission cell has shown that microwave heating of substances in the beam of a spectrometer to gain useful chemical information is possible. Furthermore, both CO alone and the CO oxidation reaction demonstrate the same infrared features under microwave heating. Taken into account with the mass spectrometry results, it can be concluded that the microwave heating of these reacting systems shows no specific microwave effect. Unfortunately, although the DRIFTS cell is an effective microreactor which also allows extraction of some spectral information, the optical restraints imposed by this technique limit its use. The application of the

transmission cell to liquid reactions demonstrates the microwave heating of liquid reactions can also be followed using similar techniques. The increasing use of microwaves in organic synthesis [85, 86, 77] suggest that this area would be highly profitable to study further.

The first iteration of a microwave heated reaction cell for *in-situ* infrared spectroscopy has shown itself to be a great success. Although a number of improvements may be made to the cell itself and the reactions involved, the first few faltering steps have been taken, and the technique shows a great deal of promise for the future.

8.7 Suggested further work

The successful use of the transmission cell to determine the adsorbed species involved in the CO oxidation reaction demonstrates its suitability for the study of microwave enhanced catalysis. It would therefore be beneficial to apply the technique to investigate systems heated by microwave radiation where unusual modifications to the reaction have been reported. Use of the cell in this manner to determine whether the reacting species adsorbed on the catalyst surface are the same under microwave and conventional heating may elucidate the mechanisms involved in producing the increased activity or modified selectivity. Whilst neither beneficial nor detrimental effect has been seen in the reaction studied, characterisation of the catalysts post reaction would also be advantageous. Reports of catalyst modification [45, 46, 33] for other reactions suggest that the application of microwave energy may affect the morphology of the materials involved.

8.7.1 Catalytic reactions

The ring-opening isomerisation of methylcyclopentane has been reported as a system where microwave heating produced a different product distribution under microwave heating [15, 32]. A comprehensive infrared study of the adsorbed species may therefore yield a productive insight into the mechanism. The reduction of NO_x is another reaction which could profit from such work, as this has been reported to occur at greatly reduced temperatures under microwave heating [56]. This reaction has the benefit of

nitrogen oxides being strong infrared chromophores, which should provide clear spectra for interpretation.

In addition to these two highlighted reactions, there is no reason why any number of systems should not be studied with this technique. Given a sensitive spectrometer, any reaction which involves infrared active species could thus be investigated.

8.7.2 Liquid phase synthesis

The microwave heating of liquid phase reactions has recently become a standard technique for organic synthesis, with a great number of reactions benefitting from the time savings possible [26, 5]. Although the rate enhancement has been shown to be due to superheating of the solvent [87], a spectroscopic confirmation of these results would be beneficial. An example of such a reaction is the generation of nitrile sulfides. A recent report [88] concerning the preparation and reaction of benzonitrile sulfide for cycloaddition reports a reduction in reaction time from 15-30 hrs to *c.* 15min. This reaction could easily be followed by *in-situ* IR, in a modified microwave cell to elucidate the processes concerned.

Bibliography

[1] R.Gedye, F.Smith, K.Westaway, H.Ali, L.Baldisera, L.Laberge, and J.Rousell. The use of microwave ovens for rapid organic synthesis. *Tetrahedron Letters*, 27(3):279–282, 1986.

[2] A.Whittaker and D.Mingos. Microwave dielectric heating effects in chemical synthesis. In R.Van Eldik and C.Hubbard, editors, *Chemistry Under Extreme or Non-Classical Conditions*, pages 479–514. Wiley and Spektrum Akademischer Verlag, 2002.

[3] C.Holcombe and N.Dykes. Microwave sintering of titanium diboride. *Journal of Materials Science*, 26:3730–3738, 1991.

[4] K.Gammampila, P.Dunscombe, B.Southcott, and A.Stacey. Thermocouple thermometry in microwave fields. *Clinical Physics and Physiological Measurement*, 2(4):285–292, 1981.

[5] S.Caddick. Microwave assisted organic reactions. *Tetrahedron*, 51(38):10403–10432, 1995.

[6] W.Perry, J.Katz, D.Rees, M.Paffet, and A.Datye. Kinetics of the microwave-heated CO oxidation reaction over alumina-supported Pd and Pt catalysts. *Journal of Catalysis*, 171:431–438, 1997.

[7] P.Debye. Anomolous dispersion for radio frequencies. In *Polar Molecules*, pages 77–108. Chemical Catalog, New York, 1929.

[8] B.Hamon. Maxwell-Wagner loss and adsorption currents in dielectrics. *Australian Journal of Physics*, 6:304–315, 1953.

[9] R.Meakins. The dielectric properties of urea occlusion compounds. *Transactions of the Faraday Society*, 51:953–961, 1955.

[10] W.Perry, D.Cooke, and J.Katz. On the possibility of a significant temperature gradient on supported metal catalysts subjected to microwave heating. *Catalysis Letters*, 47:1–4, 1997.

[11] J.Thomas. Particle size effect in microwave-enhanced catalysis. *Catalysis Letters*, 49:137–141, 1997.

[12] G.Bond, R.Moyes, S.Pollington, and D.Whan. Measurement of temperature during microwave heating. *Measurement Science and Technology*, 2:571–572, 1991.

[13] G.Robb. *The microwave effect. Non-thermal effects of microwave radiation in solid state chemistry.* PhD thesis, The University of Edinburgh, 2003.

[14] A.Reid, M.Gertner, and M.Sherar. Temperature measurement artefacts of thermocouples and fluoroptic probes during laser irradiation at 810nm. *Physics in Medicine and Biology*, 46:N149–N157, 2001.

[15] L.Seyfried, F.Garin, G.Maire, J.Thiebaut, and G.Roussy. Microwave electromagnetic field effects on reforming catalysts. *Journal of Catalysis*, 148:281–287, 1994.

[16] J.Thiebaut, G.Roussy, M.Medjram, L.Seyfried, F.Garin, and G.Mayor. Reactions de reformage des hexanes sur un catalyseur a 0,2% de Pt sur Al_2O_3 irradie par un champ microonde. *Journal de Chimie Physique et de Physico-chimie Biologique*, 89:1427–1439, 1992.

[17] J.Thiebaut, G.Roussy, M.Medjram, F.Garin, L.Seyfried, and G.Maire. Durable changes of the catalytic properties of alumina-supported platinum induced by microwave irradiation. *Catalysis Letters*, 21:133–138, 1993.

[18] R.Gedye, F.Smith, and K.Westaway. Microwaves in organic and organometallic synthesis. *Journal of Microwave Power and Electromagnetic Energy*, 26(1):3–17, 1991.

[19] D.Baghurst and D.Mingos. A new reaction vessel for accelerated syntheses using microwave dielectric super-heating effects. *Journal of the Chemistry Society, Dalton Transactions*, pages 1151–1155, 1992.

[20] A.Fung and K.Oxford. Microwave superheated Vics vapo rub: An ocular public health danger. *American Journal of Ophthalmology*, 137:379–380, 2004.

[21] D.Mingos. Microwaves in chemical syntheses. *Chemistry & Industry*, pages 596–599, 1994.

[22] J.Samuels and J.Brandon. Effect of composition on the enhanced microwave sintering of alumina-based ceramic composites. *Journal of Materials Science*, 27:3259–3265, 1992.

[23] A.Whittaker and D.Mingos. Microwave-assisted solid-state reactions involving metal powders. *Journal of the Chemistry Society, Dalton Transactions*, pages 2073–2079, 1995.

[24] D.Baghurst, A.Chippindale, and D.Mingos. Microwave syntheses for superconducting ceramics. *Nature*, 332:311, 1988.

[25] C.Landry and A.Barron. Synthesis of polycrystalline chalcopyrite semiconductors by microwave irradiation. *Science*, 260:1653–1654, 1993.

[26] A.Loupy, A.Petit, J.Hamelin, F.Texier-Boullet, P.Jacquault, and D.Mathe. New solvent-free organic synthesis using focused microwaves. *Synthesis*, (9):1213–1234, 1998.

[27] M.Hajek and M.Radoiu. Microwave activation of catalytic transformation of *t*-butylphenols. *Journal of Molecular Catalysis A: Chemical*, 160:383–392, 2000.

[28] J.Wan, Y.Chen, Y.Lee, and M.Depew. Highly effective methane conversion to aromatic hydrocarbons by means of microwave and RF-induced catalysis. *Research on Chemical Intermediates*, 26(6):599–619, 2000.

[29] G.Bond, R.Moyes, I.Theaker, and D.Whan. The effect of microwave heating on the reaction of propan-2-ol over alkalised carbon catalysts. *Topics in Catalysis*, 1:177–182, 1994.

[30] C.Cundy. Microwave techniques in the synthesis and modification of zeolite catalysts. A review. *Collection of Czechoslovak Chemical Communications*, 63:1699–1723, 1998.

[31] A.Cirera, A.Cabot, A.Cornet, and J.Morante. CO-CH_4 selectivity enhancement by *in-situ* Pd- catalysed microwave SnO_2 nanoparticles for gas detectors using active filter. *Sensors and Actuators B*, 78:151–160, 2001.

[32] G.Roussy, S.Hilaire, J.Thiebaut, G.Maire, F.Garin, and S.Ringler. Permanent change of catalytic properties induced by microwave activation on 0.3% Pt/Al_2O_3 (EuroPt-3) and on 0.3% Pt-0.3% Re/Al_2O_3 (EuroPt-4). *Applied Catalysis A: General*, 156:167–180, 1997.

[33] X.Zhang, L.Wang, Y.Cao, W.Dai, H.He, and K.Fan. A unique microwave effect on the microstructural modification of $Cu/ZnO/Al_2O_3$ catalysts for steam reforming of methanol. *Chemical Communications*, (32):4104–4106, 2005.

[34] *International Conference on High Frequency Microwave Processing and Heating*, Arnhem, Netherlands, 1989.

[35] Y.Zhenming, Z.Jinsong, C.Xiaoming, L.Qiang, X.Zhijun, and Z.Zhimin. Microwave enhanced exhaust conversion of internal combustion engines. *Applied Catalysis B: Environmental*, 34:129–135, 2001.

[36] J.Ma, M.Fang, P.Li, B.Zhu, X.Lu, and N.Lau. Microwave-assisted catalytic combustion of diesel soot. *Applied Catalysis A: General*, 159:211–228, 1997.

[37] G.Roussy, J.Thiebaut, M.Souiri, E.Marchal, A.Kiennemann, and G.Maire. Controlled oxidation of methane doped catalysts irradiated by microwaves. *Catalysis Today*, 21:349–355, 1994.

[38] G.Roussy, E.Marchal, J.Thiebaut, A.Kiennemann, and G.Maire. C_2^+ selectivity enhancement in oxidative coupling of methane over microwave-irradiated catalysts. *Fuel Processing Technology*, 50:261–274, 1997.

[39] X.Zhang, C.Lee, D.Mingos, and D.Hayward. Oxidative coupling of methane using microwave dielectric heating. *Applied Catalysis A: General*, 249:151–164, 2003.

[40] J.Wan. Microwaves and chemistry: The catalysis of an exciting marriage. *Research on Chemical Intermediates*, 19(2):147–158, 1993.

[41] C.Cha, S.Wallace, A.George, and S.Rogers. Microwave technology for treatment of fume hood exhaust. *Journal of Environmental Engineering*, 130:338–348, 2004.

[42] S.Horikoshi, H.Hidaka, and N.Serpone. Environmental remediation by an integrated microwave/UV illumination technique IV. Non-thermal effects in the microwave-assisted degradation of 2,4-dichlorophenoxyacetic acid in UV-irradiated TiO_2/H_2O dispersions. *Journal of Photochemistry and Photobiology A: Chemistry*, 159:289–300, 2003.

[43] C.Chen, P.Hong, S.Dai, and J.Kan. Microwave effects on the oxidative coupling of methane over proton conductive catalysts. *Journal of the Chemistry Society Faraday Transactions*, 91(7):1179–1180, 1995.

[44] J.Wan and M.Ioffe. Surface heating and energy transfer in pulsed microwave catalytic systems: A microwave-induced acoustic study. *Research on Chemical Intermediates*, 20(1):115–132, 1994.

[45] X.Zhang, D.Hayward, C.Lee, and D.Mingos. Microwave assisted catalytic reduction of sulfur dioxide with methane over MoS_2 catalysts. *Applied Catalysis B: Environmental*, 33:137–148, 2001.

[46] X.Zhang, D.Hayward, and D.Mingos. Apparent equilibrium shifts and hot-spot formation for catalytic reactions induced by microwave dielectric heating. *Chemical Communications*, (11):975–976, 1999.

[47] G.Maire, C.Corolleur, D.Juttard, and F.Gault. Comments on a dispersion effect in hydrogenolysis of methylcyclopentane and isomerisation of hexanes over supported platinum catalysts. *Journal of Catalysis*, 21:250–253, 1971.

[48] Y.Zhuang and A.Frennet. Kinetic studies of methylcyclopentane ring opening on EuroPt-1 (Pt/SiO_2). *Applied Catalysis A: General*, 177:205–217, 1999.

[49] G.Diaz, F.Garin, G.Maire, S.Alerasool, and R.Gonzalez. Hydrogenolysis of methylcyclopentane and isomerization of 2-methylpentane over well characterized silica-supported platinum-ruthenium catalysts. *Applied Catalysis A: General*, 124:33–46, 1995.

[50] C.Corolleur, D.Tomanova, and F.Gault. The mechanisms of hydrogenolysis and isomerisation of hydrocarbons on metals part VII. Isomerisation of labeled hexanes and hydrogenolysis of methyl (^{13}C) cyclopentane on a 10% platinum-alumina catalyst. *Journal of Catalysis*, 24:401–416, 1972.

[51] H.Will, P.Scholz, and B.Ondruschka. Microwave-assisted heterogenous gas phase catalysis. *Chemical Engineering & Technology*, 27(2):113–122, 2004.

[52] G.Bond, R.Moyes, and D.Whan. Recent applications of microwave heating in catalysis. *Catalysis Today*, 17:427–437, 1993.

[53] H.Takashima, L.Ren, and Y.Kanno. Catalytic decomposition of TCE under microwave. *Catalysis Communications*, 5:317–319, 2004.

[54] M.Turner, R.Laurence, K.Yngvesson, and W.Conner. The effect of microwave energy on three-way automotive catalysts poisoned by SO_2. *Catalysis Letters*, 71(3-4):133–138, 2001.

[55] K.Takatsu, F.Kurogi, and M.Kasaya. Development of the microwave heated catalyst system. *JSAE Review*, 20:421–438, 1999.

[56] S.Ringler, P.Girard, G.Maire, S.Hilaire, G.Roussy, and F.Garin. Mechanistic studies of NO_x reduction reactions under oxidative atmosphere on alumina supported 0.2 wt% platinum catalyst treated under microwave (part II). *Applied Catalysis B: Environmental*, 20:219–233, 1999.

[57] J.Tang, T.Zhang, D.Liang, H.Yang, N.Li, and L.Lin. Direct decomposition of NO by microwave heating over Fe/NaZSM-5. *Applied Catalysis B: Environmental*, 36:1–7, 2002.

[58] H.Roh, Y.Park, and S.Park. Superior decomposition of NO over plasma-assisted catalytic system induced by microwave. *Chemistry Letters*, 5:578–579, 2000.

[59] J.Tang, T.Zhang, D.Liang, and L.Lin. Reduction of NO by CH_4 with microwave heating. *Topics in Catalysis*, 22(1-2):59–63, 2003.

[60] M.Wójtowicz, F.Miknis, R.Grimes, W.Smith, and A.Serio. Control of nitric oxide, nitrous oxide and ammonia emissions using microwave plasmas. *Journal of Hazardous Materials*, 74:81–89, 2000.

[61] W.Perry, J.Katz, D.Rees, and M.Paffet. Kinetics of the carbon monoxide oxidation reaction under microwave heating. *Materials Research Society Symposium Proceedings*, 430:391–395, 1996.

[62] M.Schubert, M.Kahlich, H.Gasteiger, and R.Behm. Correlation between CO surface coverage and selectivity/kinetics for the preferential CO oxidation over Pt/γ-Al_2O_3 and Au/α-Fe_2O_3: An *in-situ* DRIFTS study. *Journal of Power sources*, 84:175–182, 1999.

[63] W.Epling, G.Hoflund, and J.Weaver. Surface characterisation study of Au/α-Fe_2O_3 and Au/Co_3O_4 low-temperature CO oxidation catalysts. *Journal of Physical Chemistry*, 100:9929–9934, 1996.

[64] P.Brimmer and P.Griffiths. Effect of absorbing matrices on diffuse reflectance infrared spectra. *Analytical Chemistry*, 58:2179–2184, 1986.

[65] W.Maddams. The basic physics of infrared emission spectroscopy. *Internet Journal of Vibrational Spectroscopy [www.ijvs.com]*, 5:2, 2001.

[66] J.Anderson. Infrared study of CO oxidation over Pt-Rh/Al_2O_3 catalysts. *Journal of Catalysis*, 142:153–165, 1993.

[67] M.Cavers. *Development of a Frequency Response Reactor for the Study of Heterogeneous Catalysis.* PhD thesis, The University of Edinburgh, 2000.

[68] P.Ratnasamy. Infra-red spectra of benzene and cyclohexane adsorbed on platinum-alumina. *Chemical age of India*, 21(10):889–892, 1970.

[69] P.Hendra. Recording emission spectroscopy. *Internet Journal of Vibrational Spectroscopy [www.ijvs.com]*, 5:3, 2001.

[70] B.Crawford, Jr. and P.Cross. The vibrational spectrum and thermodynamic properties of nickel carbonyl. *Journal of Chemical Physics*, 6:525–530, 1938.

[71] N.Sheppard and T.Nguyen. The vibrational spectra of carbon monoxide chemisorbed on the surfaces of metal catalysts— a suggested scheme of interpretation. In R.Clark and R.Hester, editors, *Advances in Infrared and Raman Spectroscopy*, volume 5. Heyden, London, UK, 1978.

[72] A.Burneau, O.Barrès, J.Gallas, and J.Lavalley. Comparitive study of the surface hydroxyl groups of fumed and precipitated silicas. 2. Characterization by infrared spectroscopy of the interactions with water. *Langmuir*, 6:1364–1372, 1990.

[73] A.Goodman, E.Bernard, and V.Grassian. Spectroscopic study of nitric acid and water adsorption on oxide particles: Enhanced nitric acid uptake kinetics in the presence of adsorbed water. *Journal of Physical Chemistry A*, 105:6443–6457, 2001.

[74] M.Cavers, J.Davidson, I.Harkness, L.Rees, and G.McDougall. Spectroscopic identification of the active site for CO oxidation on Rh/Al_2O_3 by concentration modulation *in situ* DRIFTS. *Journal of Catalysis*, 188:426–430, 1999.

[75] P.Marshall. *Potassium promotion of nickel alumina catalysts*. PhD thesis, The University of Edinburgh, 1994.

[76] L.J.Bellamy. *The Infra-red Spectra of Complex Molecules*. John Wiley & Sons, New York, 2nd edition, 1960.

[77] B.Hayes. *Microwave synthesis: Chemistry at the speed of light*. CEM Publishing, Matthews, NC, 2002.

[78] P.Atkins. *Physical chemistry*. Oxford University Press, Oxford, 6th edition, 1998.

[79] G.Herzberg. *Molecular spectra and molecular structure I: Spectra of diatomic molecules*. Krieger Pub. Co., Malabar, Fla., 2nd edition, 1989.

[80] J.Xu, P.Henriksen, and J.Yates, Jr. Direct spectroscopic observation of the reactive catalytic site for CO oxidation on Pt(335). *Journal of Chemical Physics*, 97:5250–5252, 1992.

[81] S.Podkolzin, J.Shen, J.de Pablo, and J.Dumesic. Equilibrated adsorption of CO on silica-supported Pt catalysts. *Journal of Physical Chemistry B*, 104:4169–4180, 2000.

[82] D.Woodruff and T.Delchar. *Modern techniques of surface science*. Cambridge University Press, Cambridge, 1988.

[83] J.Geus and P.Wells. Characterization of the standard platinum/silica catalyst EuroPt-1. 3. the size distribution of the platinum containing particles. *Applied Catalysis*, 18:231–242, 1985.

[84] B.Kramer and M.Fischbacher. Hydrogen pretreatment effects on the hydrogenolysis of methylcyclopentane on Pt/SiO_2 and Pt/Al_2O_3 catalysts. *Journal of Molecular Catalysis*, 51:247–259, 1989.

[85] P.Harris. The sintering of platinum particles in an alumina-supported catalyst: Further transmission electron microscopy studies. *Journal of Catalysis*, 97:527–542, 1986.

[86] A.Fini and A.Breccia. Chemistry by microwaves. *Pure and Applied Chemistry*, 71:573–579, 1999.

[87] R.Gedye, W.Rank, and K.Westaway. The rapid synthesis of organic compounds in microwave ovens II. *Canadian Journal of Chemistry*, 69:706–711, 1991.

[88] A.J.Morrison, R.M.Paton, and R.D.Sharp. Microwave-assisted generation and reactions of nitrile sulfides. *Synthetic Communications*, 36:807–813, 2005.